

**NANOSTRUCTURED LIPID CARRIERS (NLCs) FOR THE TREATMENT  
OF DRY EYE DISEASE**





**A Thesis Submitted to the Graduate School of Naresuan University  
in Partial Fulfillment of the Requirements  
for the Doctor of Philosophy Degree  
in Pharmaceutical Science  
August 2018  
Copyright 2018 by Naresuan University**

Thesis entitled “ Nanostructured lipid carriers (NLCs) for the treatment of dry eye disease ” by Miss Pattravee Niamprem  
has been approved by the Graduate School as partial fulfillment of the requirements  
for the Doctor of Philosophy Degree in Pharmaceutical Sciences  
of Naresuan University

**Oral Defense Committee**


  
..... Chair  
(Assistant Professor Pakawadee Sermsappasuk, Ph.D.)

  
..... Advisor  
(Associate Professor Waree Tiyafoonchai, Ph.D.)

  
..... Co – Advisor  
(Associate Professor SP Srinivas, Ph.D.)

  
..... Co – Advisor  
(Assistant Professor Pornnarin Taepavarapruk, Ph.D.)

  
..... External Examiner  
(Dr. Chirasak Kusunwiriawong, Ph.D.)

  
.....  
(Associate Professor Paisarn Muneesawang, Ph.D.)

Dean of the Graduate School

17 AUG 2018

## ACKNOWLEDGEMENT

Firstly, I would like to express my sincere gratitude to my advisor, Associated Professor Dr. Waree Tiyaboonchai, for the continuous support of my Ph.D. study, for her patience, invaluable guidance, and constant inspiration. I am thankful to my co-advisor, Associate Professor SP Srinivas from Indiana University, for his motivation, useful guidance, and intellectual support. Also, I would like to acknowledge my co-advisor, Assistant Professor Pornnarin Taepavarapruk, for her invaluable advice, and her insights in animal experiments. I am indeed deeply grateful to all the three professors for helping me in all the time of research and writing of this thesis. I could not have imagined having a better advisors and mentors for my Ph.D. study.

I am greatly thankful to Professor Thomas Millar from Western Sydney University, who provided me a great opportunity to work in his laboratory and thanks for his useful guidance, immense knowledge, and encouragement. Also, I would like to thank Dr. Burkhardt Schuett for his invaluable advice and support.

I gratefully acknowledge the financial support by the Thailand Research Fund (TRF) and Naresuan University under the Royal Golden Jubilee Ph.D. [grant number PHD/0086/2556]. This research is also partially supported by Faculty of Pharmaceutical Sciences, Naresuan University, and the Center of Excellence for Innovation in Chemistry (PERCH-CIC), Commission on High Education, Ministry of Education, Thailand.

I am also thank to my friends and all staffs in Faculty of Pharmaceutical Sciences, which made it possible for my full stay with much joy and happy moments.

Last but not the least, I would like to thank to my parents and my family for their endless love, care and supporting me spiritually throughout writing this thesis and my life in general.

Pattravee Niamprem

**Title** NANOSTRUCTURED LIPID CARRIERS (NLCs) FOR THE TREATMENT OF DRY EYE DISEASE

**Author** Patravee Niamprem

**Advisor** Associate Professor Waree Tiyafoonchai, Ph.D.

**Co-Advisor** Associate Professor SP Srinivas, Ph.D.  
Assistant Professor Pornnarin Taepavarapruk, Ph.D.

**Academic Paper** Thesis Ph.D. in Pharmaceutical Sciences,  
Naresuan University, 2018

**Keywords** nanostructured lipid carriers, dry eye disease, tear film,  
transcorneal penetration, ocular drug delivery

### ABSTRACT

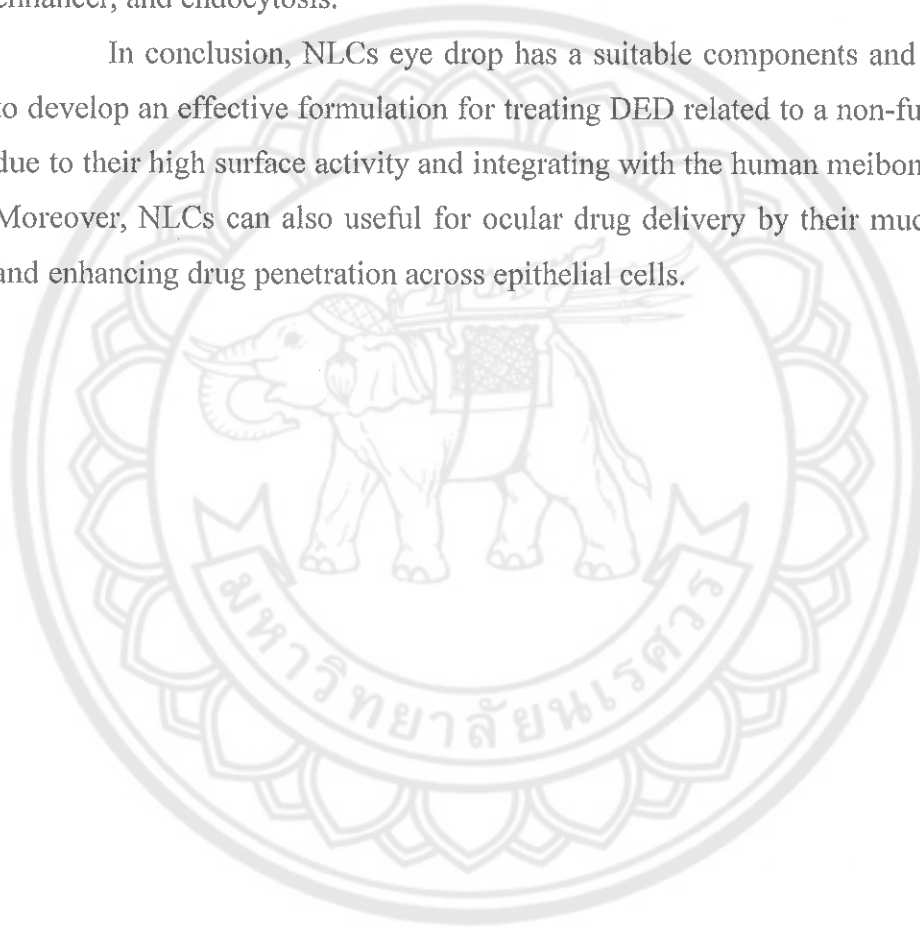
Dry eye is a disease of the tears and ocular surface involving tear hyperosmolarity and tear film instability. The tear film is a liquid layer covering the cornea and conjunctiva which acting as a barrier between the eye and environment. The outermost layer of the tear film is coated by lipids, well-known as a tear film lipid layer (TFLL), which the major component is meibum. This TFLL is responsible for reducing the surface tension of the tear film and increasing the tear film stability that related to dry eye disease (DED). It has been hypothesized that abnormal secretion of meibum or changing of the meibum composition can cause tear film instability that causes evaporative dry eye. In general, artificial tear eye drops and anti-inflammatory agents are the most widely used to relief dry eye symptomatic and suppressing the chronic inflammation, respectively. However, the efficacy of artificial tear eye drops is transient and the drop need frequent instillation. Moreover, anti-inflammatory agents are usually used as eye drops which exhibited poor bioavailability and caused of eye irritation. This puts a burden on the patient and diminishes patient compliance. To overcome this problem, the nanostructured lipid carriers (NLCs) eye drop has been developed and characterized as tear replacement formulation in order to improve the tear film stability. In addition, these NLCs formulations were designed to be a solution of the short residence time and poor drug penetration of topical eye drop.

In this study, the NLCs formulations were prepared by the high pressure homogenization technique, which type of solid lipids and surfactants affect their mean particle sizes in the range of 38 – 280 nm. One of the strongest advantages of these NLCs is possible to sterilize by an autoclaving method. NLCs prepared with Tween 80 withstood the sterilization without phase separation. In addition, the optimized NLCs eye drop, NLC3, achieved values of pH, osmolarity, and surface tension close to the physiological range that is suitable for tear replacement. Non-irritation was observed by short time exposure test in porcine corneal epithelium (PCE) cells. In order to improve tear film stability, high surface activity of NLCs eye drops was observed using a Langmuir trough. Additionally, they can interact with meibomian lipid films both directly and by diffusing from the subphase. The efficacy of NLCs eye drop as bionic tear film suggested that NLC3 eye drop exhibited significantly longer retention on the rabbit ocular surface compared with normal saline solution. In particular, the fluorescence signal of NLC3 increased in a time-dependent manner, which can be explained by NLCs would then gradually penetrate from aqueous layer to the TFLL. Also, the efficacy of NLC3 on protecting the rabbit ocular surface damaged under stress condition showed that NLC3 had a higher ability to protect the ocular surface damaged than commercial artificial tears.

Furthermore, an enhancement of the residence time and transcorneal penetration on the ocular surface was investigated. Nile red (NR) and Indomethacin (IND) was entrapped into the NLCs as a fluorescent lipophilic dye and a prototype of lipophilic drug, respectively. High entrapment efficacy (EE) of ~70 % was observed based on the type of solid lipid. In addition, the multiple type of NLCs would be achieved due to the ratio of solid lipid/oil, 5/4, used in NLCs formulations. Therefore, the release of drug from NLCs showed a prolonged release for 360 min with a burst release of 50 - 60%. As in agreement with the NLCs structure, the drugs were released from the NLCs by a diffusion-controlled mechanism. Surface modification of Nile red loaded NLCs (NR-NLCs) by polyethylene glycol 400 (PEG) or stearylamine (SA) altered the hydrophilic surface (NR-NLC-PEG) or cationic surface charge (NR-NLC-SA), respectively. By using confocal scanning micro fluorometer (CSMF), smaller NLCs (~40 nm) showed greater penetration across the epithelium compared with the larger particles (~150 nm). Moreover, both NLCs with hydrophilic surface and

cationic surface charge showed an enhancement of the mucoadhesive property on the porcine corneal surface. While, the result of PCE cells uptake by flow cytometer found that the unmodified NLCs revealed significantly higher internalization uptake compared to the NLCs modifications. These results suggested that the particle size, surface hydrophobicity, and surface charge affect the mucoadhesion and corneal penetration of ocular surface. Moreover, the common accepted penetration mechanisms of drug loaded NLCs could be explained by diffusion, penetration enhancer, and endocytosis.

In conclusion, NLCs eye drop has a suitable components and characteristics to develop an effective formulation for treating DED related to a non-functional TFLM due to their high surface activity and integrating with the human meibomian lipid film. Moreover, NLCs can also be useful for ocular drug delivery by their mucoadhesiveness and enhancing drug penetration across epithelial cells.



# LIST OF CONTENTS

Chapter	Page
<b>I INTRODUCTION.....</b>	<b>1</b>
Rational of the study.....	1
Objective of the study.....	2
Expected outputs of the study.....	3
Expected outcomes of the study.....	3
References .....	4
<b>II LITERATURE REVIEW.....</b>	<b>7</b>
Dry eye disease .....	7
Anatomy of eye .....	10
Human tears .....	11
The tear film .....	12
Structure of the tear film .....	12
Lipid layer .....	13
Aqueous layer .....	14
Mucous layer .....	14
Tear film dynamics .....	14
The correlation between the TFLL and dry eye disease.....	16
Surface tension and surface activity of the TFLL.....	17
Treatments of dry eye.....	19
Topical ocular administration.....	24
Precorneal barriers.....	25
Cornea barriers.....	25
Blood-ocular barrier.....	27
Ocular pharmacokinetics.....	27

## LIST OF CONTENTS (CONT.)

Chapter	Page
Nanostructured lipid carriers (NLCs).....	30
Introduction of NLCs.....	31
Production of NLCs .....	31
Structure of NLCs .....	32
Characterization of NLCs .....	32
Mucoadhesion theory .....	34
Animal model of dry eye .....	35
Introduction.....	35
Anatomy of rabbit eye.....	35
Examination techniques.....	37
References .....	39
<b>III INTERACTION OF NANOSTRUCTURED LIPID CARRIERS WITH HUMAN MEIBUM.....</b>	<b>47</b>
Introduction .....	47
Materials and Methods.....	49
Materials .....	49
Preparation of NLCs .....	50
Surface pressure-area (II-A) measurements of NLCs.....	50
The interaction of human meibomian lipid with optimized NLCs .....	51
The penetration of NLCs to the human meibomian lipid film....	51
Results and discussions .....	52
NLCs formulations .....	52
The surface activity of NLCs formulations .....	53



## LIST OF CONTENTS (CONT.)

Chapter	Page
The interaction of human meibomian lipid with optimized NLCs.....	57
The penetration of NLCs to human meibomian lipid film.....	61
Conclusions.....	63
Appendix.....	64
References.....	68
<b>IV NANOSTRUCTURED LIPID CARRIERS AS A BIONIC TEAR FILM IN RABBIT EVAPORATIVE DRY EYE MODEL.....</b>	<b>73</b>
Introduction.....	73
Materials and Methods.....	74
Materials .....	74
NLCs eye drop preparation.....	75
Characterization of the NLCs eye drop .....	75
Cytotoxicity of NLCs eye drop in primary porcine corneal epithelial (PCE) cells .....	76
Animals .....	77
The retention of NLCs eye drops on corneal surface.....	77
The effect of NLCs eye drops on ocular surface epithelial cells of rabbit after exposure with desiccation conditions .....	78
Results .....	79
Physicochemical characterizations of the NLCs eye drops.....	79
Cytotoxicity test of NLCs eye drop .....	79
The retention of NLCs eye drops on corneal surface in rabbit eyes .....	80

## LIST OF CONTENTS (CONT.)

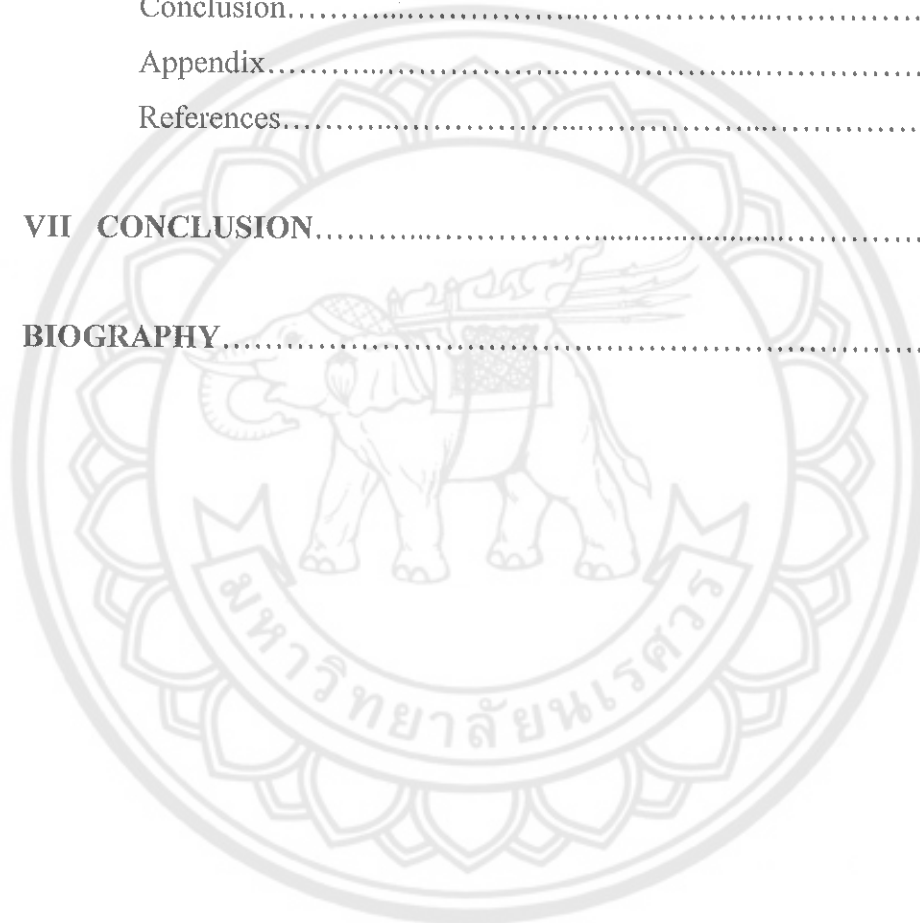
Chapter	Page
Effect of NLCs eye drops on ocular surface epithelial cells of rabbit after exposure with desiccation conditions.....	82
Discussion .....	83
Conclusion .....	87
Appendix.....	88
References .....	92
<b>V PENETRATION OF NILE RED-LOADED NANOSTRUCTURED LIPID CARRIERS ACROSS THE PORCINE CORNEA.....</b>	<b>96</b>
Introduction .....	96
Materials and Methods.....	97
Materials .....	97
Preparation of Nile red-loaded NLCs (NR-NLCs) and surface modified NR-NLCs .....	98
Physico-chemical characterization of NR-NLCs and surface modified NR-NLCs.....	98
Penetration NR-NLCs across the porcine cornea .....	99
Mucoadhesion Assay.....	99
Cellular uptake by flow cytometry.....	100
Statistic analysis .....	100
Results and discussion.....	101
Characterization of NR-NLCs.....	101
Penetration of NR-NLCs across the porcine cornea.....	103
Effect of formulations and incubation time.....	104
Effect of particle size.....	107
Effect of surface modification .....	109

## LIST OF CONTENTS (CONT.)

Chapter	Page
Mucoadhesion .....	110
Cellular uptake by flow cytometric analysis .....	113
Conclusion .....	115
Appendix .....	116
References .....	121
<b>VI DEVELOPMENT AND CHARACTERIZATION OF INDOMETHACIN-LOADED MUCOADHESIVE NANOSTRUCTURED LIPID CARRIERS FOR TOPICAL OCULAR DELIVERY .....</b>	<b>126</b>
Introduction .....	126
Materials and Methods.....	128
Materials .....	128
Preparation of blank-NLCs and IND-NLCs .....	128
Sterilization by autoclaving.....	129
Drug incorporation efficiency.....	129
Physico-chemical characterization of blank-NLCs and IND- NLCs.....	130
<i>In vitro</i> release study.....	130
<i>Ex vivo</i> mucoadhesive study.....	131
Cytotoxicity of IND-NLC in primary porcine corneal epithelial (PCE) cells.....	131
Results.....	132
Physicochemical characteristics of blank-NLCs.....	132
Physicochemical characterization of IND-NLCs.....	133
<i>In vitro</i> release study.....	135

## LIST OF CONTENTS (CONT.)

Chapter	Page
<i>Ex vivo</i> mucoadhesion test.....	136
Cytotoxicity of IND-NLC.....	136
Discussion.....	137
Conclusion.....	141
Appendix.....	142
References.....	144
<b>VII CONCLUSION.....</b>	<b>150</b>
<b>BIOGRAPHY.....</b>	<b>154</b>



## LIST OF TABLES

Table		Page
2.1	Comparison between human, rabbit, and porcine eye.....	36
3.1	The components and physicochemical properties of NLCs.....	53
4.1	Physicochemical properties of the NLCs eye drops before and after autoclaving .....	79
4.2	Summary of short time exposure (STE) tests performed by MTT assay.....	80
5.1	The effects of solid lipid type and concentration on the particle size, polydispersity index, and zeta potential of NR-NLCs.....	102
6.1	The components and physicochemical properties of NLCs.....	133
6.2	Physicochemical characterizations of the optimized IND-NLCs.....	134
6.3	Summary of short time exposure (STE) tests performed by MTT assay.....	137

## LIST OF FIGURES

Figure	Page
2.1 Mechanism of dry eye.....	8
2.2 Autoimmune cycle of chronic inflammation during the immunopathogenesis of dry eye disease. (a) An environmental stimulus initiates acute inflammation on the ocular surface stimulating upregulation of proinflammatory cytokines (e.g., TNF- $\alpha$ , IL-1 and IL-17), matrix metalloproteinases (MMPs), adhesion molecules (e.g., ICAM-1), and chemokines (e.g., CCL5 and CXCL10) within the conjunctival and corneal epithelium that act in concert to perpetuate the immune response; (b) Antigen presenting cells (e.g., dendritic cells) process autoantigen and (c) following activation, (d) traffic to the draining cervical lymph nodes (CLNs) via the afferent lymphatics, where they (e) present antigen to autoreactive CD4 <sup>+</sup> T cells. Efferent arm of the immune response: (f) Activated CD4 <sup>+</sup> T cells bearing specific adhesion molecules and chemokine receptors (e.g., CCR5 and CXCR3) migrate specifically to the ocular surface tissues (conjunctiva and cornea are shown), including the meibomian and lacrimal glands where they infiltrate the tissue and (g) release proinflammatory cytokines (IFN- $\gamma$ and IL-17) that promote chronic inflammation and tissue destruction .....	9
2.3 The human eye.....	10
2.4 Model of tear film.....	12
2.5 Scheme of the TFLL structure.....	13
2.6 Langmuir trough with two-moveable barriers.....	18

## LIST OF FIGURES (CONT.)

Figure	Page
2.7 Idealized Langmuir isotherm of the monolayer film of a typical amphiphilic molecule. The three distinct regions of the isotherm can be associated with the different level of ordering of the film as shown schematically on the figure; $\pi_c$ is the collapse pressure beyond which multilayer start forming, and $A_0$ is the zero pressure molecular area.....	19
2.8 Model showing the movement of drug into the eye after topical administration. BAB, blood-aqueous barrier; BRB, blood-retinal barrier. ....	24
2.9 The structure of cornea. ....	26
2.10 Schematic presentation of the ocular structure showing a summary of ocular pharmacokinetics. The numbers refer to following processes: 1) transcorneal permeation from the lachrymal fluid into the anterior chamber, 2) non-corneal drug permeation across the conjunctiva and sclera into the anterior uvea, 3) drug distribution from the bloodstream via the blood-aqueous barrier into the anterior chamber, 4) elimination of drug from the anterior chamber by aqueous humour passage into the trabecular meshwork and Sclemm's canal, 5) drug elimination from the aqueous humor into the systemic circulation across the blood-aqueous barrier, 6) drug distribution from the blood into the posterior eye across the blood-retina barrier, 7) intravitreal drug administration, 8) drug elimination from the vitreous via the posterior route across the blood-retina barrier, and 9) drug elimination from the vitreous via the anterior route to the posterior chamber.....	28

## LIST OF FIGURES (CONT.)

Figure	Page	
2.11	The permeation mechanisms across cornea. Passive paracellular and transcellular permeation. Transporter mediated influx and efflux across cell membrane in the apical (1 and 2) and basolateral (3 and 4) side, respectively.....	29
2.12	Three structure type of NLCs.....	32
3.1	Proposed mechanisms of NLCs after instilled into the eye. In term of ocular drug delivery, the NLCs pass through the tear film and A) endocytosis or B) slowly release the loaded drug into the corneal epithelium. Moreover, the NLCs may C) bind to the TFLL or D) break down to release the lipids and surfactants then merge with TFLL to enhance the tear film stability. ....	53
3.2	II-A curves comparing films of NLCs prepared with A) Compritol 888 ATO, B) Gelucire 43/01, and C) cetyl palmitate as solid lipid and Tween 80 as a surfactant when spread at 35 °C and then decreased to 20 °C. D) A direct comparison between the first isocycles of the three different NLCs . ....	55
3.3	II-A curves comparing films of NLCs prepared with A) Compritol 888 ATO, B) Gelucire 43/01, and C) cetyl palmitate as solid lipid and Tween 80; Span 20 as a surfactant when spread at 35 °C and then decreased to 20 °C. D) A direct comparison between the first isocycles of the three different NLCs .....	56



## LIST OF FIGURES (CONT.)

Figure	Page
<p>3.4 <math>\Pi</math>-A curves comparing films of NLCs prepared with A) Compritol 888 ATO, B) Gelucire 43/01, and C) cetyl palmitate as solid lipid and Gelucire 44/14 as a surfactant when spread at 35 °C and then decreased to 20 °C. D) A direct comparison between the first isocycles of the three different NLCs. ....</p>	57
<p>3.5 Typical <math>\Pi</math>-A curves of A) Fluoromeibum at 35 °C and B) Fluoromeibum at 20 °C before adding the NLCs. Note that at the lower temperature <math>\Pi_{\max}</math> was much higher and hysteresis greater. ....</p>	59
<p>3.6 <math>\Pi</math>-A curves comparing films of meibomian lipids mixed with A) NLC1, B) NLC2, and C) NLC3 when spread at 35 °C (red line; 1<sup>st</sup> isocycle and yellow line; 10<sup>th</sup> isocycles) and then decreased to 20 °C ( black line; 1<sup>st</sup> isocycle and blue line; 10<sup>th</sup> isocycles). ....</p>	60
<p>3.7 Micrographs comparing the appearances of meibomian lipids mixed with A) NLC1, B) NLC2, and C) NLC3 during 1<sup>st</sup> and 10<sup>th</sup> isocycles at 20 °C, respectively. The surface pressure during compression of the film and the isocycle is given, e.g. 8 iso 1 means that the pressure was 8 mN/m during compression in isocycle 1.....</p>	60
<p>3.8 <math>\Pi</math>-time curve of a fluoromeibum film with <math>\Pi_{\text{init}}</math> set to 20 mN/m at 20 °C, a further 6 <math>\mu</math>L of NR-NLCs added to the subphase (arrow), showed that NR-NLCs was able to still penetrate the film. ....</p>	62

## LIST OF FIGURES (CONT.)

Figure	Page	
3.9	Π-A curves of NR-NLCs penetrated to predeposited meibomian lipids at 20 °C (red line). The 10 <sup>th</sup> isocycles of Fluoromeibum alone at 20 °C are also shown (black line). Micrographs of the appearances of meibomian lipids mixed with NR-NLCs during 1, 3, and 4 isocycles are represented. The curve with NR-NLCs is shifted to the right by the barriers were closed to 30cm <sup>2</sup> . .....	62
3.10	SEM micrograph of NR-NLCs penetrated to fluoromeibum at 20 °C. ....	63
4.1	The fluorescence images of the rabbit preocular surface at 1, 5, 15, 30, and 60 min after administration of A) flu-NLCs and B) flu-NSS obtained with custom-built slit-lamp microscopy attached with a Nikon D5300 DSLR for digital photography (n=5).....	81
4.2	The fluorescence intensity (%) of fluorescence images of the rabbit preocular surface after instillation of flu-NLC compared with flu-NSS at various time points analyzed by ImageJ software (n = 5; mean ± SD). Student <i>t</i> test between flu-NLC and flu-NSS: * = <i>p</i> < 0.05.....	82

## LIST OF FIGURES (CONT.)

Figure	Page
<p>4.3 The absorbance of MB per mg.protein of rabbit cornea tissue in different conditions; closed eye (negative control), open eye (positive control), treated with commercial artificial tear (AT), and treated with a NLCs eye drop (NLCs) (n = 3; mean ± SD). Statistically significant differences were determined by one-way ANOVA, Turkey multiple comparison test; * = <math>p &lt; 0.05</math> compared with negative control; ** = <math>p &lt; 0.05</math> compared with positive control; *** = <math>p &lt; 0.1</math> compared with commercial artificial tears.....</p>	83
<p>5.1 Schematic illustration of multiple type Nile red-loaded nanostructured lipid carriers (NR-NLCs). .....</p>	101
<p>5.2 TEM micrographs of (A) NR-NLC-150, (B) NR-NLC-40, (C) NR-NLC-PEG, and (D) NR-NLC-SA. ....</p>	103
<p>5.3 The transcorneal fluorescence (red line) and scatter (blue line) scans obtained after topical NR-CO at (A) 4 h, (B) 6 h, and (C) 8 h. Data shown are typical results after 3 independent trials.....</p>	105
<p>5.4 The transcorneal fluorescence (red line) and scatter (blue line) scans obtained after topical NR-NSS at (A) 4 h and (B) 8 h. Data shown are typical results after 3 independent trials.....</p>	106
<p>5.5 The transcorneal fluorescence (red line) and scatter (blue line) scans obtained after topical NR-NLC-40 at (A) 4 h, (B) 6 h, and (C) 8 h. Data shown are typical results after 3 independent trials. ....</p>	107
<p>5.6 The transcorneal fluorescence (red line) and scatter (blue line) scans obtained after topical (A) NR-NLC-40 and (B) NR-NLC-150 at 4 h. Data shown are the typical result after 3 independent trials. ....</p>	108

## LIST OF FIGURES (CONT.)


Figure	Page
5.7 The transcorneal fluorescence (red line) and scatter (blue line) scans obtained after topical (A) NR-NLC-40, (B) NR-NLC-PEG, and (C) NR-NLC-SA at 4 h. Data shown are the typical result after 3 independent trials. ....	110
5.8 Fluorescence images of vertical slices of the cornea surface after instillation of different NR-NLCs compared with NR-NSS at 5, 15, 60, and 360 min. Magnification $\times 20$ . ....	112
5.9 The fluorescence intensity (%) of fluorescence images of the cornea tissue after instillation of different NR-NLCs compared with NR-NSS at 5, 15, 60, and 360 min analyzed by ImageJ software. Statistically significant differences were determined by one-way ANOVA, Turkey multiple comparison test; <sup>a</sup> $p < 0.05$ compared with NR-NSS; <sup>b</sup> $p < 0.05$ compared with NR-NLC-40; <sup>c</sup> $p < 0.05$ compared with NR-NLC-PEG. ....	113
5.10 Cell uptake of NR-NLC-40, NR-NLC-PEG, and NR-NLC-SA in PCE cells analyzed by flow cytometry. Histogram for different samples corresponds to the mean NR fluorescence intensity (%). Statistically significant differences were determined by one-way ANOVA, Turkey multiple comparison test; <sup>a</sup> $p < 0.05$ compared with NR-NLC-40; <sup>b</sup> $p < 0.05$ compared with NR-NLC-PEG. ....	114
6.1 TEM micrographs of (A) IND-NLC2 and (B) IND-NLC2-PEG	134
6.2 <i>In vitro</i> release profiles of IND from IND-NLC1, IND-NLC2, and IND-NLC2-PEG in NSS with 0.6% (w/v) Tween 80 at 34°C. Error bars represent standard deviation for $n=3$ . ....	135

## LIST OF FIGURES (CONT.)

Figure	Page
6.3 The percentage of IND remaining on porcine cornea tissue after a steady flow of NSS for 60 min. Error bars represent standard deviation for n=3.....	136




## ABBREVIATIONS




$\alpha$	=	alpha
$\beta$	=	beta
$\gamma$	=	gamma
$\delta$	=	delta
$\epsilon$	=	dielectric constant
$\zeta$	=	zeta potential
$U_E$	=	electrophoretic mobility
$\eta$	=	viscosity of the medium
$^{\circ}\text{C}$	=	degree celsius
$\mu\text{g}$	=	microgram
$\mu\text{L}$	=	microliter
$\mu\text{M}$	=	micrometer
ANOVA	=	analysis of variance
AT	=	artificial tear
BAB	=	blood-brain barrier
$\text{cm}^2$	=	square centimeter
Cont.	=	continued
Cps	=	centipoise
CSMF	=	confocal scanning microfluorometer
CSLM	=	custom-built slit-lamp microscopy
CsA	=	cyclosporin A
DED	=	dry eye disease
DI water	=	deionized water
DLS	=	dynamic light scattering
EE	=	entrapment efficiency
EFA	=	essential fatty acids
FDA	=	food and drug administration
HCl	=	hydrochloride
$\text{HO}_2^{\cdot}$	=	hydroperoxyl radical
HPH	=	high pressure homogenization

## ABBREVIATIONS (CONT.)



HPLC	=	high pressure liquid chromatography
IND	=	indomethacin
IND-NLCs	=	indomethacin loaded nanostructured lipid carriers
kDa	=	kilodaltons
LFU	=	lacrimal functional unit
MAPK	=	mitogen-activated protein kinase
MB	=	methylene blue
MCT	=	medium chain triglyceride
MDR1	=	multi-drug resistance gene
mg	=	milligram
MGD	=	meibomian gland dysfunction
min	=	minute
mOsm	=	milliosmole
ml	=	milliliter
mM	=	millimolar
MMP9	=	metalloproteinases
mN	=	millinewtons
MTT	=	methyl thiazol diphenyl-tetrazolium bromide
mV	=	millivolt
MW	=	molecular weight
nm	=	nanometer
NGF	=	nerve growth factor
NLCs	=	nanostructured lipid carriers
NR-NLCs	=	nile red loaded nanostructured lipid carriers
NR	=	nile red
NSS	=	normal saline solution
O <sub>2</sub>	=	oxygen
O/F/W	=	oil-in-fat-in-water
p38 MAPK	=	mitogen-activated protein kinase p38
PCE	=	porcine corneal epithelial

## ABBREVIATIONS (CONT.)



PEG	=	polyethylene glycol
PEG400	=	polyethylene glycol 400
PGE <sub>3</sub>	=	prostaglandin E <sub>3</sub>
P-gp	=	P-glycoprotein
pH	=	power of hydrogen ion concentration
PI	=	polydispersity index
q.s.	=	quantity sufficient
RH	=	relative humidity
RPE	=	retinal pigment epithelium
rpm	=	revolutions per minute
RT	=	room temperature
SD	=	standard deviation
SEM	=	scanning electron microscopy
STE	=	short time exposure
TBUT	=	tear break-up time
TEM	=	transmission electron microscopy
TFL	=	tear film lipid layer
T80	=	tween 80
USA	=	united states of america
UV	=	ultraviolet
UV-Vis	=	ultraviolet-visible
v/v	=	volume by volume
w/w	=	weight by weight
ZP	=	zeta potential



# CHAPTER I

## INTRODUCTION

This chapter contains the rationale of the study along with specific objectives, expected outputs, and expected clinical outcomes of the study.

### **The rationale for the study**

Dry eye is a disease of the tear film and ocular surface. It involves hyperosmolarity of the tears and instability of the tear film [1, 2]. Age, female sex, hormonal imbalance, autoimmune diseases, abnormal corneal innervation, vitamin A deficiency, environmental stress, contact lens, infections, topical drugs and ophthalmic surgery are the well-known risk factors for the development of dry eye disease (DED) [3, 4]. It is estimated that almost 5 million Americans, 50 years and older, have DED [1]. Moreover, nearly 30 million Americans suffer from the less severe form of DED, and approximately two-thirds are women [1, 5]. The progression of DED may lead to corneal ulceration when left untreated [6].

The tear film is a liquid layer covering the cornea and conjunctiva. It forms a barrier between the eye and environment. The outermost layer of the tear film is coated by lipids, well-known as a tear film lipid layer (TFLL), which has meibum as the significant component [7]. This TFLL is responsible for reducing the surface tension of the tear film and increasing the tear film stability that related to dry eye disease (DED). It has been hypothesized that abnormal secretion of meibum or changing of the meibum composition can cause tear film instability that causes evaporative dry eye [1, 5]. In general, artificial tears drops are widely used to relieve signs and symptoms of DED [8]. However, the efficacy of the drop is transient, and the drop requires frequent application as the instilled drops are drained rapidly with the continuous tear secretion and blinking [9]. This puts a burden on the patient and diminishes patient compliance.

These drawbacks of artificial tears have led to the development of novel lipid-based nanocarriers for significant enhancement in tear film stability and increase the residence time of the drop on the ocular surface [8, 10, 11]. Among the new lipid-based nanocarriers, NLCs possess significant advantages [12]. NLCs are made from physiological lipids, and hence they are biodegradable, biocompatible, and do not cause any acute and chronic toxicity to the eye [12, 13, 14]. In addition, they possess high drug loading capacity, long-term physical stability, and potential for controlled drug release and drug targeting. NLCs also protect the encapsulated drug against chemical degradation in storage. Finally, it exhibits high mucoadhesiveness [13, 15].

The primary goal of this study is to develop NLCs eye drop as tear replacement formulation in order to resemble natural tears and replenish the tear film. In addition, these NLCs formulations designed to be a solution of the short residence time and poor drug penetration of topical eye drop.

#### **Objectives of the study**

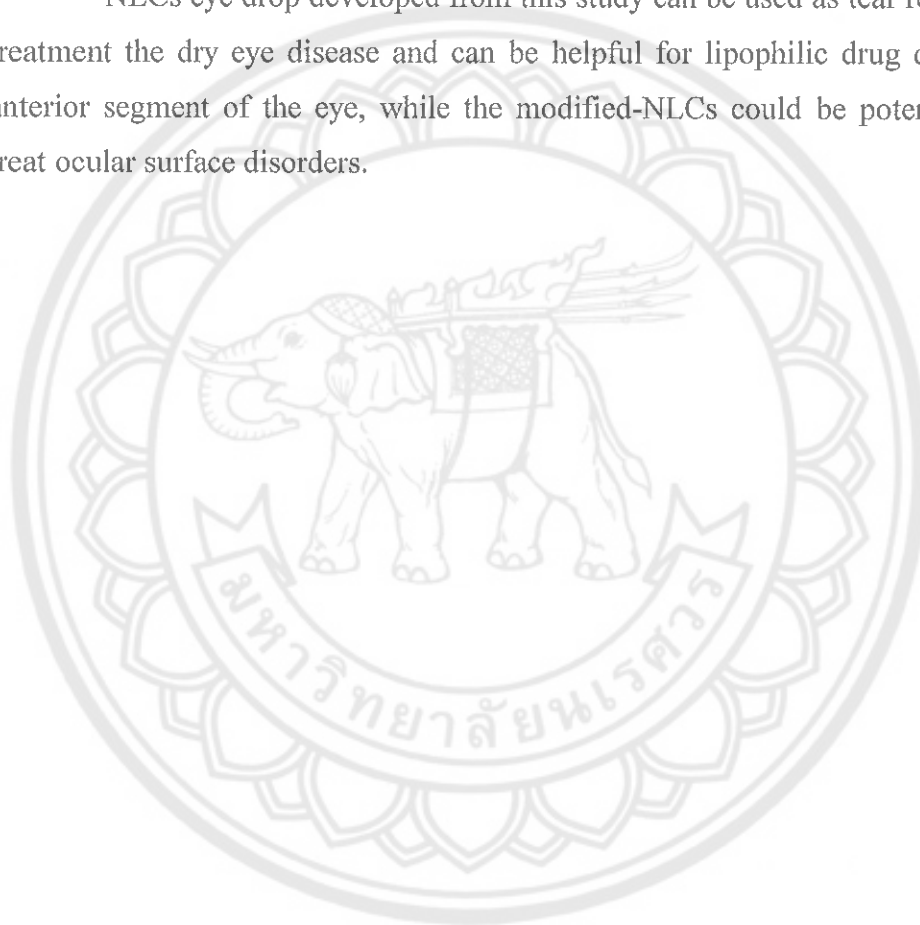
1. To develop and characterize the NLCs eye drop like a tear replacement
2. To investigate the surface activity of NLCs eye drop and interaction of NLCs eye drop with human meibum
3. To evaluate the efficacies of NLCs eye drop in order to improve the stability of tear film and decrease the ocular surface epithelial cells damaged from desiccation condition in a rabbit model.
4. To develop and characterize of Nile Red-loaded NLCs (NR-NLCs) and Indomethacin-loaded NLCs (IND- NLCs)
5. To assess the toxicity of NLCs eye drop in porcine corneal epithelial (PCE) cells
6. To evaluate the mucoadhesiveness of Nile Red-loaded NLCs (NR-NLCs) and Indomethacin-loaded NLCs (IND- NLCs)
7. To evaluate transcorneal permeation of NR-NLCs across porcine eye *ex vivo*

**Expected outputs of the study**

NLCs eye drop could be successfully developed with the potentially resemble natural tears and replenish the tear film to serve as tear replacement. In addition, the developed NLCs can be useful for topical ocular drug delivery system with enhanced transcorneal penetration and mucoadhesion.

**Expected outcomes of the study**

NLCs eye drop developed from this study can be used as tear replacement for treatment the dry eye disease and can be helpful for lipophilic drug delivery to the anterior segment of the eye, while the modified-NLCs could be potentially used to treat ocular surface disorders.





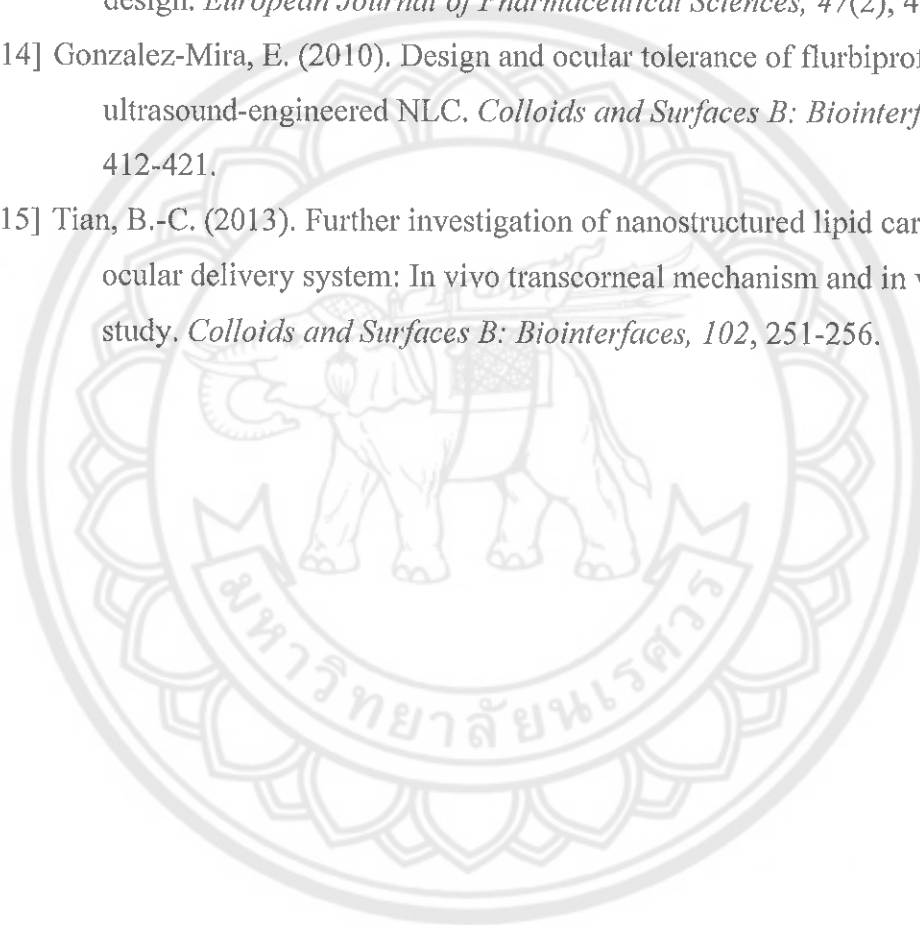
**REFERENCES**

## REFERENCES

- [1] Stevenson, W., S.K. Chauhan, & R. Dana. (2012). Dry eye disease: An immune-mediated ocular surface disorder. *Arch Ophthalmol*, 130(1), 90-100.
- [2] Stern, M.E., & S.C. Pflugfelder. (2004). Inflammation in dry eye. *Ocul Surf*, 2(2), 124-130.
- [3] Pflugfelder, S.C. (2003). Anti-inflammatory therapy of dry eye. *Ocul Surf*, 1(1), 31-36.
- [4] Wander, A.H., & B.H. Koffler. (2009). Extending the duration of tear film protection in dry eye syndrome: review and retrospective case series study of the hydroxypropyl cellulose ophthalmic insert. *Clinical Practice*, 7(3), 154-162.
- [5] Barabino, S. (2012). Ocular surface immunity: Homeostatic mechanisms and their disruption in dry eye disease. *Progress in Retinal and Eye Research*, 31(3), 271-285.
- [6] Aksungur, P., Demirbilek, M., Denkbay, E.B., Vandervoort, J., Ludwig, A., & Unlü, N. (2011). Development and characterization of Cyclosporine A loaded nanoparticles for ocular drug delivery: Cellular toxicity, uptake, and kinetic studies. *Journal of Controlled Release*, 151(3), 286-294.
- [7] Cwiklik, L. (2016). Tear film lipid layer: A molecular level view. *Biochimica et Biophysica Acta (BBA) - Biomembranes*, 1858(10), 2421-2430.
- [8] Vicario-de-la-Torre, M. (2018). Novel Nano-Liposome Formulation for Dry Eyes with Components Similar to the Preocular Tear Film. *Polymers*, 10(4), 425.
- [9] Gan, L., Wang, J., Jiang, M., Bartlett, H., Ouyang, D., Eperjesi, F., Liu, J., & Gan, Y. (2013). *Recent advances in topical ophthalmic drug delivery with lipid-based nanocarriers*. N.P.: n.p.
- [10] Gan, L., Wang, J., Jiang, M., Bartlett, H., Ouyang, D., Eperjesi, F., Liu, J., & Gan, Y. (2013). Recent advances in topical ophthalmic drug delivery with lipid-based nanocarriers. *Drug Discovery Today*, 18(5-6), 290-297.
- [11] Acar, D., Molina-Martínez, I.T., Gómez-Ballesteros, M., Guzmán-Navarro, M., Benítez-Del-Castillo, J.M., & Herrero-Vanrell, R. (2018). Novel liposome-

based and in situ gelling artificial tear formulation for dry eye disease treatment. *Contact Lens and Anterior Eye*, 41(1), 93-96.

- [12] Araújo, J., Gonzalez, E., Egea, M.A., Garcia, M.L., & Souto, E.B. (2009). Nanomedicines for ocular NSAIDs: safety on drug delivery. *Nanomedicine: Nanotechnology, Biology and Medicine*, 5(4), 394-401.
- [13] Hao, J. (2012). Development and optimization of baicalin-loaded solid lipid nanoparticles prepared by coacervation method using central composite design. *European Journal of Pharmaceutical Sciences*, 47(2), 497-505.
- [14] Gonzalez-Mira, E. (2010). Design and ocular tolerance of flurbiprofen loaded ultrasound-engineered NLC. *Colloids and Surfaces B: Biointerfaces*, 81(2), 412-421.
- [15] Tian, B.-C. (2013). Further investigation of nanostructured lipid carriers as an ocular delivery system: In vivo transcorneal mechanism and in vitro release study. *Colloids and Surfaces B: Biointerfaces*, 102, 251-256.



## CHAPTER II

### LITERATURE REVIEW

#### **Dry eye disease**

Dry eye is a disease of the tears and ocular surface involving tear hyperosmolarity and tear film instability that results in symptoms of discomfort, visual disturbance, eye dryness, irritation, foreign body sensation and potential damage to the ocular surface [1, 2]. Age, female sex, hormonal imbalance, autoimmune diseases, abnormal corneal innervation, vitamin A deficiency, environmental stress, contact lens, infections, topical drugs and ophthalmic surgery are the well-known risk factors for the development of dry eye disease (DED) [3, 4]. It is estimated that almost 5 million Americans, 50 years and older, have DED [1]. Moreover, nearly 30 million Americans suffer from the less severe form of DED and approximately two - thirds are women [1, 5]. The progression of DED may lead to corneal ulceration when left untreated [6].

As mentioned above, tear hyperosmolarity and tear film instability are core mechanisms of DED. Then, the interaction of various etiologies with these core mechanism are summarized in Figure 2.1 [7]. Tear hyperosmolarity is regarded as the central mechanism causing ocular surface inflammation, damage, and symptoms, and the initiation of compensatory events in dry eye. It is a result of water evaporation from the exposed ocular surface by excessive evaporation or/and a low aqueous tear flow. Hyperosmolarity stimulates a cascade of inflammatory events in the epithelial surface cells, involving mitogen-activated protein (MAP) kinases and nuclear factor (NF)- $\kappa$ B signaling pathways and produce of a variety of proinflammatory cytokines such as interleukin (IL) 1, IL-6, tumor necrosis factor (TNF) and matrix metalloproteinases (MMP9). In addition, desiccating stress can initiates ocular surface epithelial cells to release proinflammatory cytokines and chemokines [1, 7].

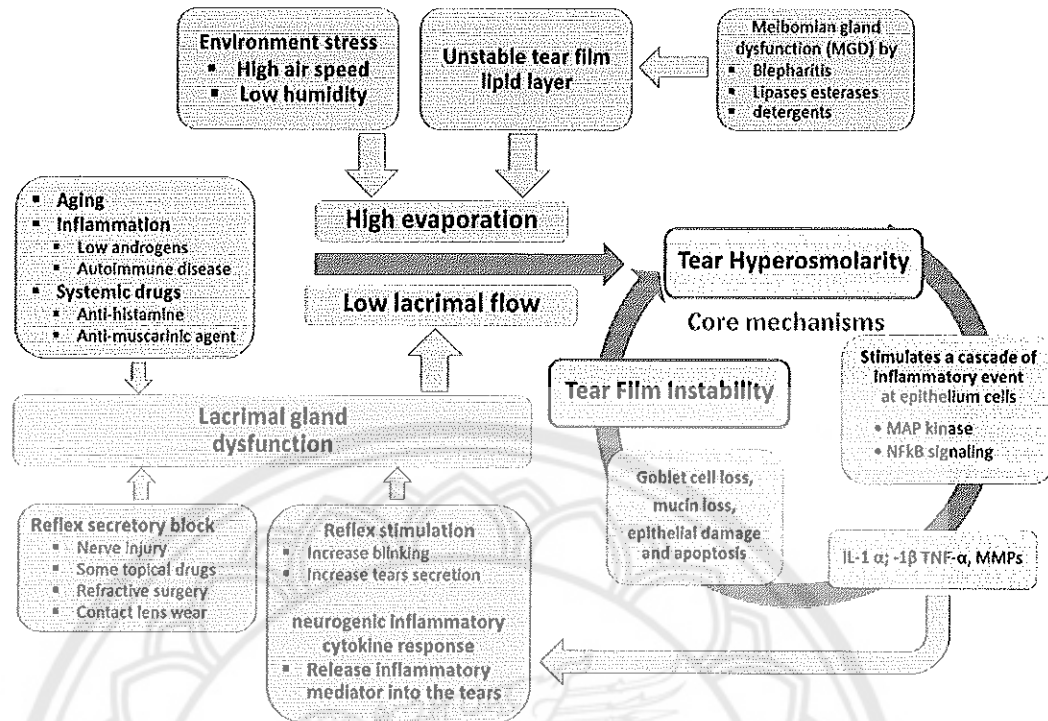


Figure 2.1 Mechanism of dry eye [7]

Source: Modified from the report of the International Dry Eye WorkShop (DEWS), 2007

The immunoinflammatory pathway can be described in Figure 2.2. These inflammatory events resulting in epithelial damage involves cell death by apoptosis, a loss of goblet cells, and disturbance of mucin expression, leading to tear film stability. Moreover, the epithelial injury caused by dry eye stimulates corneal nerve endings, leading to symptoms of discomfort, increased blinking, and potentially compensatory reflex lacrimal tear secretion. However, tear film instability can be initiated, without the prior occurrence of tear hyperosmolarity, by several etiologies, including xerophthalmia, ocular allergy, topical preservative use, and contact lens wear.

The major causes of tear hyperosmolarity are reduced aqueous tear flow, resulting from lacrimal failure, and/or high evaporation from the tear film. Increased evaporation loss is favored by environmental conditions of low humidity and high air flow. In addition, meibomian gland dysfunction (MGD) leads to an unstable tear film lipid layer. The factors that can be reduced aqueous tear flow include aging, low



androgens levels, and systemic drugs. Tear delivery may be obstructed by reflex secretory block that resulting from refractive surgery, contact lens wear and chronic abuse of topical anesthetics.

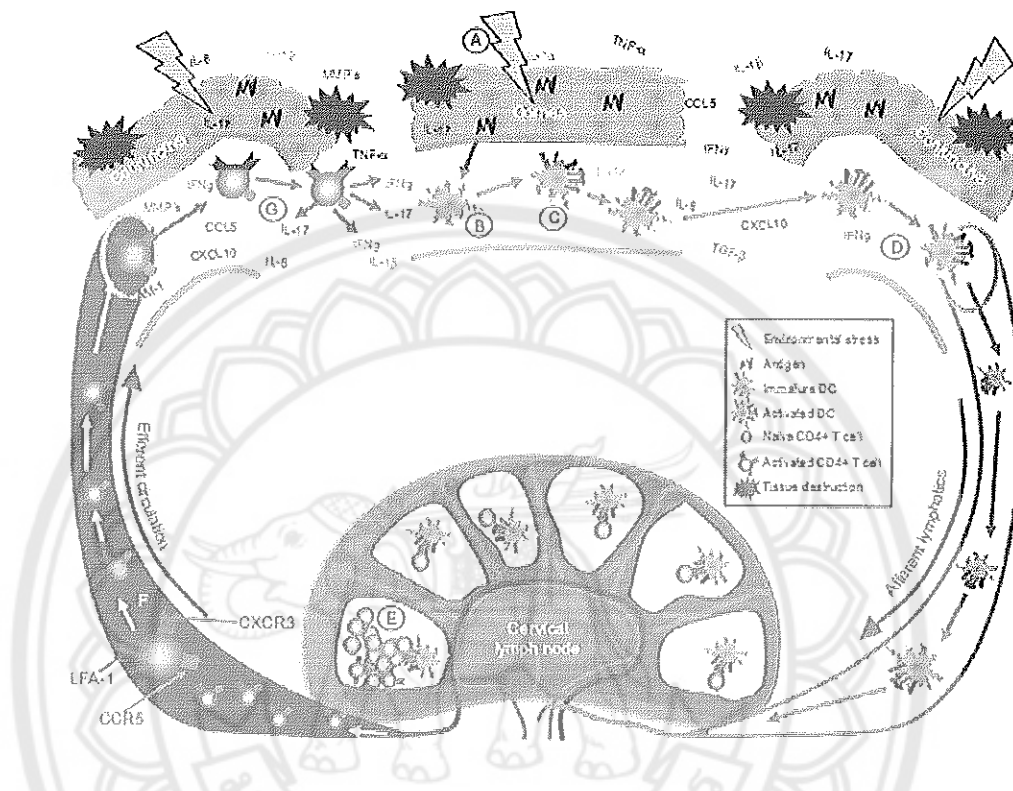


**Figure 2.2 Autoimmune cycle of chronic inflammation during the immunopathogenesis of dry eye disease [1]. (a) An environmental stimulus initiates acute inflammation on the ocular surface stimulating upregulation of proinflammatory cytokines (e.g., TNF- , IL-1 and IL-1 ), matrix metalloproteinases (MMPs), adhesion molecules (e.g., ICAM-1), and chemokines (e.g.,CCL5 and CXCL10) within the conjunctival and corneal epithelium that act in concert to perpetuate the immune response; (b) Antigenpresenting cells (e.g., dendritic cells) process autoantigen and (c) following activation, (d) traffic to the draining cervical lymph nodes (CLNs) via the afferent lymphatics, where they (e) present antigen to autoreactive CD4<sup>+</sup> T cells. Efferent arm of**

**the immune response:(f) Activated CD4<sup>+</sup> T cells bearing specific adhesion molecules and chemokine receptors (e.g., CCR5 and CXCR3) migratespecifically to the ocular surface tissues (conjunctiva and cornea are shown), including the meibomian and lacrimal glands where theyinfiltrate the tissue and (g) release proinflammatory cytokines (IFN- and IL-17) that promote chronic inflammation and tissue destruction [1]**

### Anatomy of eye

The human eye is a slightly asymmetrical globe, about an inch in diameter. It can be divided into the anterior and the posterior segments [8]. The anterior segments include the iris, cornea, pupil, sclera, ciliary body, lens and conjunctiva. The posterior segments comprise the choroid, retina, macular and vitreous humor. Behind the eye, the optic nerve carries electrical impulses to the brain (Figure 2.3).

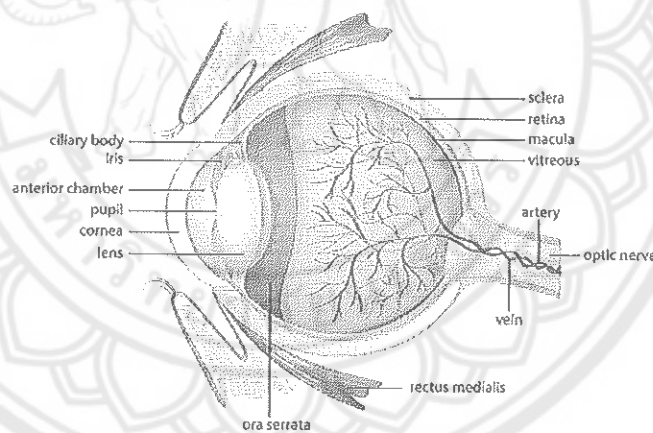


**Figure 2.3 The human eye**

**Source:** <http://www.wisegeek.com/what-is-the-cornea.htm>

The lacrimal functional unit (LFU) includes the lacrimal glands, ocular surface (cornea and conjunctiva), eyelids, meibomian glands, and associated sensory and motor nerves. These unique physiologies constrains such as the blinking reflex, lachrymal secretion, and nasolacrimal drainage that are the barriers to remove the drug

from the ocular surface for topical administration. The short residence time (only a few minutes) for drug absorption leading to ocular bioavailability is very low (less than 5%).

### **Human tears**

Under normal condition, the volume of tear fluid is around 5 – 10  $\mu\text{L}$  and the secretion rate is about 1.2  $\mu\text{L}/\text{min}$ , with a turnover rate of approximately 16% per minute [9]. The tears can be divided into three type including basal, reflex, and crying tears. The basal tears are secreted by accessory lacrimal gland and distributed cover the cornea by blinking of the eye lid while the reflex tear is secreted by main lacrimal gland. The reflex tear is resulted from the corneal or blink reflex which occurs at a rapid rate as 0.1 s. The corneal or blink reflex is an automatic blinking of the eyelid elicited by the stimulation of the cornea such as touching, foreign body, and foreign particle. The blink reflex is a true reflex, with a sensory afferent limb, intervening synapses, and a motor efferent. The afferent limb of the blink reflex is mediated by sensory fiber of the supraorbital branch of the ophthalmic division of the trigeminal nerve (cranial nerve V1) and the efferent limb by motor fibers of the facial nerve (cranial nerve VII). Just as with the corneal reflex, ipsilateral electrical stimulation of the supraorbital branch of the trigeminal nerve elicits a facial nerve (eye blink) response bilaterally. Stimulation of the ipsilateral supraorbital nerve results in an afferent volley along the trigeminal nerve to both the main sensory nucleus of V (mid-pons) and the nucleus of the spinal tract of V (lower pons and medulla) in the brainstem [10].

Although small in volume, the human tear fluid is an extremely complex biological mixture containing proteins/peptides, electrolytes, lipids, mucin, and small molecule metabolites. The sources for the tears include the main and accessory lacrimal glands, ocular surface epithelial cells, Meibomian glands, goblet cells, and an ultrafiltrate of blood all contribute to the composition of the tear fluid. Thus, an extensive literature exists reporting various substances (inflammatory mediators, cytokines, growth factors, invading white cells, remodelling enzymes, mucin, and complement component) that have been detected in tears in various disorders [9, 11].

An increase in tear osmolarity is a hallmark of dry eye disease and it thought to be the central mechanism in the pathogenesis of ocular surface damage in the disease, as noted in the Dry Eye Workshop Report [12]. It is suggested that osmolarity values of 296 - 302 mOsms/L are the normal patients and range of values from 300 - 360 mOsms/L or higher are indicative of moderate to severe dry eye. Clinical cutoffs for the diagnosis of dry eye vary based on the study and the severity of dry eye, but most fit within the range of 305 - 318 mOsms/L [13].

### The tear film

The tear film is a thin layer of an extracellular fluid that covers the underlying cornea and conjunctiva and forming the anterior component of the ocular surface. The role and function of the tear film has been extensively reviewed. Briefly, this film is of particular importance to the cornea because unlike other tissues, the cornea lacks a vascular system and therefore, the tear film serves as a source for nutrients, oxygen, growth factors, immune and antimicrobial proteins, and cells of the immune system.

#### 1. Structure of the tear film

Generally, the tear film is composed of three layers: the outermost lipid layer, the middle aqueous layer, and the innermost mucus layer (Figure 2.4). Each layer contains various macromolecules that have specific role and assist in maintaining ocular health and function of the eye.

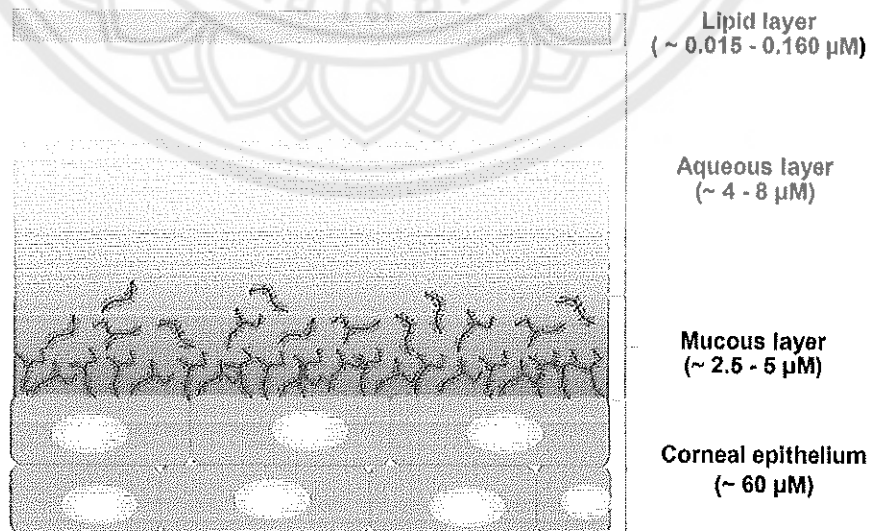


**Figure 2.4 Model of tear film**

## 2. Lipid layer

The lipid layer is the outermost layer that consists of polar and non-polar lipid which produced by meibomian gland in the eye. These meibomian glands are lined in the parallel to each other in the upper and lower tarsal plates, perpendicular to the lid margins [14]. As showed in Figure 2.5, the lipid layer can be divided into two phase, a polar and non-polar phase [15]. The non-polar lipid, which is closest to the external environment, is composed of phospholipids such as phosphatidylcholine, phosphatidylethanolamine and sphingosine, and makes up less than 10% of lipid layer. In contrast, the non-polar lipid, which is located closest to the aqueous layer and forms the major component of the lipid layer, is composed of cholesterol, cholesterol ester, mono-di-triglyceride and hydrocarbon. This layer is approximately  $0.015 - 0.160 \mu\text{M}$  thick that serves as a protective barrier for both the eye and the tear film from foreign contaminants. In addition, it provides stability for the tear film as it prevents the evaporation of tears when eyelids are opened, as well as maintaining a smooth tear film for the refraction of incoming light. Lastly, the lipid layer acts as a lubricant which assists in eyelid movement during the process of blinking.

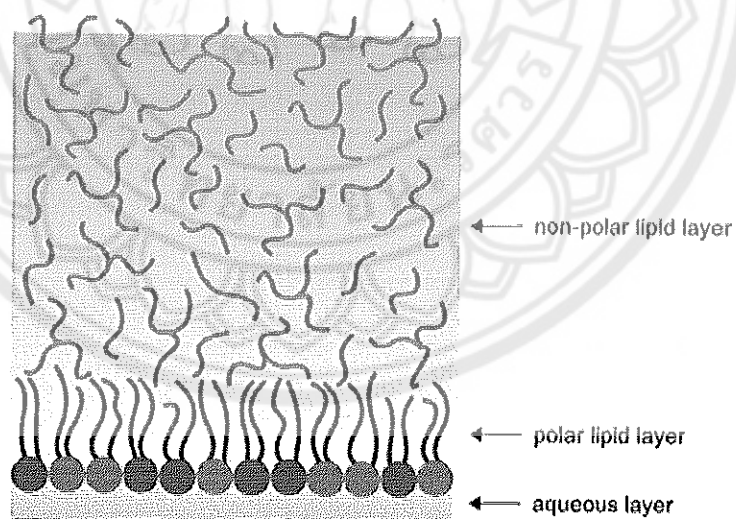


**Figure 2.5 Scheme of the TFL structure [15]**

### 3. Aqueous layer

The aqueous layer is the middle layer that produced by the lacrimal gland in the eye. The aqueous layer makes up the bulk of the tear film, with a thickness of about 4 - 8  $\mu\text{M}$  and is composed of water and various water-soluble proteins, vitamins, cytokines, immunoglobulins, hormones, electrolytes and metabolites [11]. The various electrolytes present in the aqueous layer include sodium, potassium, calcium, magnesium, bicarbonates, chloride, and phosphate ions. These electrolytes regulate tear osmolality, as well as acting as a buffer to maintain the physiological pH of tears. In addition, more than 400 proteins have been identified in human tear fluid. These different proteins and antimicrobial agents in the aqueous layer are largely responsible for the prevention of viral and bacterial infections in the eye. Amongst the large class of proteins, lysozyme, lactoferrin, lipocalin and secretory immunoglobulin A are found to be the most abundant in tears, and are all commonly involved in antibacterial activities [16].

### 4. Mucous layer

The mucin innermost layer is 2.5 - 5.0  $\mu\text{M}$  thick that contains immunoglobulins, enzymes, urea, salts, and glucose. Mucins are secreted from conjunctival goblet cells, which form the mucous layer to maintain a wettable of corneal surface. Mucins are large glycoproteins with molecular weights ranging from  $3 \times 10^5 - 4 \times 10^7$  kDa and are classified as transmembrane or secretory mucins. Transmembrane mucins form a protective barrier against pathogens at cell-tear film interface, whereas secretory mucins move within the tear film. This layer can be lubricating the palpebral conjunctiva leading to smooth movement of the eyelid during blinking. Mucin is the most effective of a number of different proteins found in tears at lowering the surface tension of an aqueous surface that enable the tear film to spread properly over the eye. The researchers suggested that mucin have a direct and active role in the TFL, and more broadly in the tear film in terms of their relationship with lipids [17].

### 5. Tear film dynamics

Tear film is not a static system because of three key process: tear flow, tear evaporation, and blinking [15]. While the dynamic associated with tear flow and evaporation can lead to a stationary process, the blinking is a source of significant

non-regular disturbances of the tear film. The lipids, which have a melting point range 19 - 32°C, are squeezed out from the meibomian gland orifices located in the lid margin as pressure is put on the tarsal plates during blinking [18]. Tear film thinning after blinks is usually attributed to evaporation of water from the aqueous subphase. On the other hand, during deterioration of the tear film after blinks, variations of diffraction patterns occur clearly pointing to alterations of TFL structure. Nevertheless, one can expect that the most important dynamic processes regarding TFL occur due to action of eyelids. Namely, it is presumable that the eyelids both laterally compress/decompress the lipids and interact with the lipid layer from the top. It has been noted that the details of the eyelids action on TFL are not fully understood. It is usually assumed that eyelids either slide atop of the lipid film which acts as a lubricant or that the eyelids remove the film by compression and hence the film has to be completely re-spread upon eyelid opening. Although, the dynamic of these processes are not well understood as they are relatively difficult to address experimentally. Some insight can be gained from Langmuir balance experiments with lateral compression-decompression cycling [17].

The time of eyelid down- and up-movement in a spontaneous blink is approximately 100 ms and 250 ms, respectively. After each blink, the tear film must be at least partially re-spread at the surface of cornea. This process is characterized by a complex and not fully understood dynamics. Such factors as osmolality, gravitational forces, and evaporation were demonstrated to play a significant role during tear film spreading and the methods of fluid dynamics are typically applied for description of these phenomena [19]. Following each blink, the tear film moves upward over the corneal surface with a decaying velocity, and stabilizes after approximately 1 s [20]. Regarding lipids, their movement and TFL reconstruction is relatively fast and is assumed to be driven by Marangoni effect due to a concentration gradient of polar lipid [20]. After some period of time, so-called tear film tear break-up time (TBUT), the film deteriorates, thins, and breaks. TBUT in humans is typically in the range of seconds, up to one minute; although in the dry eye disease it can be reduced to few seconds or the break-up can even occur instantaneously after a blink [21, 22]. The break-up can be macroscopically observed in a form of specific patterns, e.g., dots or streaks, occurring at the surface of cornea. Note however, that the macroscopic-level

break-up of the tear film must be preceded and then accompanied by structural changes at the molecular level.

#### **6. The correlation between the TFLL and dry eye disease**

As previously mentioned, TFLL is the most outward part of the tear film, residing at the very eye-air interface. Functions of the lipid layer include providing a smooth optical surface for the cornea, enhancing the stability of the tear film, enhancing the spreading of the tear film, preventing spillover of tears from the lid margin, preventing contamination of the tear film by sebum, and sealing the apposed lid margins during sleep [23]. Its main function is to reduce surface tension of the tear film and plays a big role in tear film stability. This surface tension is reduced to approximately two-thirds of that of water which stabilizes the tear film at the cornea surface that could be retard water evaporation. Studies suggest that normally, much of the tear film lipid layer is a structure that remains stable over a series of blinks, folding concertina-like, as it approaches the lower lid margin in the down-phase of the blink and unfolding in the up-phase, with little mixing of lipid within the lipid layer or between the lipid layer and the reservoirs [24]. When this dynamic stability of the tear film is disturbed there is functional disturbance such as variability of functional visual acuity and increased optical aberration [15].

There is some evidence that evaporation is affected by lipid layer thickness, but it is currently not known specifically how lipid composition alters either the stability or thickness of the lipid layer, despite the fact that thicker TFLL correlates with better tear stability [18]. It has been proposed, though, that the polar lipids act as a surfactant that helps spread the nonpolar lipids over the aqueous component of the tear film, provide a barrier between the two layers, and provide a structure that supports the nonpolar phase, which is responsible for creating a seal that decreases evaporation from the tear film [23].

The most common cause of increased evaporation from the eye is meibomian gland dysfunction (MGD), which leads to a reduced delivery of oil to the lid margin and to the tear film. MGD is a chronic disease that is characterized by blockage of, or changes in, meibomian secretions. Obstructive MGD has been described as having an unstable tear film, increased evaporation, gland drop out, viscous lipid, and low lipid volume, causing dry eye [25]. Hence, the lipid layer is



considered an important component in the tear film in maintaining the tear film intact over the anterior surface of the eye.

### **7. Surface tension and surface activity of the TFLL**

The functions of the TFLL are underpinned by physicochemical properties such as surface tension that allow the TFLL to spread over the aqueous phase and to maintain its structural integrity under enormous stresses of a blink cycle [21, 26]. Surface tension involves various aspects of the tear film, both at the air-liquid interface and the corneal epithelium. The wettability of solid surfaces such as the corneal epithelium is dictated by surface tension i.e. the tear film is able to lubricate the ocular surface because its surface tension is lower than that of the corneal epithelium. Surface tension is also responsible for the thickness of the tear film and the distribution of tears between compartments [26]. It has been suggested that a low surface tension in tears is important for tear film stability [27]. As mentioned above, the dynamic of TFLL spread are not well understood as they relatively difficult to address experimentally. Thus, some insight can be gain from Langmuir balance experiments with lateral compression-decompression cycling [17].

Analysis of surface pressure/tension in tears have been measured through the contact angle method, capillary tube measurement or a Langmuir film balance, which comprises a Langmuir trough with moveable barriers and a Wilhelmy plate for monitoring pressure changes [28, 29, 30]. A Langmuir trough with moveable barriers (Figure 2.6) possesses the suitable method to assess the movement of lipids and proteins onto the surface, removal from the surface at different surface pressures, the elastic properties of meibomian lipid films and the effects of repeated compression, or the expansion cycles on films in response to various lipids or proteins. Thin lipid films spread on an aqueous subphase of a Langmuir trough have been well established as model systems for cell membrane, pulmonary lipid, and tear film systems [31, 32]. In addition, the microscopic structure of the films can be observed and correlated with the surface pressure. Other variables such as pH, temperature and salt concentrations of the subphase can also be controlled.

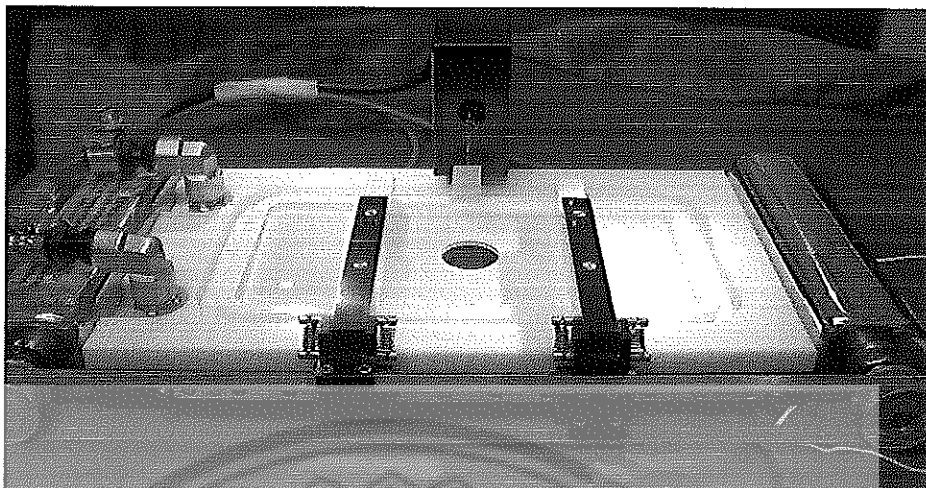


**Figure 2.6 Langmuir trough with two-moveable barriers**

The accumulation of surface active molecules at the interface tends to reduce the surface tension. Thus the surface tension (or surface pressure) is a function of the molecular surface density (number of molecules per unit area), and can be affected by “compressing” a particular monolayer. This can be observed and quantified by sweeping closed a barrier to reduce the area occupied by the film under study while the surface tension is continuously monitored. The obtained plot (surface pressure versus area occupied at a given temperature) is the pressure-area isotherm which has a shape characteristic of molecule involved in film formation. Typically for simple amphiphilic molecules, the isotherm shows usually three distinct regions (Figure 2.7). When no external pressure is applied to the monolayer, the molecules behave like a two-dimensional “gas”. As the barrier is closing, the surface pressure increases causing first partial ordering of the film to produce a two-dimensional “liquid” and next, upon further ordering to force the film to behave like a “quasi-solid”. For a clean system (no contaminants affecting the surface tension), each of these states of the film has a characteristic trace on the isotherm (Figure 2.7) with a sharp transition at the change of state. Eventually, the collapse pressure,  $\pi_c$ , is reached beyond which multilayer start forming. It is noted that the collapse is not uniform; there still might be regions of monolayer broken up by “ridges” and aggregates. The collapse pressure can also be defined as the maximum pressure that a monolayer can sustain before expelling molecules from the Langmuir film.

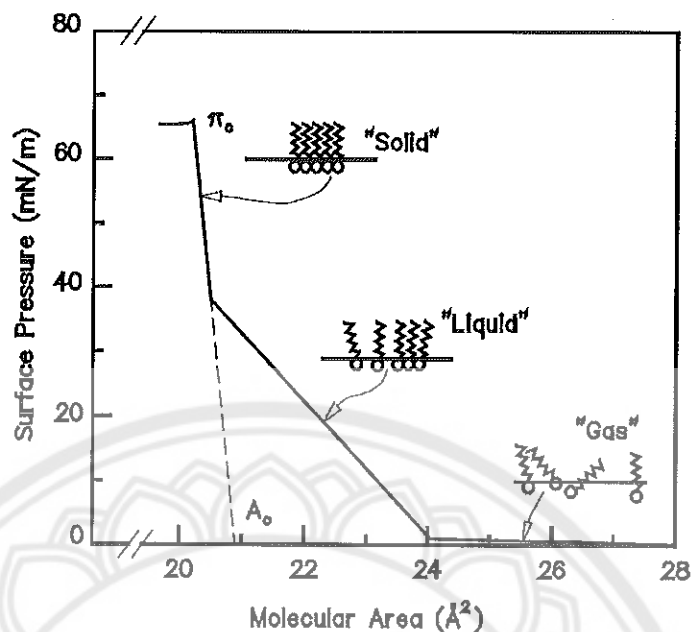


**Figure 2.7** Idealized Langmuir isotherm of the monolayer film of a typical amphiphilic molecule. The three distinct regions of the isotherm can be associated with the different level of ordering of the film as shown schematically on the figure;  $\pi_c$  is the collapse pressure beyond which multilayer start forming, and  $A_0$  is the zero pressure molecular area [33]

### Treatments of dry eye

The goals for DED treatment are overcome the signs and symptoms of disorder by enhancing the tear film stability and suppressing the chronic sub-clinical inflammation of the ocular surface. Thus, the most widely accepted treatment of dry eye patients are ocular lubricant and topical anti-inflammatory drugs. However, there are several new treatment agents and delivery systems have been studied. The advantages, specific indications and limitations of each type of DED treatment are summarized below.

#### 1. Ocular lubricants

In classical dry eye treatment, ocular lubricants or so called “artificial tear” have been developed. These ocular lubricants formulations have been accepted and widely used in mild and moderate DED by relieving symptoms of discomfort. These

formulation consist of hypotonic or isotonic buffered solution with electrolyte to mimic the natural tear, and various type of polymeric viscosity agent to extend residence time on ocular surface [34]. The popular polymeric viscosity agents include hydroxymethyl cellulose, carboxymethyl cellulose, hydroxyl propylcellulose, polyvinyl alcohol, propylene glycol, and polyethylene glycol 400. Conventional formulation have been used to develop for DED treatments, such as solutions, ointments and gels. Ointments are formulated with mineral oil and petrolatum that usually use at nighttime because their blurring effects. Gels have longer retention times than solutions but less visual blurring effect than ointments [4].

It has been demonstrated that treatment of meibomian gland disease (MGD) through manual expression of the meibomian glands does increase the tear film lipid layer thickness and tear film stability [23]. Thus, therapies targeted at replenishing or stabilizing the lipid layer are key to the treatment of dry eye, either as monotherapy or in conjunction with therapies designed to enhance aqueous production. Over the past decade, lipid-base nanocarrier formulations, such as emulsion (Refresh dry eye therapy<sup>®</sup>, Lipimix<sup>®</sup>, Soothe<sup>®</sup>XP Emollient), liposome (Tear again<sup>®</sup>), and cationic emulsion (Cationorm<sup>®</sup>) have been clinically approved and marketed for dry eye patient [35]. These formulations is still extensively interested and developed by new novel lipid-base nanocarrier (such as solid lipid nanoparticle (SLN) and nanostructured lipid carrier (NLC)) with supportive laboratory and clinical evidence [35, 36].

## 2. Corticosteroids

Methylprednisolone, loteprednol etabonate and fluorometholone have been used as topical corticosteroids that effect to reduce the sign of inflammation and improve the integrity of ocular surface in dry eye patients [37]. These drugs inhibit cytokine and chemokine production, decrease the synthesis of Matrix metalloproteinases (MMPs) and arachidonic acid derivatives, suppress the expression of cell adhesion molecules, and induce lymphocyte apoptosis [38]. The topical corticosteroids, usually use for short-term (1-2 weeks), can rapidly and effectively relieve the symptoms and signs of moderate or severe dry eye. They should not be used for long-term due to their adverse effects such as ocular hypertension, cataracts, and opportunistic bacterial or fungal infection [34].

### 3. Cyclosporin A (CsA)

CsA is a very promising treatment for DED because it is the first agent focused on the pathogenesis of this disease. CsA can be controlled ocular surface inflammation by partial immunodulatory effects that increasing tear secretion and tear film stability [13]. CsA binds to nuclear protein required for T-cell activation, which results in a decrease in T-cell-stimulated inflammatory cytokines [38]. The drug also has the ability to block c-Jun NH2-terminal kinase and p38 MAPK cascades, which contribute to T-cell activation. In addition, conjunctiva epithelial apoptosis may decrease. It can be used for long-term without the adverse effects. However it also has some side effect such as burning and irritation on ocular surface [39]. It is lipophilic drug leading to low bioavailability and challenge for preparation. Moreover, another consideration that could also affect CsA permeability is the presence of an efflux pump such as P-glycoprotein (P-gp; MDR1) in the both of conjunctiva and cornea epithelium cells in human, rabbit and rabbit corneal cell line [40-42]. Although, these efflux pumps are one of barrier to ocular drug delivery, we did not find strong evidence on cornea epithelium cells. However, the formulation that inhibit P-gp activity are suggested.

CsA initially prepared for topical with oil and ointment which were messy, uncomfortable to use, and the permeation to ocular is limited. Thus, CsA was developed by lipid emulsion formulation. This 0.05% CsA oil in water emulsion (Restasis®) was approved by FDA in December 2002 and still used for dry eye treatment [43]. Unfortunately, the most common side effect is ocular burning or irritation following the long-term use of Restasis®. Moreover, poor ocular tolerance, low bioavailability, and instability are also the major drawbacks report with Restasis®. Therefore, the new CsA delivery systems have been developed. Cationic emulsions have been formulated with CsA (Cyclokate®) and studied in Phase III clinical trials [44]. Another types of drug delivery systems such as liposome, SLN and NLC have been also studied [6, 43, 45].

### 4. Tetracycline derivative

Tetracyclines antibiotic (such as azithromycin, minocycline, and doxycycline) usually use in severe dry eye patient with effect to improve of Meibimian gland dysfunction and contact lens wear [46]. They can be inhibited the

expression of pro-inflammatory cytokine such as MMPs activity. Oral administration is the most common route. However, topical formulations are available, and liposomal-bound topical doxycycline may be useful in increasing bioavailability [37, 46].

### **5. Hormonal therapy**

The previous study reported that adequate androgen, prolactin and estrogen levels are essential for normal lacrimal gland function and structural organization [13]. The administration of topical androgen and estrogen steroid hormones for 3 – 4 months have been showed increasing tear production and lipid layer thickness in dry eye patients. In addition, the combined esterified estrogen and methyl-testosterone for 4 – 24 months can be reduced symptoms and promote clinical improvement in postmenopausal women with DED. Today, clinical trials evaluating topical testosterone are in Phase II trials [37].

### **6. Essential fatty acids (Omega 3)**

Omega-3 fatty acid is polyunsaturated essential fatty acids (EFAs) that has anti-inflammatory effect [5]. The human body cannot synthesize EFAs. Therefore, EFAs must be obtained from the diet. Omega-3's are elongated by enzymes to produce largely anti-inflammatory prostaglandin E<sub>3</sub> (PGE<sub>3</sub>), anti-inflammatory leukotriene B<sub>5</sub> (LTB<sub>5</sub>), thromboxane (which reduces vascular permeability) and resolvins [47]. Interestingly, there are several studied reported that topical EFAs showed therapeutic effect by decrease ocular staining, cytokine expression, and immune cell infiltration, increase tear production, and maintain ocular surface integrity in animal model [48]. However, more evidence is needed to identify the most efficacy form and dose of EFAs. The EFAs has completed Phase II investigation in clinical trial [46].

### **7. Nerve growth factor (NGF)**

The previous studies observed that NGF can be increased ocular surface sensitivity, inhibited inflammatory reaction and regulated tear film production [13]. NGF seem to a play role in the pathophysiology of DED and may be a promising therapeutic option. Thus, they are interested to develop the efficacy form and dose and study in clinical trials.

## 8. Secretagogues

The secretagogues can increase tear volume, stimulated mucin production, improved symptoms, and surface staining in dry eye. One drug of secretagogues is name “Cevimeline” is approved by FDA in USA for dry mouth treatment only. Cevimeline is a parasympathomimetic and muscarinic agonist, with particular effect on M1 and M3 receptors leads to stimulate the secretion of salivary gland. However, there are two secretagogues under investigation by major drug company for dry eye treatment include diquafosol tetrasodium and hydroxyecosatetraenoic acid. Diquafosol is a dinucleotide, purinoreceptor P2Y<sub>(2)</sub> receptor agonist. Basic pharmacological studies have shown that it acts on P2Y<sub>(2)</sub> receptors at the ocular surface, to promote tear and mucin secretion via elevated intracellular Ca<sup>+2</sup> concentrations. Diquafosol also improves tear and mucin secretion in experimental dry eye models. Thus, the clinical studies of diquafosol for DED treatment are under evaluation in Phase II and expected to be in Phase III very near future [37, 49].

## 9. Autologus serum

The topical of autologous serum has been found to be beneficial in severe dry-eye patient when other treatments have failed [37]. This serum contains a number of anti-inflammatory factors that can inhibit the mediators of the ocular surface. Autologous serum drops (diluted 1% with saline) have been reported to improve ocular irritation symptoms and conjunctival and corneal dye staining in several small clinical trials [3].

In conclusion, a number of different dry eye treatment and new candidate are commercially available, and many other approaches have been studied, indicating that the number of treatment will increase dramatically in the near future. The best treatment for DED remains unknown; it depends on type and level of severity in patient. The combinations of artificial tears, oral omega-3 essential fatty acid, secretagogues, short-term steroids, and daily cyclosporine A (CsA) are used to treat the inflammation and restore normal tear film in patients with mild-to-moderate disease. The use of more aggressive treatment such as autologous serum and oral tetracyclines is restricted to severe dry eye patients. Additionally, the optimal designs of DED treatment have also been studied.

## Topical ocular administration

Most ocular medications may be administered topically in order to treat ocular disorders. This route is often preferred for the management of various pathological diseases that affect the anterior chamber of the eye. The two main reasons are; it is more conveniently administered and provides a higher ratio of ocular to systemic drug level [50]. Typically topical ocular drug administration is accomplished by eye drops, but they have only a short contact time on the eye surface that resulting from precorneal barrier leading to low ocular bioavailability (Figure 2.8). The contact time, and thereby duration of drug action, can be prolonged by formulation design (e.g. gels, ointments, and inserts). Usually, 1 – 5 % of the instilled dose is absorbed and only 1% reaches the aqueous humor.

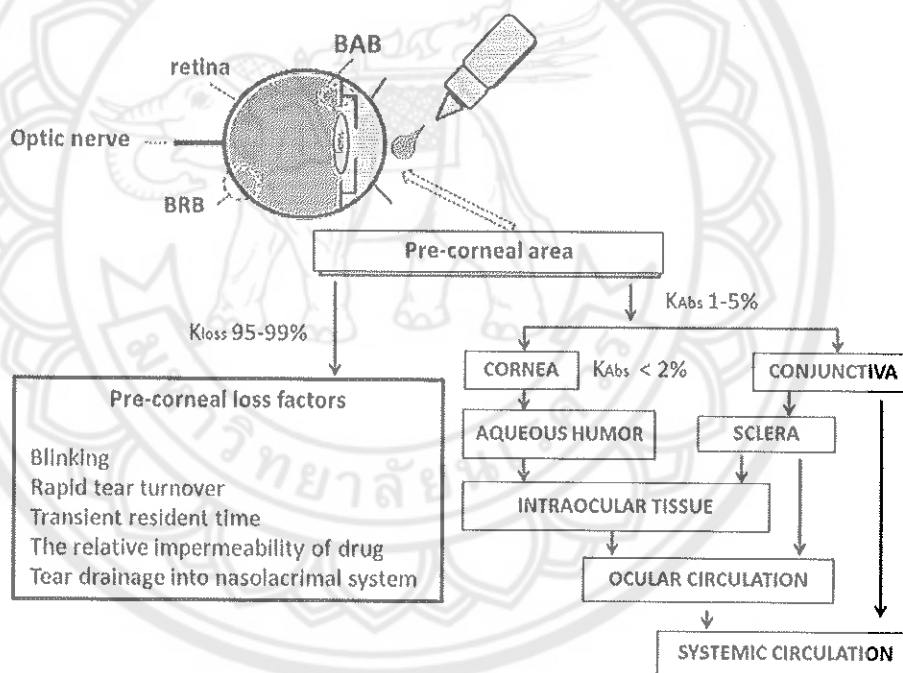


**Figure 2.8** Model showing the movement of drug into the eye after topical administration. BAB, blood-aqueous barrier; BRB, blood-retinal barrier. Modified from Bucolo et al. [51]



When compared with drug delivery to the other part of the body, ocular drug delivery has significant challenges because they have various ocular barriers. Almost of these ocular barriers are occurred by the unique of ocular anatomy and physiology that challenging for drug delivery scientists. These barriers are specific depending upon the route of administration such as topical, systemic and injectable. The ocular barriers are divided into three parts including precorneal barrier, cornea barrier and blood ocular barrier.

### **1. Precorneal barriers**

The loss of drug from the precorneal area is a result of drainage, tear secretion, non-corneal absorption and corneal absorption rate process. There are three possible of the precorneal barriers causing loss of drug.

#### **1.1 High turnover rate.**

As the lacrimal functional unit function, the basal tear flow is  $\sim 1.2$   $\mu\text{L}/\text{min}$  ( $0.5 - 2.2$   $\mu\text{L}/\text{min}$ ). This results in a tear turnover rate of 16 % per minute during waking hours. Reflex stimulation might increase lachrymation 100-fold, up to 300  $\mu\text{L}/\text{min}$ . Topical administration, mostly in the form of eye drops, is quickly washed away by the tear film after application on the surface of the eye.

#### **1.2 Gel-like mucus layer.**

Approximately 2 – 3 mL mucus are secreted daily. Mucin presented in the tear film has a protective role by forming a hydrophilic gel layer that moves over the glycocalyx of the ocular surface and clears cell debris, foreign bodies and pathogens. At the same time, it acts as a barrier to drug delivery systems.

#### **1.3 Protein binding**

Protein binding of drugs in the tear fluid is a factor affecting drug bioavailability [52]. Tear normally, contain about 0.7 % protein and the protein level increase during infection or inflammation. When the drug-protein complex continue to circulate, tears are replaced quickly thus removing both free and bound forms of the drug [53].

### **2. Cornea barrier**

The cornea is a  $\sim 500 - 800$   $\mu\text{M}$  thick transparent collagenous structure. It provides the majority of the refractive power of the eye and is the primary barrier to topical drug absorption. The cornea is consisted of the 6 layers, epithelium, Bowman's

membrane, stroma, Dua's layer, Descemet's membrane and endothelium (Figure 2.9) [8].

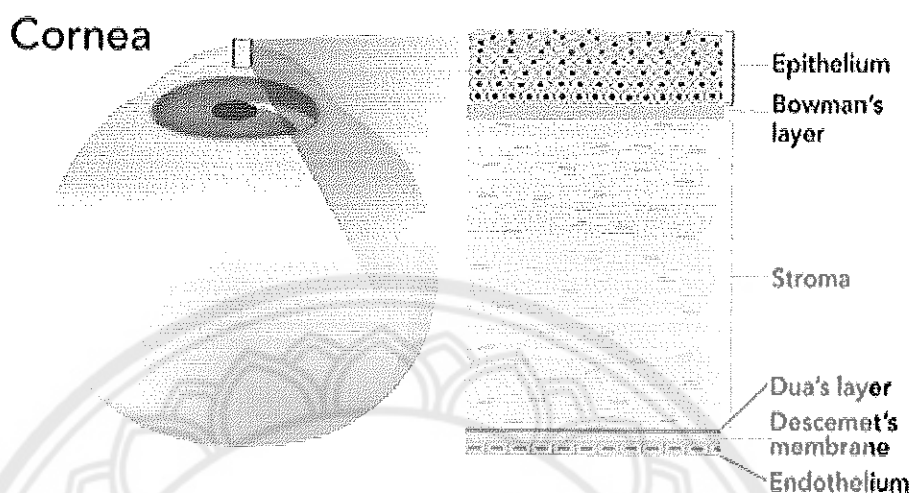


**Figure 2.9 The structure of cornea**

**Source:** <http://www.brussels-vision-specialists.eu/en/corneal-anatomy>

The corneal epithelium consists of 5 - 6 layers of cells packed closely by tight junctions that limit the paracellular drug permeation [35, 54]. The epithelium is impermeable to polar or hydrophilic compounds with molecular weight greater than 60 - 100 Da [53]. Immediately underneath the epithelium is the Bowman's membrane, a thin homogeneous layer forming a transition toward the stroma, and it's not considered to be a barrier to drug diffusion. The stroma makes up 90 % of the corneal thickness. It consists of 75 % water in a collagenous extracellular matrix. So it shows hydrophilic nature. Thus, the stroma allow hydrophilic molecule to pass through easily. However, it limits the penetration of highly lipophilic or large molecular weight compound. Descemet's membrane is a tough, homogeneous band supporting the endothelium, a single layer of cells important to keep the hydration of the stroma constant. Finally, the corneal endothelium is a leaky monolayer that easier permeated than epithelium. It maintains an effective barrier between the stroma and aqueous humor. In the conclusion, these layers make cornea a crucial barrier to most lipophilic

and hydrophilic drugs. To penetrate the cornea, optimal lipophilicity for the permeant corresponds to log P values of 2 - 3 [44].

### **3. Blood-ocular barrier**

The eye is protected from the xenobiotics in the blood stream by blood-ocular barriers. These barriers have two parts: blood-aqueous barrier and blood-retina barrier. The blood-aqueous barrier, located in anterior segment, is composed of the endothelial cells in the uvea. This barrier prevents the access of plasma albumin into the aqueous humor, and also limits the access of hydrophilic drugs from plasma into the aqueous humor. The blood-retina barrier, located in posterior segment between blood stream and eye is comprised of retinal pigment epithelium (RPE) and the tight walls of retinal capillaries. Unlike retinal capillaries the vasculature of the choroid has extensive blood flow and leaky walls. Drugs easily gain access to the choroidal extravascular space, but thereafter distribution into the retina is limited by the RPE and retinal endothelia.

#### **Ocular pharmacokinetics**

The main routes of drug administration and elimination from the eye have been shown schematically in Figure 2.10. For topical administration, the ocular routes of absorption are divided into corneal and non-corneal. For the corneal route, the drug go to the systemic circulation by across the cornea to aqueous humor and intraocular circulation while the non-corneal route the drug go to the systemic circulation by conjunctiva and sclera (Figure 2.10).

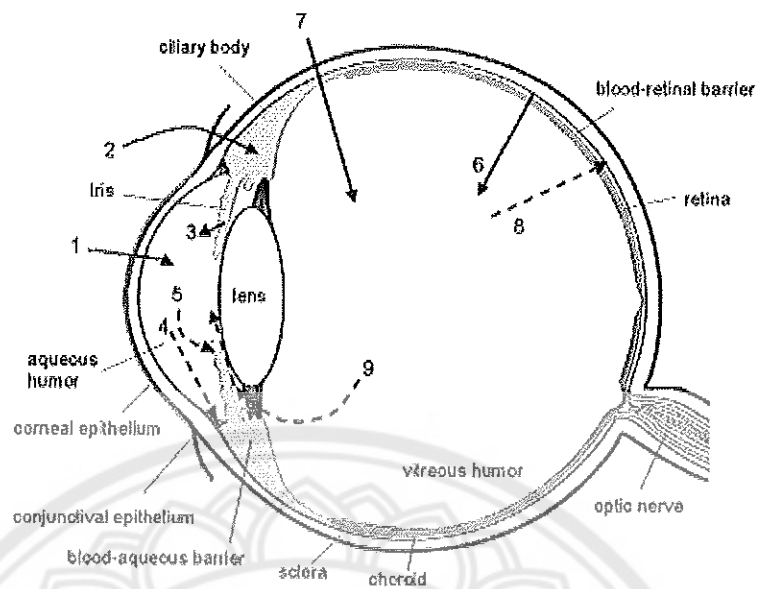


**Figure 2.10 Schematic presentation of the ocular structure showing a summary of ocular pharmacokinetics. The numbers refer to following processes:**

- 1) transcorneal permeation from the lachrymal fluid into the anterior chamber,**
- 2) non-corneal drug permeation across the conjunctiva and sclera into the anterior uvea,**
- 3) drug distribution from the bloodstream via the blood-aqueous barrier into the anterior chamber,**
- 4) elimination of drug from the anterior chamber by aqueous humour passage into the trabecular meshwork and Schlemm's canal,**
- 5) drug elimination from the aqueous humor into the systemic circulation across the blood-aqueous barrier,**
- 6) drug distribution from the blood into the posterior eye across the blood-retina barrier,**
- 7) intravitreal drug administration,**
- 8) drug elimination from the vitreous via the posterior route across the blood-retina barrier,**
- and 9) drug elimination from the vitreous via the anterior route to the posterior chamber [54]**

Corneal route is the most common pathway of drug absorption across cornea. The major permeation mechanisms across the cornea include passive transport and active transport (Figure 2.11). There are three mechanisms of passive transport including passive transcellular, passive paracellular, and facilitated diffusion. Passive transcellular and paracellular are not dependent on transporter proteins, but they are dependent on drug properties that can determine the partitioning and diffusion of the molecule in the lipid bilayer of the cell membrane. The drugs can move from higher to lower concentration to maintain equilibrium in cells. Passive transcellular permeability of drugs across the cornea is influenced by various factors, such as lipophilicity (i.e. partition coefficient), molecular weight, charge, and degree of ionization. In particular, lipophilicity is a major factor in corneal drug penetration. Passive paracellular diffuse via the spaces between the cells. These spaces are limited by the tight junctions in the cornea epithelium.

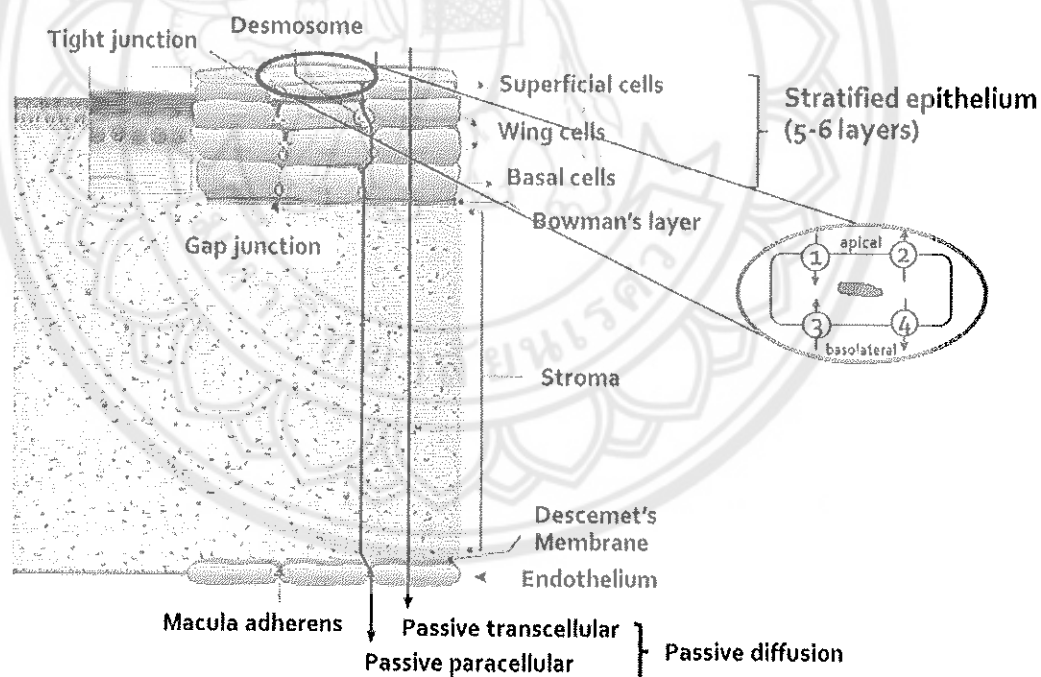


**Figure 2.11** The permeation mechanisms across cornea. Passive paracellular and transcellular permeation. Transporter mediated influx and efflux across cell membrane in the apical (1 and 2) and basolateral (3 and 4) side, respectively. Modified from Eliisa Mannermaa et al. [55]

There are many reported that the intercellular spaces are smaller than 3 nm. Only small drugs (MW < 350 Da) and ions can permeate through the paracellular route. In addition, facilitate diffusion or so called carrier-mediated diffusion, requires expression of transporters in the corneal epithelium. Many large molecules such as glucose will bind with a specific carrier proteins and then move through the cell membrane. The drugs move down the concentration gradient and do not use ATP (cellular energy) to move. Active transport requires ATP to move the drugs across the cell membrane in the direction against their concentration gradient. Other types of transporters perform efflux of drugs from the cells. The efflux transporters such as MRP, P-gp, and BCRP express on the corneal epithelium that facilitate the export of drug from the cell.

Although the corneal route is the primary route of enter drug into the eye, studies have also shown that absorption can occur via the non-corneal (conjunctival-scleral) route, particularly for large hydrophilic molecule such as protein and peptide. The conjunctiva is composed of 3 layers include outer epithelium, stroma and submucosa. It is more permeable or leaky than the cornea that allows drugs to permeate through the paracellular as well as transcellular route. The conjunctiva is highly vascularized so drug absorption often results in systemic distribution of the drug away from the eye. The sclera is the white eye which outer coat of the eye. Sclera anatomy is similar to corneal stroma. Thus, drug permeation through the sclera occurs via the aqueous intercellular space between the collagen fibers. The sclera is more permeable (10 times) than cornea and half permeable as the conjunctiva such as drug with a MW of more than 1kDa are almost impermeable through the cornea whereas dextran (40 kDa) and albumin (69 kDa) have good permeability through the sclera.

### **Nanostructured lipid carriers (NLCs)**

Recently, the lipid-based nanocarriers have been developed for ophthalmic drug delivery. The aims are to improve ocular contact time, enhance the permeability of drug into target site, sustained and controlled-release drugs that leading to improve ocular bioavailability of the drugs. Among the lipid-based nanocarriers, NLCs possess significant advantages.

## 1. Introduction of NLCs

NLCs are colloidal carriers with mean particle size in the nanometer range. NLCs are considered to be the new generation of lipid-based nanocarriers that developed to avoid disadvantages of solid lipid nanoparticles (SLNs) by composing of solid and liquid lipid [56]. NLCs can be made from physiological lipids so that they are biodegradable, biocompatible, and without any acute and chronic toxicity [57, 58, 59]. In addition, they possess high drug loading capacity, physical long-term stability, and potential for controlled drug release and drug targeting. NLCs also protect the encapsulated drug against chemical degradation in storage. Finally, it exhibits high mucoadhesiveness due to their small particle size as well as their lipophilic characters lead to longer residence time in the lung and eye [57, 60, 61]. Sterilization of ophthalmic formulation is critical for topical application as microbial contamination should be prevented [62]. One of the strongest advantages of these NLCs is the possibility to sterile by an autoclaving method which is a commonly used and reliable technique. Thus, the advantages above make NLCs an attractive candidate for topical administration of eye drop [63, 64, 65].

## 2. Production of NLCs

Many different methods have been described in the literature for production of NLCs. The hot homogenization is the most used method for fabrication of NLCs. This method has many advantages include easy scale up, lack of organic solvents and short production time, compared to the other method [66]. Briefly, the drug is initially dissolved or dispersed in the melted lipid mixture. Then, the melted lipid is dispersed in aqueous emulsifier solution at the same temperature by high speed stirring. The obtained hot emulsion may further be homogenized at the same temperature, by instruments such as high pressure homogenizer (HPH) to produce a hot nanoemulsion. This technique is known as high pressure homogenization technique. This technique is used to homogenize the hot emulsion to obtain the smaller particles with lower polydispersity index usually below 0.3. Subsequently, NLCs are produced by cooling the hot nanoemulsion in cold water, room temperature or by a heat exchanger to crystalize lipid droplet and precipitate the lipid nanoparticles.

### 3. Structure of NLCs

The structure of NLCs has been proposed for three types including imperfect, amorphous, and multiple type NLCs, depends on the formulation composition and the production parameters [56, 66]. Imperfect type NLCs can be obtained by mixing solid lipid with different type of liquid lipids (oils). These imperfections/holes accommodate the drug in molecular form and amorphous clusters; increase the drug payload. Amorphous type NLCs can be produced by mixing solid lipids with special lipid such as hydroxyoctacosanylhydroxystearate, isopropylmyristate or medium chain triglyceride, which the lipidic core congeals in an amorphous rather than crystalline state. Finally, multiple type NLCs or multiple oil-in-fat-in-water (O/F/W) carrier are produced by mixing a solid lipid with a higher amount of oils. These solid matrixes of lipid nanoparticle contains tiny liquid oil nano-compartments that caused high drug solubility. This solid matrix prevents drug leakage and allowing controlled drug release.

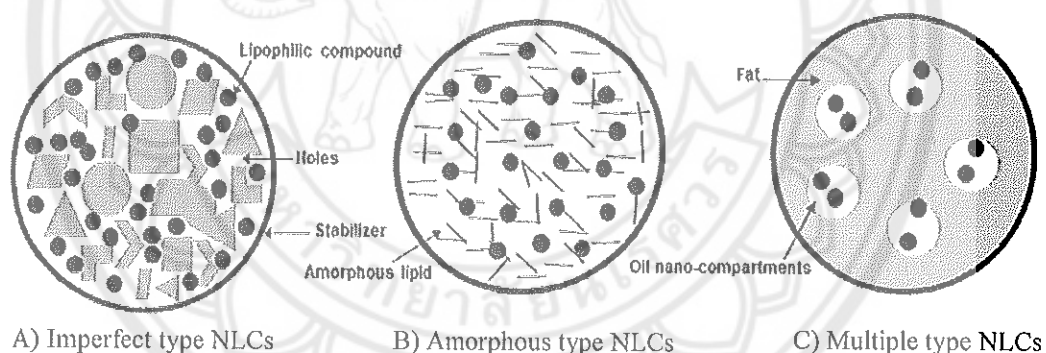


Figure 2.12 Three structure type of NLCs [66]

### 4. Characterization of NLCs

The various techniques for major characterization of NLCs are particle size, polydispersity index, particle charge, particle morphology, chemical stability during processing and storing, encapsulation efficiency, crystalline status, and release manner [56, 67]. Here, a brief description of some of these properties is provided.



The mean particle size and polydispersity index (PI) are the most important characteristics for NLCs dispersions to confirm the production of the particles in nano-range which regarding to the physical stability, solubility, biological performance, release rate, turbidity, and chemical stability [66, 68]. The most common tool for analyzing the size of NLCs dispersions is dynamic light scattering (DLS). The basic principle of this method is to observe the movement of particles and measure their Brownian motion. The PI indicates the width of the particle size distribution, which ranges from 0 to 1. Theoretically, PI values of 0.1-0.3 show a fairly narrow size distribution where a PI value greater than 0.5 indicates a very broad distribution [66]. PI has an important effect on physical stability of NLCs dispersions and as much as possible should be low for the long-term stability of NLCs dispersions.

The particle charge or known as zeta-potential is the electrical potential at the shear plane, which is defined as the distance away from the particle surface below which the counter-ions remain strongly attached to the particle when it moves in an electrical field. Zeta-potential is a useful parameter to predict the physical stability of the NLCs dispersions. Particles with a large negative or positive zeta potential (more negative than  $-30$  mV or more positive than  $+30$  mV) will achieve a nanodispersions with good stability [69].

Particle morphology is referred to the shape of lipid nanoparticles which has impact to many characteristics of NLCs formulation such as physical and chemical stability, encapsulation efficacy, drug loading, and drug release rate [66]. Thus, the advance microscopic techniques such as scanning electron microscopy (SEM) and transmission electron microscopy (TEM) are frequently used to provide critical information with respect to size, size distribution, morphology, and internal structure of lipid nanoparticles.

The encapsulation efficacy (EE) is defined as the ratio of encapsulated drug in nanoparticles to whole drug first incorporated into the lipid phase of NLCs multiplied by 100 [66]. The EE influences the release characteristics of NLCs and depends on the NLCs ingredients, production method, and condition used.

### **Mucoadhesion theory**

Mucoadhesion may be defined as adhesion of a delivery system to the mucosal surface for releasing the drug at the site in a controlled fashion [70]. In general, mucoadhesive polymers are responsible for the mucoadhesion phenomenon in mucoadhesive drug delivery systems. Their advantages include the prolonged residence time of the dosage form at the site of absorption leading to enhanced absorption and hence the therapeutic efficacy of the drug. In addition, mucoadhesion approach can be advantageous in improving bioavailability of ocular drugs by increasing the residence time of the drug in the eye.

In general, the mucoadhesion phenomenon could be explained by diffusion theory (physical entanglement and/or interpenetration of polymer chains and mucus chains), wetting theory (ability of mucoadhesive polymer to spread and develop intimate contact with the mucous layer), adsorption theory (surface forces resulting in chemical bonding), and electronic theory (attractive electrostatic forces between glycoprotein mucin network and the mucoadhesive polymer).

The mucus in the eye is mainly produced by the conjunctival goblet cells, and it forms the bottom layer of the tear film wetting the corneal epithelium. Mucoadhesive polymers can adhere to the mucin coat covering the conjunctival and the corneal surfaces of the eye by hydrogen bonding, electrostatic, covalent and hydrophobic interactions, which forms the basis of ocular mucoadhesion.

The lipid base nanocarriers have been reported that it can exhibit mucoadhesive property [60, 71]. The previous study indicated that the NLCs form films of densely packed spheres on the surface of the cornea which exert an occlusive effect by increasing corneal hydration [72]. Moreover, nanospheres coated polymer, such as polyethylene glycol (PEG), chitosan, and carbopol, suggested that the coating layers affected the interaction of the colloidal systems with the corneal epithelial cells [72-74]. The surface composition of colloidal systems may affect its affinity towards the ocular mucosa. The positive surface charge exhibits mucoadhesive effect by electrostatic interaction with the negative charge of mucus [70, 75].

## **Animal model of dry eye**

### **1. Introduction**

Generally, the type of dry eye can be divided into aqueous deficient and evaporative dry eye. Considering the complicated etiology, a huge variety of animal models are available to mimic the difference pathophysiology mechanism of DED. The different animal models such as monkey, rabbit, rat, mice, and dog have been developed. The measurement of tear secretion, gland secretion, tear production, tear film stability, tear film instability, corneal uptake, and ocular surface staining have been performed to determine the DED in animal models. The mouse and rat are the model most commonly used to study autoimmune mechanisms of DED, because of the diversities of different knockout and transgenic strains and good availability of antibody [76]. However, there are no data exist concerning altered tear secretion, ocular surface changes, or any signs related to lacrimal gland insufficiency or dry eye in mouse or rat model [77].

The rabbit and dog models are more suitable to use for dry eye study due to they can presented the tear secretion, ocular surface changes, and offer better accessibility of the ocular surface [77]. The New Zealand white rabbits are the usual choice for vision research [6, 43, 64, 76, 77]. They have large eyes and corneal lesions easily accessible for imaging and quantification by eye observation, when compared to the mouse model [77]. They have gentle nature, relative low cost to maintain and more similar to human eyes than the mouse models [78, 79]. Moreover, the rabbit model have been suggested to address specific problem and useful for developing new treatment in dry eye [76, 77].

### **2. Anatomy of rabbit eye**

The rabbit eye has a larger lacrimal gland, unique lacrimal and aqueous drainage systems, and its cornea is devoid of a significant Bowman's membrane. The differences between rabbit and human eye are summarized in Table 1. The rabbit cornea is unusually prominent and wide, transmitting almost 100 % of light in the visible spectrum. The corneal thickness is approximately 0.3 - 0.4 mm at its center and approximately 0.45 mm near the limbus. The rabbit corneal epithelium is thinner than that of human, approximately 30 - 40  $\mu\text{M}$  thick. In addition, volumetric differences (a difference in the relative volumes of the lens and vitreous), the presence of vascular

medullary rays in an otherwise avascular retina, and the presence of a visual streak in the absence of a true macula lutea. Despite these shortcomings, the rabbit is the most commonly used animal model for the study of vitreous and retina pathologies and for the evaluation of the effects of medical and surgical interventions.

The rabbit inter-blink time is approximately 10 minutes that known to be one of the longest among animals whereas a typical inter-blink time for healthy adult human is 5 - 8 seconds. Thus, the long inter-blink time of rabbit is suitable for investigate the tear film stability [80].

**Table 2.1 Comparison between human, rabbit, and porcine eye [79, 80, 81, 82]**

Comparisons	Human	Rabbit	Porcine
<b>Ocular dimensions</b>			
<b>Globe (mm)</b>			
Anteroposterior	24	16 - 19	23.9
Horizontal	23.5	18 - 20	16.6
Vertical		17 - 18	15
<b>Cornea</b>			
<b>Diameter (mm)</b>			
Horizontal	11.7	13	10.8
Vertical	10.6	13.5 - 14	9.1
Radius of curvature (mm)	7.5 - 8.0	7.0 - 7.5	7.2
<b>Cornea thickness (mm)</b>			
Center	0.5	0.3 - 0.4	0.8
Peripheral	0.7 - 1.0	0.45	0.9-15
Epithelial thickness ( $\mu\text{m}$ )	30 - 40	30 - 40	50 - 70
Epithelial cell layers	5 - 7	5 - 7	6 - 9
Bowman's layer	Present	Absent	Present
Endothelial cell density ( $\text{cell}/\text{mm}^2$ )	4,003 - 1,547	3,200	4,000
	at 12 - 74		
	year		

Table 2.1 (cont.)

Comparisons	Human	Rabbit	Porcine
Anterior chamber depth (mm)	3.05	2.9	2.47
Vitreous chamber depth (mm)	16.32	6.2	11.39
Typical inter-blink time	5-7 seconds	10 minutes	6 seconds

### 3. Examination techniques

The common clinical tests to diagnose DED in humans (such as the Schirmer test, fluorescein, and rose bengal staining of the ocular surface) have been used in dogs and rabbits. Some examinations are explained below [83].

#### 3.1 Measurement of tear secretion by Schirmer test

The filter paper (5 mm wide and 35 mm long) is folded 5 mm from one end, with its two corners cut to minimize conjunctival irritation. It is inserted at the junction of the middle and outer third of the lower lid, after gently removing the excess secretion from the lower lid margin. The standard time used to measure tear production in humans is 5 min. The test can be performed without anesthesia to measure the total tear secretion. In addition, this test can be performed after the instillation of topical anesthetic, which measuring mainly basal tear production [84].

#### 3.2 Tear film stability

Tear break-up time (TBUT) is widely used in clinical method of measuring tear film stability. It is defined as the time interval following a blink to the occurrence of break in the tear film. After applying liquid fluorescein to the ocular surface by means of a micropipette, or by a wetted fluorescein strip, the time from opening the eyes to the appearance of the first spot on the corneal surface is measured [84].

#### 3.3 Ocular surface evaluation

Evaluating the condition of the ocular surface is an important aspect of DED diagnosis and treatment, and therefore can play a central role in the use of animal models of dry eye. Fluorescein, is a water soluble vital dye, has been used in animal models of dry eye for ocular surface staining, corneal uptake measurement, and for the clearance test [84]. In rabbit's dry eye models, fluorescein is applied into the

inferior conjunctival sac by drop or strips, and the staining examined with a slit lamp microscope.





**REFERENCES**

## REFERENCES

- [1] Stevenson, W., S.K. Chauhan, & R. Dana. (2012). Dry eye disease: An immune-mediated ocular surface disorder. *Arch Ophthalmol*, 130(1), 90-100.
- [2] Stern, M.E., & S.C. Pflugfelder. (2004). Inflammation in dry eye. *Ocul Surf*, 2(2), 124-130.
- [3] Pflugfelder, S.C. (2003). Anti-inflammatory therapy of dry eye. *Ocul Surf*, 1(1), 31-36.
- [4] Wander, A.H., & B.H. Koffler. (2009). Extending the duration of tear film protection in dry eye syndrome: review and retrospective case series study of the hydroxypropyl cellulose ophthalmic insert. *Clinical Practice*, 7(3), 154-162.
- [5] Barabino, S. (2012). Ocular surface immunity: Homeostatic mechanisms and their disruption in dry eye disease. *Progress in Retinal and Eye Research*, 31(3), 271-285.
- [6] Aksungur, P., Demirbilek, M., Denkbaşı, E.B., Vandervoort, J., Ludwig, A., & Unlü, N. (2011). Development and characterization of Cyclosporine A loaded nanoparticles for ocular drug delivery: Cellular toxicity, uptake, and kinetic studies. *Journal of Controlled Release*, 151(3), 286-294.
- [7] Lemp, M.A., Baudouin, C., & Baum, J. (2007). The definition and classification of dry eye disease: report of the Definition and Classification Subcommittee of the International Dry Eye WorkShop (2007). *Ocul Surf*, 5(2), 75-92.
- [8] Kim, Y.C. (2014). Ocular delivery of macromolecules. *Journal of Controlled Release*, 190, 172-181.
- [9] Zhou, L., & R.W. Beuerman. (2012). Tear analysis in ocular surface diseases. *Progress in Retinal and Eye Research*, 31(6), 527-550.
- [10] Johnson, M.E., & P.J. Murphy. (2004). Changes in the tear film and ocular surface from dry eye syndrome. *Progress in Retinal and Eye Research*, 23(4), 449-474.
- [11] Tiffany, J.M. (2003). Tears in health and disease. *Eye*, 17(8), 923-926.



- [12] Utine, C.A. (2011). Tear osmolarity measurements in dry eye related to primary Sjogren's syndrome. *Curr Eye Res*, 36(8), 683-690.
- [13] Lin, H., & S.C. Yiu. (2014). Dry eye disease: A review of diagnostic approaches and treatments. *Saudi Journal of Ophthalmology*, 28(3), 173-181.
- [14] Pucker, A.D., & J.J. Nichols. (2012). Analysis of Meibum and Tear Lipids. *The Ocular Surface*, 10(4), 230-250.
- [15] Cwiklik, L. (2016). Tear film lipid layer: A molecular level view. *Biochimica et Biophysica Acta (BBA) - Biomembranes*, 1858(10), 2421-2430.
- [16] Molloy, M.P. (1997). Establishment of the human reflex tear two-dimensional polyacrylamide gel electrophoresis reference map: new proteins of potential diagnostic value. *Electrophoresis*, 18(15), 2811-2815.
- [17] Millar, T.J., & B.S. Schuett. (2015). The real reason for having a meibomian lipid layer covering the outer surface of the tear film – A review. *Experimental Eye Research*, 137, 125-138.
- [18] Bron, A.J., & J.M. Tiffany. (2004). The contribution of meibomian disease to dry eye. *Ocul Surf*, 2(2), 149-165.
- [19] Braun, R.J. (2011). Dynamics of the Tear Film. *Annual Review of Fluid Mechanics*, 44(1), 267-297.
- [20] Braun, R.J. (2015). Dynamics and function of the tear film in relation to the blink cycle. *Progress in Retinal and Eye Research*, 45, 132-164.
- [21] Holly, F.J. (1993). Diagnostic methods and treatment modalities of dry eye conditions. *Int Ophthalmol*, 17(3), 113-125.
- [22] Norn, M.S. (1969). Desiccation of the precorneal film. I. Corneal wetting-time. *Acta Ophthalmol (Copenh)*, 47(4), 865-880.
- [23] Foulks, G.N. (2007). The Correlation Between the Tear Film Lipid Layer and Dry Eye Disease. *Survey of Ophthalmology*, 52(4), 369-374.
- [24] Bron, A.J. (2004). Functional aspects of the tear film lipid layer. *Experimental Eye Research*, 78(3), 347-360.
- [25] Peng, C.-C., Cerretani, C., Braun, R.J., & Radke, C.J. (2014). Evaporation-driven instability of the precorneal tear film. *Advances in Colloid and Interface Science*, 206, 250-264.

- [26] Iwata, S. (1969). Evaporation rate of water from the precorneal tear film and cornea in the rabbit. *Invest Ophthalmol*, 8(6), 613 - 619.
- [27] Tiffany, J.M., N. Winter, & G. Bliss. (1989). Tear film stability and tear surface tension. *Curr Eye Res*, 8(5), 507-515.
- [28] Herok, G.H., P. Mudgil, & T.J. Millar. (2009). The effect of Meibomian lipids and tear proteins on evaporation rate under controlled in vitro conditions. *Curr Eye Res*, 34(7), 589-597.
- [29] Millar, T.J. (2009). Adsorption of Human Tear Lipocalin to Human Meibomian Lipid Films. *Investigative Ophthalmology & Visual Science*, 50(1), 140-151.
- [30] Schuett, B.S., & T.J. Millar. (2012). Lipid Component Contributions to the Surface Activity of Meibomian Lipids. *Investigative Ophthalmology & Visual Science*, 53(11), 7208-7219.
- [31] Dennison, S.R., F. Harris, & D.A. Phoenix. (2014). Chapter Three - Langmuir-Blodgett Approach to Investigate Antimicrobial Peptide-Membrane Interactions. In A. Iglič, & C.V. Kulkarni. (Eds.), *Advances in Planar Lipid Bilayers and Liposomes* (pp. 83-110). N.P.: Academic Press.
- [32] Dwivedi, M. (2014). Biophysical investigations of the structure and function of the tear fluid lipid layers and the effect of ectoine. Part B: Artificial lipid films. *Biochimica et Biophysica Acta (BBA) - Biomembranes*, 1838(10), 2716-2727.
- [33] Shen Y.R. (2016). *Molecular adsorption at interfaces*, in *Fundamentals of Sum-Frequency Spectroscopy*. Cambridge: Cambridge University.
- [34] Colligris, B., H.A. Alkozi, & J. Pintor. (2014). Recent developments on dry eye disease treatment compounds. *Saudi Journal of Ophthalmology*, 28(1), 19-30.
- [35] Gan, L. (2013). Recent advances in topical ophthalmic drug delivery with lipid-based nanocarriers. *Drug Discovery Today*, 18(5-6), 290-297.
- [36] Urban-Morlan, Z. (2010). Preparation and characterization of solid lipid nanoparticles containing cyclosporine by the emulsification-diffusion method. *International journal of nanomedicine*, 5(1178-2013), 611-620.
- [37] Foulks, G.N. (2008). *Chapter 6 - New Therapies for Dry Eye Disease*, in *Ocular Therapeutics*. London: Academic Press.

- [38] McCabe, E., & S. Narayanan. (2009). Advancements in anti-inflammatory therapy for dry eye syndrome. *Optometry - Journal of the American Optometric Association*, 80(10), 555-566.
- [39] Theng, J.T.S. (2003). Pharmacokinetic and Toxicity Study of an Intraocular Cyclosporine DDS in the Anterior Segment of Rabbit Eyes. *Investigative Ophthalmology & Visual Science*, 44(11), 4895-4899.
- [40] Kawazu, K. (1999). Characterization of Cyclosporin A Transport in Cultured Rabbit Corneal Epithelial Cells: P-Glycoprotein Transport Activity and Binding to Cyclophilin. *Investigative Ophthalmology & Visual Science*, 40(8), 1738-1744.
- [41] Dey, S. (2003). Molecular Evidence and Functional Expression of P-Glycoprotein (MDR1) in Human and Rabbit Cornea and Corneal Epithelial Cell Lines. *Investigative Ophthalmology & Visual Science*, 44(7), 2909-2918.
- [42] Barot, M. (2013). Mitochondrial localization of P-glycoprotein and peptide transporters in corneal epithelial cells – Novel strategies for intracellular drug targeting. *Experimental Eye Research*, 106, 47-54.
- [43] Karn, P.R. (2014). Supercritical fluid-mediated liposomes containing cyclosporin A for the treatment of dry eye syndrome in a rabbit model: comparative study with the conventional cyclosporin A emulsion. *International journal of nanomedicine*, 9(1178-2013), 3791-3800.
- [44] Gan, L., Wang, J., Jiang, M., Bartlett, H., Ouyang, D., Eperjesi, F., Liu, J., & Gan, Y. (2013). *Recent advances in topical ophthalmic drug delivery with lipid-based nanocarriers*. N.P.: n.p.
- [45] Gokce, E.H. (2008). Cyclosporine A loaded SLNs: Evaluation of cellular uptake and corneal cytotoxicity. *International Journal of Pharmaceutics*, 364(1), 76-86.
- [46] Skalicky, S.E. (2013). New agents for treating dry eye syndrome. *Current Allergy and Asthma Reports*, 13(1534-6315), 322-328.
- [47] Roncone, M., H. Bartlett, & F. Eperjesi. (2010). Essential fatty acids for dry eye: A review. *Contact Lens and Anterior Eye*, 33(2), 49-54.
- [48] Rashid, S. (2008). Topical omega-3 and omega-6 fatty acids for treatment of dry eye. *Archive of Ophthalmology*, 126(2), 219-225.

- [49] Matsumoto, Y. (2012). Efficacy and Safety of Diquafosol Ophthalmic Solution in Patients with Dry Eye Syndrome: A Japanese Phase 2 Clinical Trial. *Ophthalmology*, 119(10), 1954-1960.
- [50] Lallemand, F. (2003). Cyclosporine A delivery to the eye: A pharmaceutical challenge. *European Journal of Pharmaceutics and Biopharmaceutics*, 56(3), 307-318.
- [51] Bucolo, C., F. Drago, & S. Salomone. (2012). Ocular drug delivery: a clue from nanotechnology. *Frontiers in Pharmacology*, 3, 188.
- [52] Sasaki, H. (1996). Delivery of drugs to the eye by topical application. *Progress in Retinal and Eye Research*, 15(2), 583-620.
- [53] Malhotra, M., & D.K. Majumdar. (2001). Permeation through cornea. *Indian Journal of Experimental Biology*, 39(0019-5189), 11-24.
- [54] Urtti, A. (2006). Challenges and obstacles of ocular pharmacokinetics and drug delivery. *Advanced Drug Delivery Reviews*, 58(11), 1131-1135.
- [55] Mannermaa, E., K.-S. Vellonen, & A. Urtti. (2006). Drug transport in corneal epithelium and blood–retina barrier: Emerging role of transporters in ocular pharmacokinetics. *Advanced Drug Delivery Reviews*, 58(11), 1136-1163.
- [56] Müller, R.H., M. Radtke, & S.A. Wissing. (2002). Solid lipid nanoparticles (SLN) and nanostructured lipid carriers (NLC) in cosmetic and dermatological preparations. *Advanced Drug Delivery Reviews*, 54(Supplement), S131-S155.
- [57] Hao, J. (2012). Development and optimization of baicalin-loaded solid lipid nanoparticles prepared by coacervation method using central composite design. *European Journal of Pharmaceutical Sciences*, 47(2), 497-505.
- [58] Araújo, J. (2009). Nanomedicines for ocular NSAIDs: safety on drug delivery. *Nanomedicine: Nanotechnology, Biology and Medicine*, 5(4), 394-401.
- [59] Gonzalez-Mira, E. (2010). Design and ocular tolerance of flurbiprofen loaded ultrasound-engineered NLC. *Colloids and Surfaces B: Biointerfaces*, 81(2), 412-421.
- [60] Tian, B.-C. (2013). Further investigation of nanostructured lipid carriers as an ocular delivery system: In vivo transcorneal mechanism and in vitro release study. *Colloids and Surfaces B: Biointerfaces*, 102, 251-256.

- [61] Pardeike, J. (2011). Development of an Itraconazole-loaded nanostructured lipid carrier (NLC) formulation for pulmonary application. *International Journal of Pharmaceutics*, 419(1–2), 329-338.
- [62] Baudouin, C. (2010). Preservatives in eyedrops: The good, the bad and the ugly. *Progress in Retinal and Eye Research*, 29(4), 312-334.
- [63] Zhang, W. (2014). Nanostructured lipid carrier surface modified with Eudragit RS 100 and its potential ophthalmic functions. *International journal of nanomedicine*, 9(1178-2013), 4305-4315.
- [64] Shen, J. (2010). Thiolated nanostructured lipid carriers as a potential ocular drug delivery system for cyclosporine A: Improving in vivo ocular distribution. *International Journal of Pharmaceutics*, 402(1–2), 248-253.
- [65] Li, X. (2008). A controlled-release ocular delivery system for ibuprofen based on nanostructured lipid carriers. *International Journal of Pharmaceutics*, 363(1–2), 177-182.
- [66] Tamjidi, F. (2013). Nanostructured lipid carriers (NLC): A potential delivery system for bioactive food molecules. *Innovative Food Science & Emerging Technologies*, 19, 29-43.
- [67] Fathi, M., M.R. Mozafari, & M. Mohebbi. (2012). Nanoencapsulation of food ingredients using lipid based delivery systems. *Trends in Food Science & Technology*, 23(1), 13-27.
- [68] Das, S., W.K. Ng, & R.B.H. Tan. (2012). Are nanostructured lipid carriers (NLCs) better than solid lipid nanoparticles (SLNs): Development, characterizations and comparative evaluations of clotrimazole-loaded SLNs and NLCs?. *European Journal of Pharmaceutical Sciences*, 47(1), 139-151.
- [69] Loo, C. (2013). Effect of compositions in nanostructured lipid carriers (NLC) on skin hydration and occlusion. *Int J Nanomedicine*, 8, 13-22.
- [70] Ludwig, A. (2005). The use of mucoadhesive polymers in ocular drug delivery. *Advanced Drug Delivery Reviews*, 57(11), 1595-1639.
- [71] Liu, Z. (2011). Preparation and evaluation of solid lipid nanoparticles of baicalin for ocular drug delivery system in vitro and in vivo. *Drug Development and Industrial Pharmacy*, 37(4), 475-481.

- [72] Liu, C.-H. (2014). Novel Lutein Loaded Lipid Nanoparticles on Porcine Corneal Distribution. *Journal of Ophthalmology*, 2014, 1-11.
- [73] Luo, Q. (2011). Nanostructured lipid carrier (NLC) coated with Chitosan Oligosaccharides and its potential use in ocular drug delivery system. *International Journal of Pharmaceutics*, 403(1-2), 185-191.
- [74] Tian, B. (2012). Novel surface-modified nanostructured lipid carriers with partially deacetylated water-soluble chitosan for efficient ocular delivery. *J Pharm Sci*, 101(3), 1040-1049.
- [75] Li, N. (2009). Liposome coated with low molecular weight chitosan and its potential use in ocular drug delivery. *International Journal of Pharmaceutics*, 379(1), 131-138.
- [76] Schrader, S., G. Mircheff Ak Fau - Geerling, & G. Geerling. (2008). Animal models of dry eye. *Dev Ophthalmol*, 41(0250-3751), 298-312.
- [77] Barabino, S., & M.R. Dana. (2004). Animal Models of Dry Eye: A Critical Assessment of Opportunities and Limitations. *Investigative Ophthalmology & Visual Science*, 45(6), 1641-1646.
- [78] Li, N. (2013). Establishment of the mild, moderate and severe dry eye models using three methods in rabbits. *BMC Ophthalmology*, 13(1), 50.
- [79] Los, L.I. (2008). The rabbit as an animal model for post-natal vitreous matrix differentiation and degeneration. *Eye*, 22(10), 1223-1232.
- [80] Wei, X.E. (2013). Tear film break-up time in rabbits. *Clin Exp Optom*, 96(1), 70-75.
- [81] Coats, B. (2010). Ocular Hemorrhages in Neonatal Porcine Eyes from Single, Rapid Rotational Events. *Investigative Ophthalmology & Visual Science*, 51(9), 4792-4797.
- [82] Meltendorf, C. (2007). Endothelial cell density in porcine corneas after exposure to hypotonic solutions. *Graefes Arch Clin Exp Ophthalmol.*, 245(1), 143-147.
- [83] Williams, D. (2007). Rabbit and rodent ophthalmology. *European Journal of Companion Animal Practice*, 17(3), 242-252.
- [84] Barabino, S., W. Chen, & M.R. Dana. (2004). Tear film and ocular surface tests in animal models of dry eye: uses and limitations. *Experimental Eye Research*, 79(5), 613-621.

## CHAPTER III

### INTERACTION OF NANOSTRUCTURED LIPID CARRIERS WITH HUMAN MEIBUM

This chapter has been submitted to the International Journal of Applied Pharmaceutics and is currently being reviewed. This chapter focus on determining the nanostructured lipid carriers (NLCs) eye drop as tear replacement formulation in order to resemble natural tears and replenish the tear film. In our approach, nanostructured lipid carriers (NLCs) were produced with the aim to bind to the surface of the corneal epithelium and slowly release their lipid contents into the tear film. Consequently, the lipids would adsorb to the TFLL and will modify the TFLL's physical properties and hence the tear film stability. In this study, the surface activities of different NLCs formulation were tested in a Langmuir trough, and their surface pressure area (II-A) profiles were compared. Moreover, the ability of NLCs to adsorb and change the activity of meibomian lipid films was examined under fluorescence microscopy.

#### Introduction

A mainly aqueous tear film covers the exposed ocular surface. For it to spread across the surface of the eye and form a stable thin film, its surface tension at the air interface has to be lowered, otherwise, it would form tiny beads across the ocular surface. The tear film lipid layer (TFLL) reduces the surface tension of the tear film and therefore plays a major role in the spreading of the tear film [1]. The major component of the TFLL is meibum, a lipid secretion from holocrine glands in the eyelid [2]. The lipids in meibum are mainly hydrophobic wax and cholesterol esters with some triglycerides [3, 4, 5]. Meibum also contains a small proportion of amphipathic lipids, particularly (O-acyl) omega hydroxy fatty acids, which act as surfactants. The exact structure of the TFLL is unknown because once meibum is secreted onto the ocular surface, it has the opportunity to interact with components of the aqueous layer that include mucins, other proteins, and lipids from other sources

than meibum. Through these interactions, it self-assembles so that a normal tear film is resistant to evaporative loss [6].

It has been hypothesized that abnormal secretion of meibum or changes in its composition can cause tear film instability leading to dry eye disease (DED) [6, 7]. In general, artificial tear drops are used to give symptomatic relief from DED. These drops are designed to target the TFL or to provide a viscous aqueous substitute. However, they are washed out over time and hence require frequent instillation. This puts a burden on the patient and diminishes patient compliance. Accordingly, there is unmet need to enhance the artificial tear drops with agents that can provide sustained efficacy against signs and symptoms of DED.

Nanostructured lipid carriers (NLCs) [8] could be a solution to the problem of the short residence time of topical eye drops for DED. In particular, the NLCs made from lipid assemblages have been shown to have strong mucoadhesiveness to corneal epithelium [9, 10]. This means that they have a higher dwell time in the eye and hence will release its lipids through disintegration over a much longer period. This would markedly decrease the application frequency of a lipid-based eye drop. For example, NLCs designed to target the TFL with the lipids, they are comprised of would ideally bind to mucous components of the tear film, for example at glycocalyx at the surface of the corneal epithelium, and slowly release their lipid contents into the tear film. These released lipids would then adsorb and penetrate the TFL to improve the stability of TFL (Figure 3.1). Furthermore, a release of other drugs incorporate into the NLCs is also possible.

For this to happen, the NLCs would first need to pass through the tear film and hence have the opportunity to interact with the TFL. Therefore, this study focused on determining if the NLCs were able to interact directly with the TFL. To study this potential interaction in more detail, films of meibomian lipids formed by spreading meibomian lipids in a Langmuir trough [11-13] were used as a simple emulation of the TFL [14, 15]. NLCs were then added to the subphase or mixed with the meibomian lipids, and their effect on the meibomian lipid film was examined.



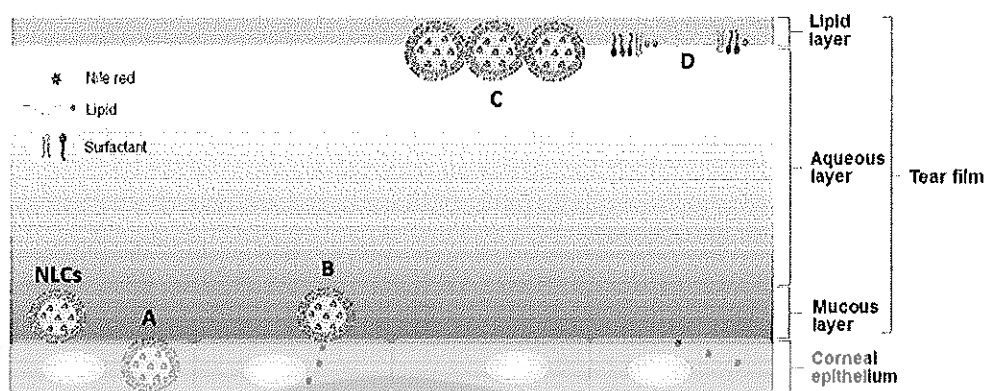


**Figure 3.1 Proposed mechanisms of NLCs after instilled into the eye. In term of ocular drug delivery, the NLCs pass through the tear film and A) endocytosis or B) slowly release the loaded drug into the corneal epithelium. Moreover, the NLCs may C) bind to the TFL or D) break down to release the lipids and surfactants then merge with TFL to enhance the tear film stability**

## Materials and Methods

### 1. Materials

Gelucire 44/14 (lauryl macrogol-32 glyceride), Gelucire 50/13 (G50/13), and Compritol 888 ATO (CATO, glyceryl behenate) were kindly gifted by Gattefossé (Cedex, France). Lexol GT865 (medium chain triglyceride), cetyl palmitate (CP), and squalene were purchased from Namsiang trading (Bangkok, Thailand). Tween 80 (T80), Span 20 (S20) was purchased from AjexFinechem (Sydney, Australia). Emulmetik 900 was purchased from Lucas Meyer (Ludwigshafen, Germany). Amicon Ultra 10K centrifugal filter was purchased from Merck Millipore (Massachusetts, USA).

Nile red was purchased from Sigma Aldrich (Massachusetts, USA). NBD-DPPC(1-plamitoyl-2-[12-[(7-nitro-2-1,3-benzoxadiazol-4-yl)aminododecanoyl]-sn-glycero-3-phosphatidylcholine) was obtained from Avanti Polar Lipids Inc. (Tullamarine, USA). Chloroform (HPLC grade) used for dissolving lipids was purchased from LabScan (NSW, Australia). There was no surface activity associated with this solvent. Ion exchange purified water (Milli-Q; Millipore, Billerica, MA) with

a resistance of 18.2 M $\Omega$  was used in all experiments. An artificial tear (AT) buffer that emulates ion concentrations in human tears was prepared (6.6 g/L NaCl, 1.7 g/L KCl, 1.4 g/L NaHCO<sub>3</sub>, 0.15 g/L CaCl<sub>2</sub>, 0.1 g/L NaH<sub>2</sub>PO<sub>4</sub>, 4.18 g/L MOPS, pH 7.4) and used as the subphase in the surface pressure experiments described below.

## 2. Preparation of NLCs

NLCs were prepared by a high-pressure homogenization (HPH) technique with a variation of solid lipid and surfactant (Table 3.1). Briefly, the lipid phase contained 2% (w/w) squalene, 2% (w/w) Emulmetik 900, 2% (w/w) Lexol GT865, and 3% (w/w) solid lipid (water comprised the remaining mass of the final NLCs). It was heated to 85°C to melt the lipids. The aqueous phase, consisting of 5% (w/w) surfactant dispersed in distilled water was slowly added to the oil phase at the same temperature while gently stirring with a glass rod. This primary emulsion was then stirred at 5000 rpm using a high-speed homogenizer (IKA<sup>®</sup>-T18, Staufen, Germany) for 1 min and then subjected to a high-pressure homogenizer (Microfluidics M-110P, Massachusetts, USA) applying 5 cycles at 1500 bar. The resulting hot o/w microemulsion was rapidly cooled to 25°C, re-solidifying the lipid and forming the NLCs. The resulting NLCs were washed twice with 0.9% NaCl solution in purified water using an ultrafiltration system (Amicon 8400, Massachusetts, USA) fitted with a molecular weight cut off 100kDa membrane to remove the excess starting components.

The mean particle size and polydispersity index (PI) of NLCs were determined by dynamic light scattering (DLS) with a ZetaPALS<sup>®</sup> analyzer (Brookhaven 90Plus, New York, USA). The zeta potential of NLCs was determined by measuring the particle electrophoretic mobility using ZetaPAL<sup>®</sup> analyzer.

## 3. Surface pressure-area (II-A) measurements of NLCs

The surface activity at an air-water interface of different formulations of NLCs was assessed by measuring changes to pressure-area (II-A) isocycles in a double barrier Langmuir trough (NIMA 102M, Coventry, UK). The individual components of NLCs and NLCs were spread onto the surface of ATB at 35°C in a double barrier Langmuir trough, isocycles performed and then the trough was cooled to 20 °C and further isocycles made. The samples were deposited by touching micro-drops of the solution to the surface of the subphase. The quantity of lipids that was

spread was chosen so that the initial  $\Pi$  was lower than 1 mN/m. The surface was compressed and expanded at a rate of 15 cm<sup>2</sup>/min with using a maximum surface area of 79 cm<sup>2</sup> and minimum surface area of 16 cm<sup>2</sup>. A Whilhelmy balance with Whatman filter paper type No.1 was used to record surface pressure during isocycles.

#### **4. The interaction of human meibomian lipid with optimized NLCs**

Meibomian lipids were collected using a metal spatula [16] from one of the authors, a 62-year-old male with no known ocular pathology. Samples from different collection dates (all within a week) were dissolved in chloroform and pooled, and the one sample was used for all experiments. The sample was dried under nitrogen gas and reconstituted to 1 mg/mL in chloroform and stored -20°C.

For microscopic analysis, the meibomian lipid films were doped with fluorescent marker 1% (w/w) NBD-DPPC, and 20  $\mu$ L of the mixture was spread at the air-buffer interface between two movable barriers in the Langmuir trough to form the meibomian lipid films. After 10 min, to allow chloroform evaporation,  $\Pi$ -A isocycles were carried out at 35°C as described above until equilibrium was reached (about 10 isocycles). The NLCs dispersions (3  $\mu$ L) were applied to the surface of the meibomian lipid film and further  $\Pi$ -A isocycles recorded. After 10 isocycles, the temperature was decreased to 20°C and further isocycles recorded.

The surface film was observed microscopically at a 400x magnification using a Leica epifluorescence microscope. The microscope was equipped with an excitation band to pass filter of 450-490 nm, a dichroic mirror with a reflection short pass of 510 nm and a barrier filter with a line pass of 515 nm for labeled lipid which fluoresced green. The filters could be swapped using a manual slide. Digital images were recorded using an Andor Ixon back-illuminated DV887ECS-BV camera at a shutter speed of 10<sup>-2</sup> s or less.

#### **5. The penetration of NLCs to the human meibomian lipid film**

Nile red (0.0005% w/v), a lipophilic fluorescent dye, was added to the lipid phase of some NLCs formulation during preparing process to give fluorescence tagged NR-NLCs. . NBD-DPPC doped meibomian lipid films were prepared at 20°C as described above. After equilibrium of these films were reached (10 isocycles), the barriers of the trough were moved so that the surface area was 30 cm<sup>2</sup>. Six microliters of NR-NLCs were injected into the subphase outside of the barrier, and  $\Pi$  monitored

over time with the area fixed at 30 cm<sup>2</sup>. When there was no further change in  $\Pi$  observed over time, a series of isocycles were performed, and  $\Pi$ -A profiles were recorded.

Again, the surface films were observed under a Leica epifluorescence microscope as described above. In case of investigation NR-NLC, an excitation band pass filter of 535-550 nm, dichroic mirror with a reflection short pass of 590 and a barrier filter with band pass of 610-675 nm were used. The filters could be swapped using a manual slide. Digital images were recorded using an Andor Ixon back-illuminated DV887ECS-BV camera at a shutter speed of 10<sup>-2</sup> s or less.

Scanning electron microscopy (SEM, JSM-7001F, JEOL, Tokyo, Japan) was used to visualize the surface morphology of NR-NLCs at the air interface. A silicon wafer was gently touched to the interface avoiding dipping it into the subphase. The sample was allowed to air-dry at room temperature and sputter-coated with gold. Then photomicrographs were taken at an acceleration voltage of 15 kV at a magnification of 10,000X.

## Results and discussions

### 1. NLCs formulations

In this study, NLCs were successfully prepared by a high-pressure homogenization technique with different types of solid lipid and surfactant. The physicochemical properties of different NLCs formulations are summarized in Table 3.1. The particle sizes were various from 38 – 280 nm based on types of solid lipid and surfactant. As previously reported the number of the fatty acid side chain on solid lipid and surfactant had a significant effect on the particle size of NLCs [17].

With regard to the different solid lipids, NLC1, NLC4, and NLC7, prepared with Compritol 888 ATO (fatty acid side chains, C<sub>22</sub>), showed larger particle sizes of 280 ± 9, 229 ± 11, and 154 ± 5 nm, respectively. Whereas preparing with Gelucire® 43/01 ((fatty acid side chains, C<sub>18</sub>); NLC2, NLC5, and NLC8) and cetyl palmitate ((fatty acid side chains, C<sub>16</sub>); NLC3, NLC6, and NLC9), reduced the particle size to ~ 40 nm. In the case of NLCs prepared with Compritol 888 ATO, the type of surfactant had a significant effect on the mean particle size (P<0.05). Indeed, NLC1 prepared with Tween 80 (fatty acid side chains, C<sub>18</sub>) as a surfactant, demonstrated a

larger particle size compared to NLC4 prepared with mix of Tween 80 and Span 20 (fatty acid side chains, C<sub>16</sub> and C<sub>12</sub>) and NLC7 prepared with Gelucire 44/14 (fatty acid side chains, C<sub>12</sub>). These larger size can be attributed to the solid lipid and surfactant with long fatty acid side chain [18]. However, in case of NLCs prepared with Gelucire 43/01 and cetyl palmitate, the different surfactants used appeared to have a minimal role in their particle size (Table 3.1). Also, all NLCs formulations exhibited a high zeta potential of -30 mV, which would provide long-term physical stability. The negative charge is most likely due to the presence of medium chain triglyceride carboxylic group on the particle surface [19].

**Table 3.1 The components and physicochemical properties of NLCs**

Formula	Solid lipid	Surfactant	PS (nm) ± SD	PI ± SD	ZP (mV) ± SD
NLC1	Compritol 888 ATO	T80	280 ± 9	0.22 ± 0.06	-33 ± 3
NLC2	Gelucire 50/13	T80	35 ± 6	0.27 ± 0.02	-29 ± 4
NLC3	cetyl palmitate	T80	39 ± 5	0.25 ± 0.00	-30 ± 2
NLC4	Compritol 888 ATO	T80; S20	229 ± 11	0.25 ± 0.03	-29 ± 3
NLC5	Gelucire 50/13	T80; S20	44 ± 4	0.22 ± 0.04	-27 ± 5
NLC6	cetyl palmitate	T80; S20	38 ± 3	0.25 ± 0.03	-25 ± 3
NLC7	Compritol 888 ATO	G 44/14	154 ± 5	0.27 ± 0.01	-31 ± 4
NLC8	Gelucire 50/13	G 44/14	38 ± 3	0.28 ± 0.04	-27 ± 1
NLC9	cetyl palmitate	G 44/14	35 ± 6	0.23 ± 0.02	-26 ± 3

SD: standard deviation for n=3, PS = particle size, PI = polydispersity index, ZP = zeta potential

## 2. The surface activity of NLCs formulations

An appropriate model for studying the behavior of these NLCs at air/water interface is to monitor their ability to spread using a Langmuir trough and measuring changes in  $\Pi$ . This has been used previously to study films of pure lipid and models of the TFL [11, 12, 13]. Typically experiments are carried out at both 20 °C and at

about the temperature of the ocular surface at  $\sim 35$  °C. The lower temperature is used because it is a temperature commonly used by physical chemists who use these techniques and hence allows the results to be compared more broadly with current literature. It should also be noted that molar quantities of nanoparticles could not be determined because there was a small variance in size of the particles. The amounts chosen to apply to the trough were such that take-off of the  $\Pi$ -A isotherms (having a measurable pressure) was below the maximum surface area ( $\sim 79\text{cm}^2$ ).

The  $\Pi$ -A isocycles of NLCs prepared with various solid lipid types as well as the effects of different surfactants are shown in Figures 3.2-4. All NLCs formulations showed high surface activity requiring only  $\sim 100$  ng of material to be applied to the surface. Surface activity was slightly higher at  $35$  °C versus  $20$  °C, which is to be expected based on the enhanced movement of the NLCs at higher temperatures. There was little change in the  $\Pi$ -A curves over multiple isocycles except for a slight decrease in  $\Pi$ , which would most likely indicate a reorganization of the NLCs on the surface. Films of NLC2 at  $35$  °C were an exception and showed a slight increase in  $\Pi_{\text{max}}$  over multiple isocycles (Figure 3.2B). There was no collapse of any of the films due to high surface pressures, and so it is most likely that the small changes to take-off area and  $\Pi_{\text{max}}$  were due to changes in packing of the NLCs during the course of multiple isocycles. For NLCs that used Compritol 888 as their solid lipid (NLC1, 4, and 7) slightly more preparation had to be applied to the surface to achieve a targeted take-off area comparable to the other NLC preparation. The reason for this is unclear, but it could be related to the size of the particles because these NLCs were much larger than the others (NLC2, 3, 5, 6, 8, and 9 having similar sizes  $\sim 37\text{nm}$  and NLC1  $\sim 280\text{nm}$ ; NLC4  $\sim 230\text{nm}$  and NLC7  $\sim 150\text{nm}$ ).

In general, the structure of NLCs particles is composed of the lipid phase matrix which is covered by the surfactant. To ensure that the  $\Pi$ -A profiles of the NLCs were not due to the surface activity of unincorporated starting products, the  $\Pi$ -A profiles of the individual components used to form the NLCs were examined (Appendix C-E). The  $\Pi$ -A profiles of the individual components of NLCs required larger amounts to be applied to the surface and showed unique patterns characteristic to the component and starkly different to the NLCs, which were made of these components. This confirms that the surface activity observed for the NLCs are not

caused by free surface-active components, which were not removed during the purification of the NLCs, but rather by the NLC themselves.

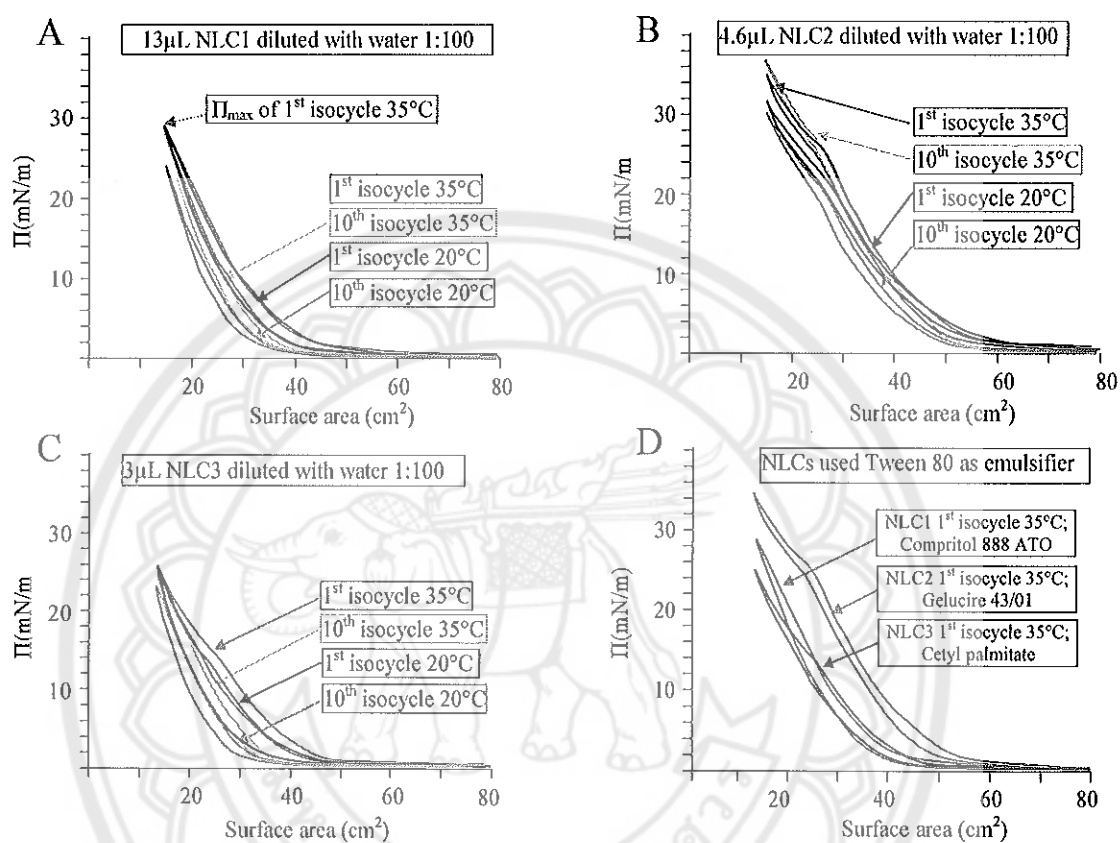


**Figure 3.2**  $\Pi$ -A curves comparing films of NLCs prepared with A) Compritol 888 ATO, B) Gelucire 43/01, and C) cetyl palmitate as solid lipid and Tween 80 as a surfactant when spread at 35 °C and then decreased to 20 °C. D) A direct comparison between the first isocycles of the three different NLCs

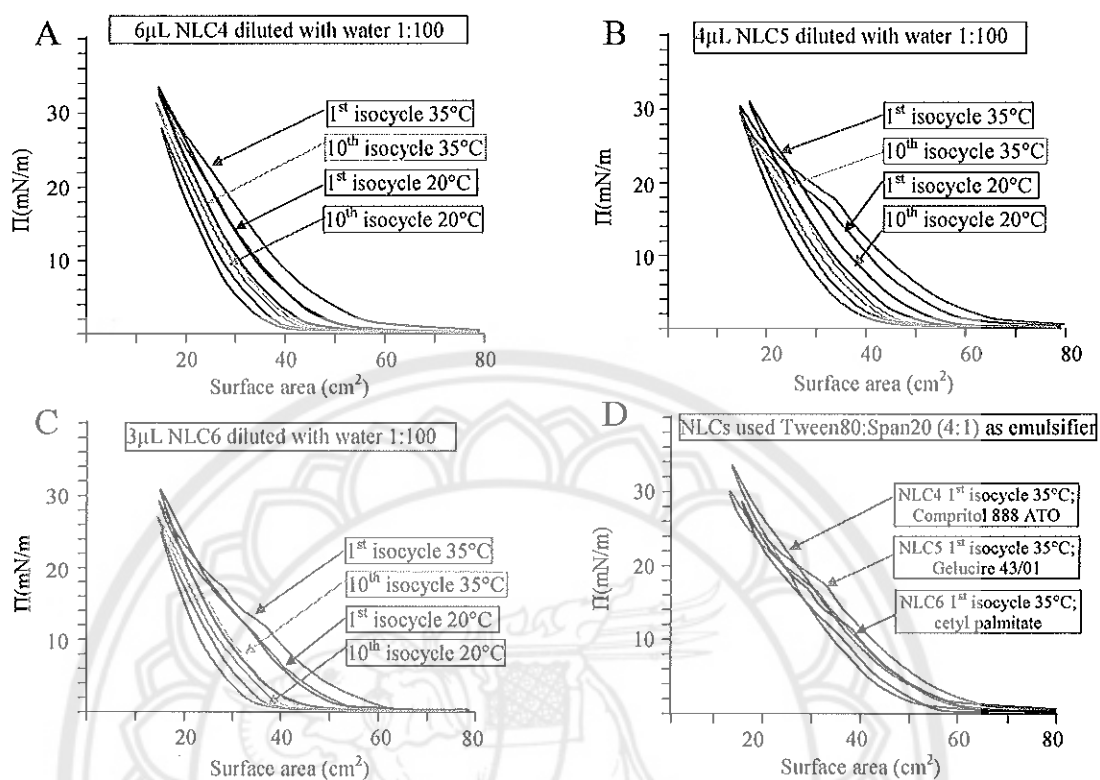


**Figure 3.3**  $\Pi$ -A curves comparing films of NLCs prepared with A) Compritol 888 ATO, B) Gelucire 43/01, and C) cetyl palmitate as solid lipid and Tween 80: Span 20 as a surfactant when spread at 35 °C and then decreased to 20 °C. D) A direct comparison between the first isocycles of the three different NLCs



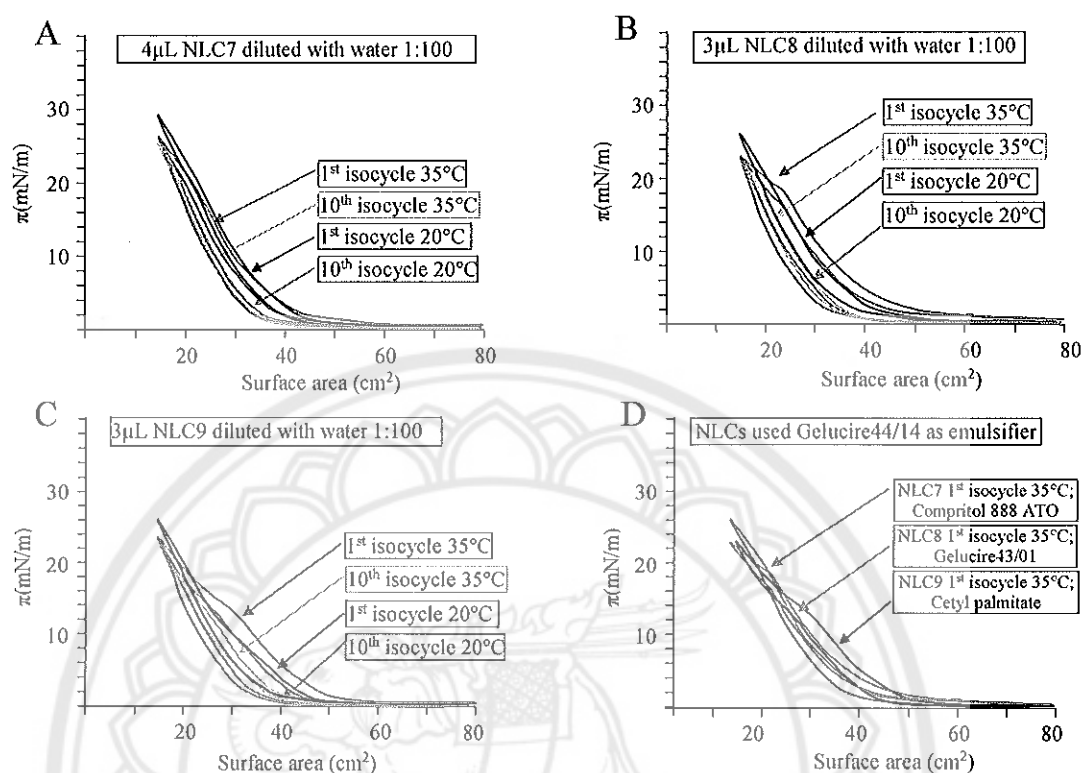


**Figure 3.4**  $\Pi$ -A curves comparing films of NLCs prepared with A) Compritol 888 ATO, B) Gelucire 43/01, and C) cetyl palmitate as solid lipid and Gelucire 44/14 as a surfactant when spread at 35 °C and then decreased to 20 °C. D) A direct comparison between the first isocycles of the three different NLCs

### 3. The interaction of human meibomian lipid with optimized NLCs

To study the interaction of meibum with NLCs, only NLCs prepared with Tween 80 as the surfactant component was used (NLC 1, 2, 3, see Table 3.1). The surface activity of meibomian lipid films has been well documented [14, 15]. Commonly, isocycles of meibum spread on a Langmuir trough are examined [20]. In this study, sample  $\Pi$ -A curves of meibomian lipid films doped with 1% (w/w) NBD-DPPC (a fluorescent marker) before adding the NLCs at 35 °C and 20 °C are shown in Figure 3.5. The effects of NLCs (NLC1, NLC2, and NLC3) applied to fluoromeibomian lipid films are shown in Figure 3.6. The  $\Pi$ -A profiles of fluoromeibomian lipid films seeded with NLCs showed an increase in  $\Pi_{\text{max}}$  and the  $\Pi$ -

A profiles were dominated by the meibomian lipids. Furthermore, the shape of the curves of the meibomian films mixed with NLCs was also similar and did not collapse at the smallest surface areas compared to meibomian lipid films, although it had more lipids applied to the surface (data not shown). This clearly indicated that the NLCs were contributing to the surface activity of the film and were most likely at the surface. There was a slight decrease in  $\Pi$  over multiple isocycles, and  $\Pi_{\max}$  decreased over time at 35°C, which was not observed with pure meibomian films. This could indicate some reorganisation of the NLCs at the surface or that some NLCs might be moving off the surface. There were some slight differences in the  $\Pi$ -A isocycle curves between the different NLCs mixed with meibum. Most notable was a slight phase shift (flattening of the profile) for the NLC2 seeded film at 35°C.

These data indicate that the NLCs are surface active and interact with or are at least incorporated in meibomian lipid films. This ability of the NLCs to interact with meibomian lipids has to be taken into account when using those NLCs as a potential vehicle for delivery of drugs to the ocular surface. It also opens the possibility of designing NLCs to treat deficiencies in the tear film lipid layer in some forms of dry eye.

Fluorescence microscopy was then used to gauge the distribution of the NLCs in the meibomian films (Figure 3.7). The films observed at 35 °C were too fluid and their fast changes did not allow photography of them. Thus only data for the film at 20 °C are reported. Brightly fluorescent regions in the films indicate regions rich in meibomian lipids and darker regions indicate areas depleted in meibomian lipids, and hence probably more abundant in NLCs.

In general terms, the mixed films with the different NLCs gave different appearances, which means that the different NLCs interacted with the meibomian lipids differently. Since each of the different NLCs were prepared with the same surfactant, the difference must be attributed the effect of the solid lipid component of the NLCs or their sizes. Most notable was that NLC2 seemed to disperse within the film but not evenly mix with the film irrespective of the surface pressure or the number of isocycles. Similarly, NLC1 also did not mix evenly with the meibomian lipids, but different to NLC2 tended to remain in specific regions rather than dispersed throughout the film. This distribution pattern remained stable throughout many

isocycles. At higher pressures, the darker zones, indicating meibomian lipid depletion, disappeared. This is likely to be due to NLC1 was being forced off the surface which would correspond to the inflection at higher pressures in the  $\Pi$ -A isocycle curves (Figure 3.7). NLC3 seemed to mix more evenly with the meibomian lipids, at least in part, giving relatively even gray areas to the film when compared to NLC1 or NLC2. In the 1<sup>st</sup> isocycle there were bright fluorescing zones suggesting that initially, NLC3 did not mix well with the meibomian lipids. However, within the next and the following isocycles the resulting film displayed an even appearance.

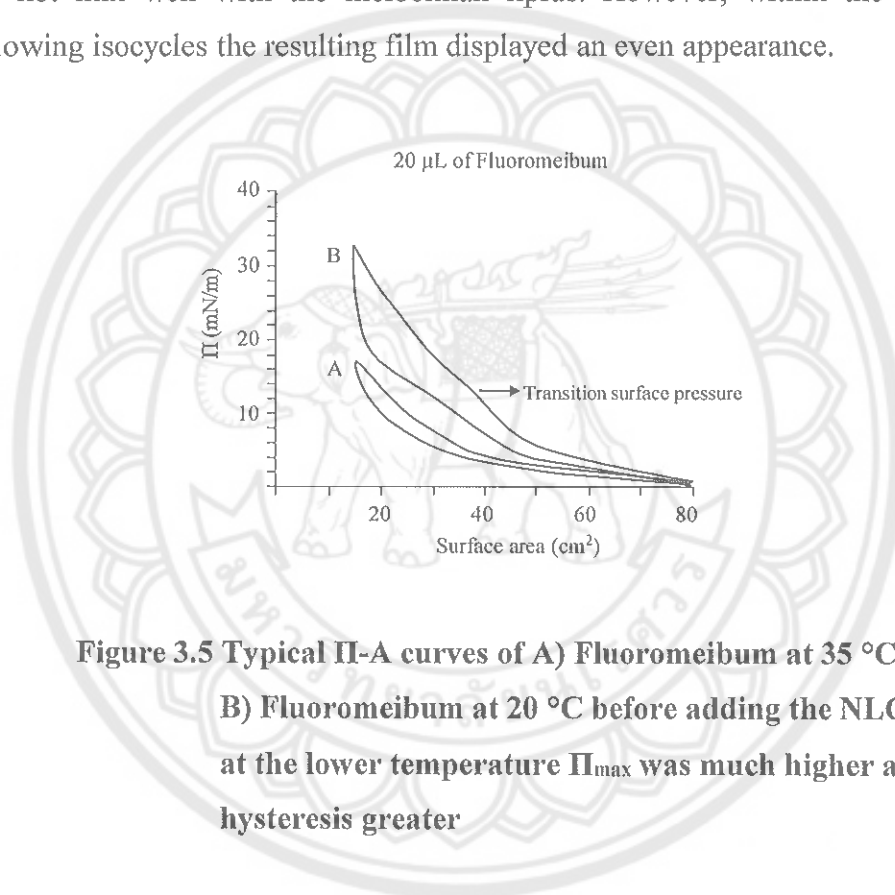


**Figure 3.5 Typical  $\Pi$ -A curves of A) Fluoromeibum at 35 °C and B) Fluoromeibum at 20 °C before adding the NLCs. Note that at the lower temperature  $\Pi_{\max}$  was much higher and hysteresis greater**

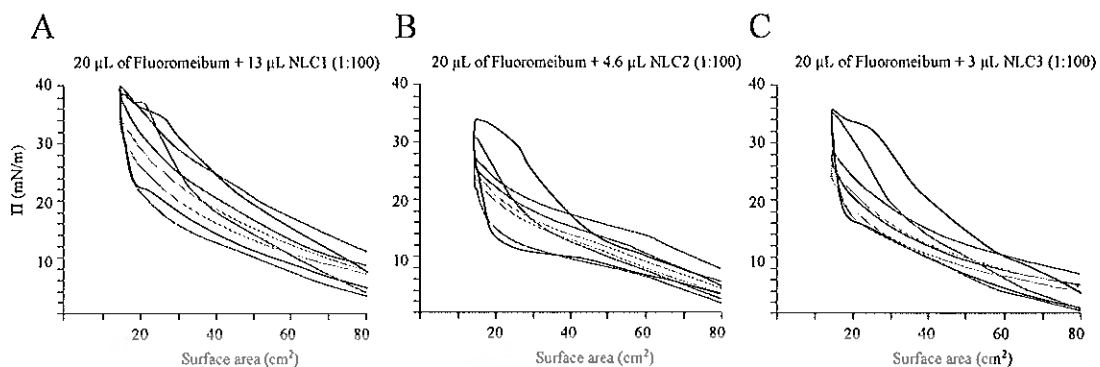


**Figure 3.6**  $\Pi$ -A curves comparing films of meibomian lipids mixed with A) NLC1, B) NLC2, and C) NLC3 when spread at 35 °C (red line; 1<sup>st</sup> isocycle and yellow line; 10<sup>th</sup> isocycles) and then decreased to 20 °C (black line; 1<sup>st</sup> isocycle and blue line; 10<sup>th</sup> isocycles)

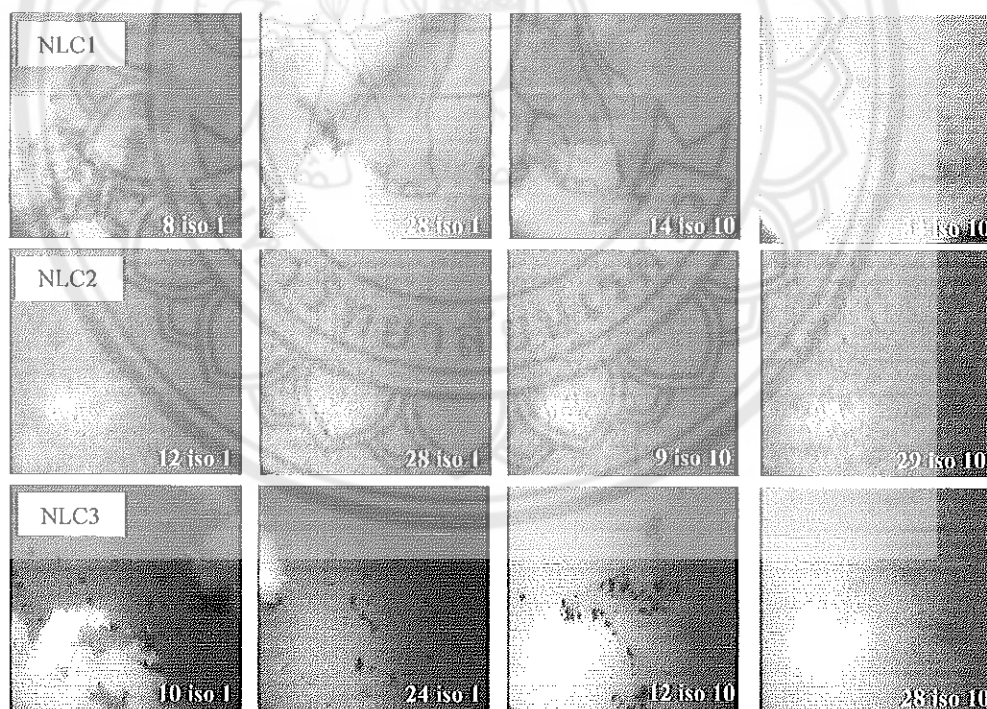


**Figure 3.7** Micrographs comparing the appearances of meibomian lipids mixed with A) NLC1, B) NLC2, and C) NLC3 during 1<sup>st</sup> and 10<sup>th</sup> isocycles at 20 °C, respectively. The surface pressure during compression of the film and the isocycle is given, e.g. 8 iso 1 means that the pressure was 8 mN/m during compression in isocycle 1

#### 4. The penetration of NLCs to human meibomian lipid film

It is anticipated that pharmaceutical formulations of NLCs would be applied to the ocular surface as aqueous-based drops and therefore in addition to interacting directly with the tear film lipid layer (simulated above), some NLCs could become incorporated in the aqueous component of the tear film and therefore in theory would have to diffuse to the TFL in order to interact with it. This was tested by evaluating the penetration of NLCs from the subphase into a meibomian lipid film. Such penetration by NLCs from the subphase is indicated by an increase in  $\Pi$  over time of a meibomian lipid film kept at a fixed area. Following injection of NLCs into the subphase outside the barriers,  $\Pi$  slowly increased over time and then stabilised (Figure 3.8). After there was no further change in  $\Pi$ , a series of isocycles at 20 °C were performed and  $\Pi$ -A profiles were recorded. The  $\Pi$ -A profile showed similar characteristics to a pure meibomian lipid film. In addition, the NLCs penetrated to meibomian lipids had greater surface activity (higher  $\Pi_{\max}$ ) than the meibomian lipid alone, which was further evidence that the NLCs had integrated into the meibomian lipid layer. In this case the Nile Red tagged were used and the meibomian lipids were seeded with a green fluorescing lipid (NBD-DPPC). By swapping filters, the distribution of the NLCs in the films could be seen (Figure 3.9). The micrographs showed that there were regions of clumping of the fluorophores and this clumping increased with the number of isocycles. Both fluorophores showed the same pattern rather than complementary patterns indicating that there was mixing of the meibomian lipids, or at least of the fluorophores the meibum was doped with, with the Nile red NLCs, while other areas of the film were depleted of those fluorophores (Figure 3.9).

To determine if NLCs had reached the surface and had interacted with the meibomian lipid film, rather than possible breakdown products from the NLCs, samples of the film were collected using a silicon wafer. To allow space on the trough to collect the sample, the barriers were compressed to 30cm<sup>2</sup> rather than the maximal normal 15cm<sup>2</sup>. These were not true Blodgett films as the wafer was not placed in the subphase, but rather those films were collected from the air/lipid interface. This was to minimise the possibility of any particles being seen coming from the subphase rather than the surface. Scanning electron microscopy of these wafers showed that the NLCs had integrated with the meibomian lipid film (Figure 3.10).

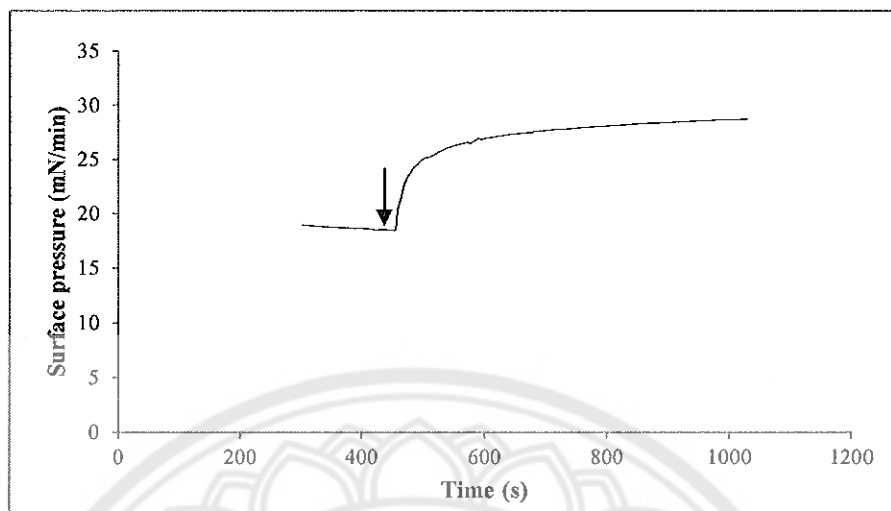


**Figure 3.8**  $\Pi$ -time curve of a fluoromeibum film with  $\Pi_{init}$  set to 20 mN/m at 20 °C, a further 6  $\mu$ L of NR-NLCs added to the subphase (arrow), showed that NR-NLCs was able to still penetrate the film

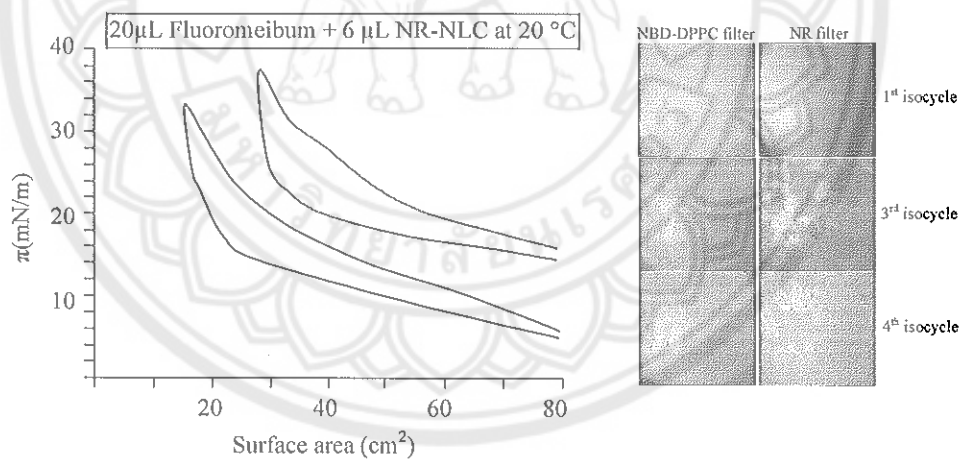


**Figure 3.9**  $\Pi$ -A curves of NR-NLCs penetrated to predeposited meibomian lipids at 20 °C (red line). The 10<sup>th</sup> isocycles of Fluoromeibum alone at 20 °C are also shown (black line). Micrographs of the appearances of meibomian lipids mixed with NR-NLCs during 1, 3, and 4 isocycles are represented. The curve with NR-NLCs is shifted to the right by the barriers were closed to 30cm<sup>2</sup>

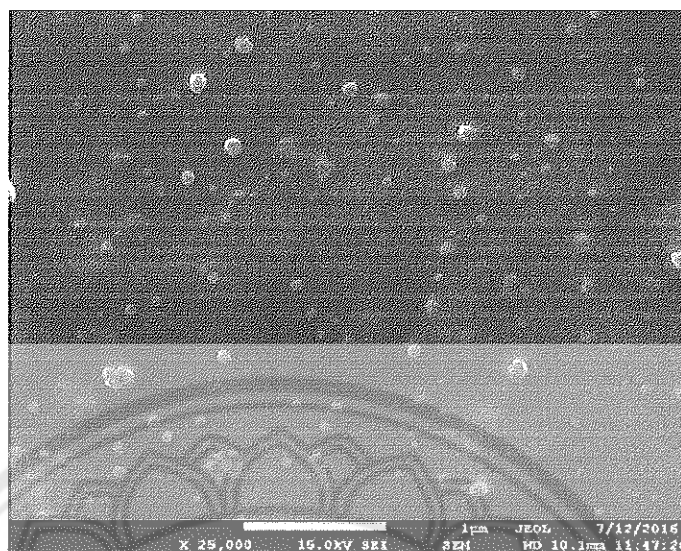


**Figure 3.10 SEM micrograph of NR-NLCs penetrated to fluoromeibum at 20 °C**

### **Conclusions**

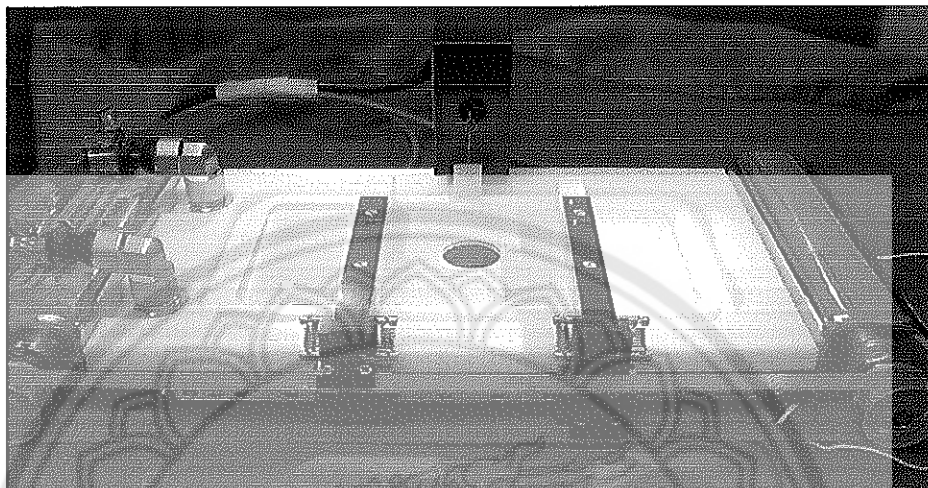
In summary, NLCs designed to attach to the ocular surface for the delivery of their drugs can also interact with meibomian lipid films both directly and by diffusing from the subphase. It is therefore likely that in vivo, NLCs applied in eye drop formulations to the ocular surface will also in part integrate with the tear film lipid layer. Therefore, development of these types of drug delivery mechanisms must take this into account because disruption of the tear film lipid layer is associated with dry eye. On the other hand, different types of NLCs interact with meibomian lipid films differently, and so it theoretically would be possible to tailor the NLCs to bind strongly to the ocular surface and at the same time have minimum effect on the lipid layer or even improve the performance of the lipid layer.



**APPENDIX**

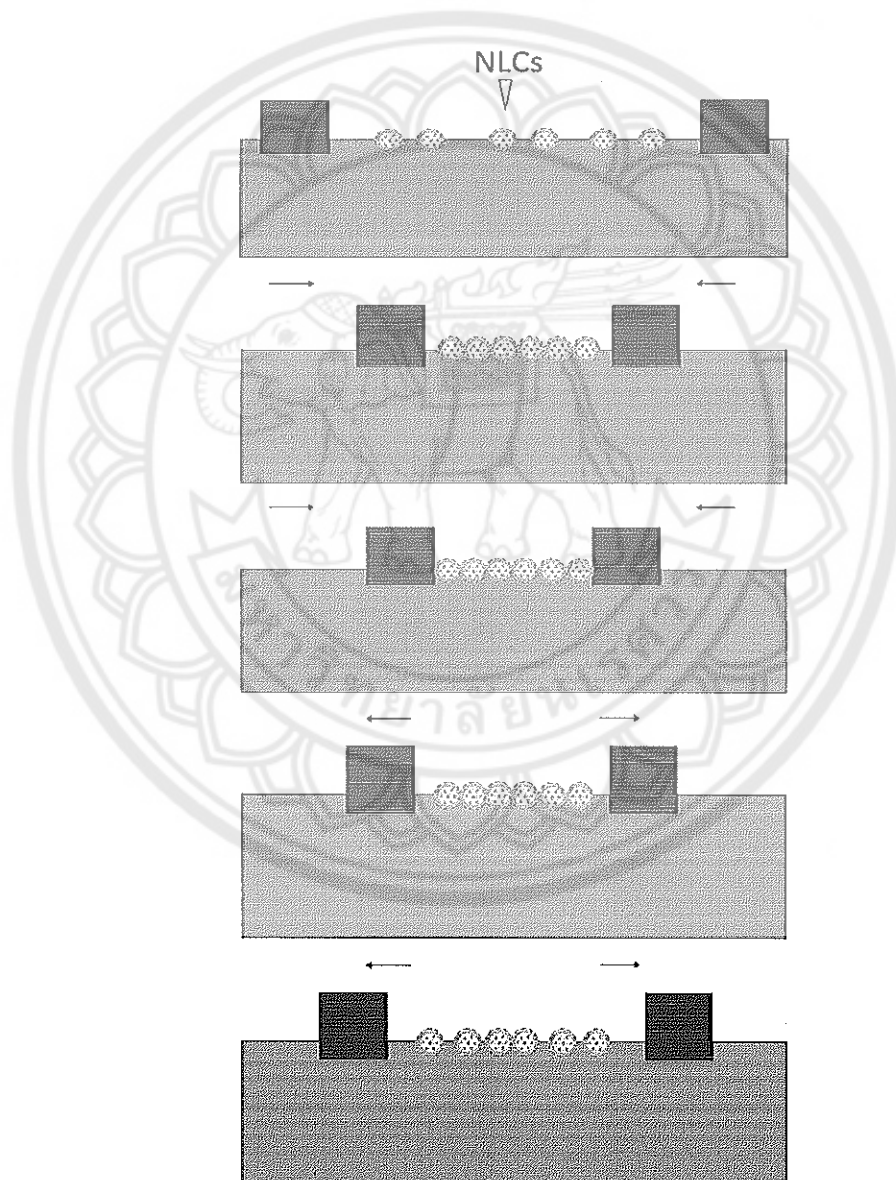


**Appendix A Langmuir trough with two-moveable barriers and the pressure sensor to measure the surface pressure change at interface**

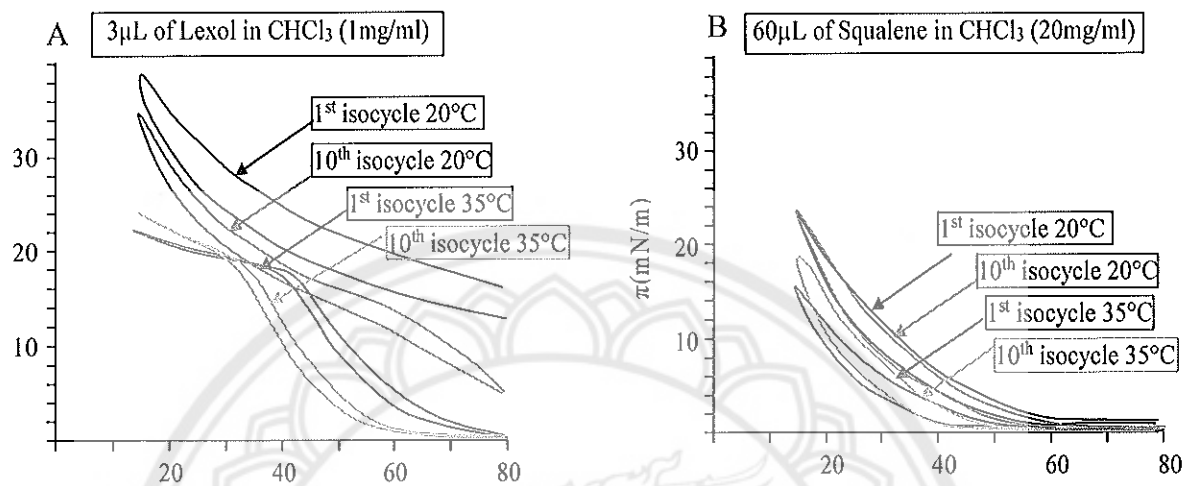


**Appendix B Schematic diagram of the experimental trough apparatus showing the NLCs particles confined in the area between barriers.**

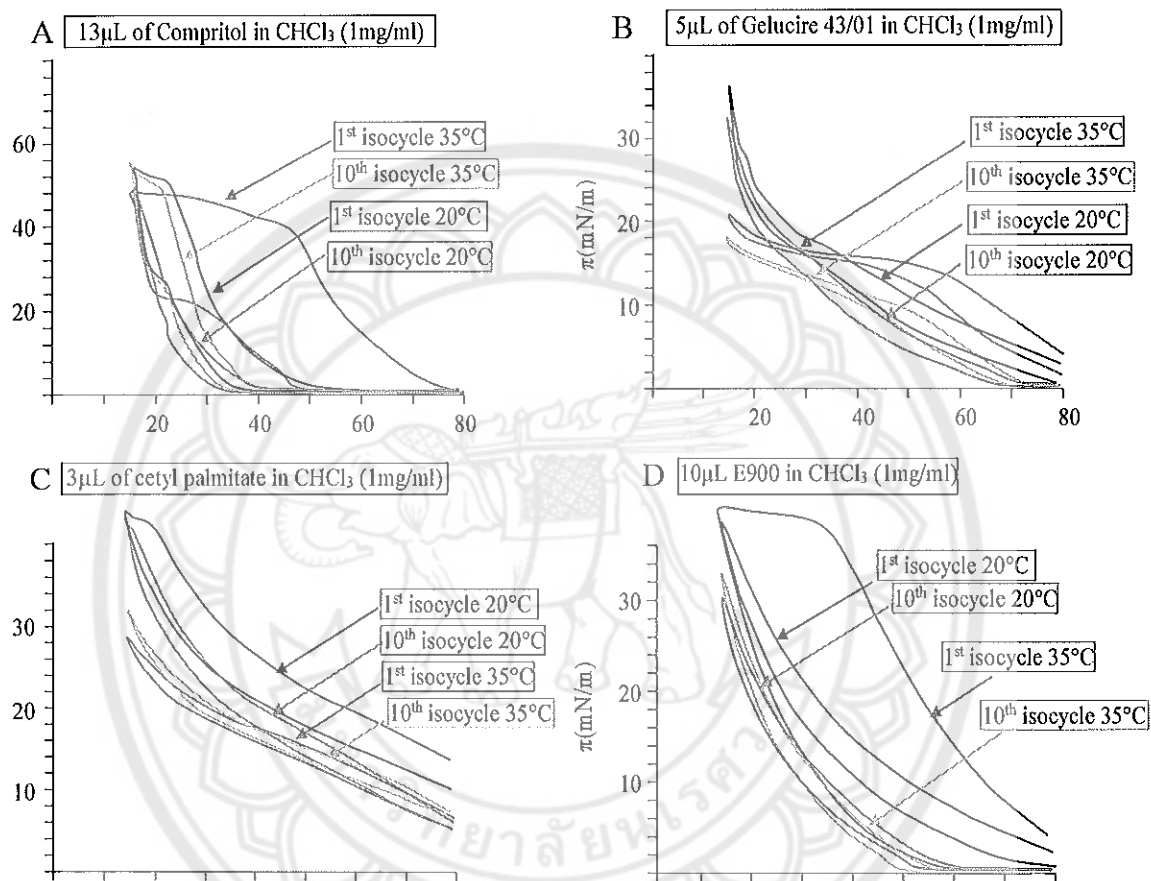
**By closing the coupled barriers, the NLCs forced to attach with other particles, thus, the surface pressure is increasing. In contrast, the surface pressure is decreasing while the barriers are opening and the NLCs particles are separated**



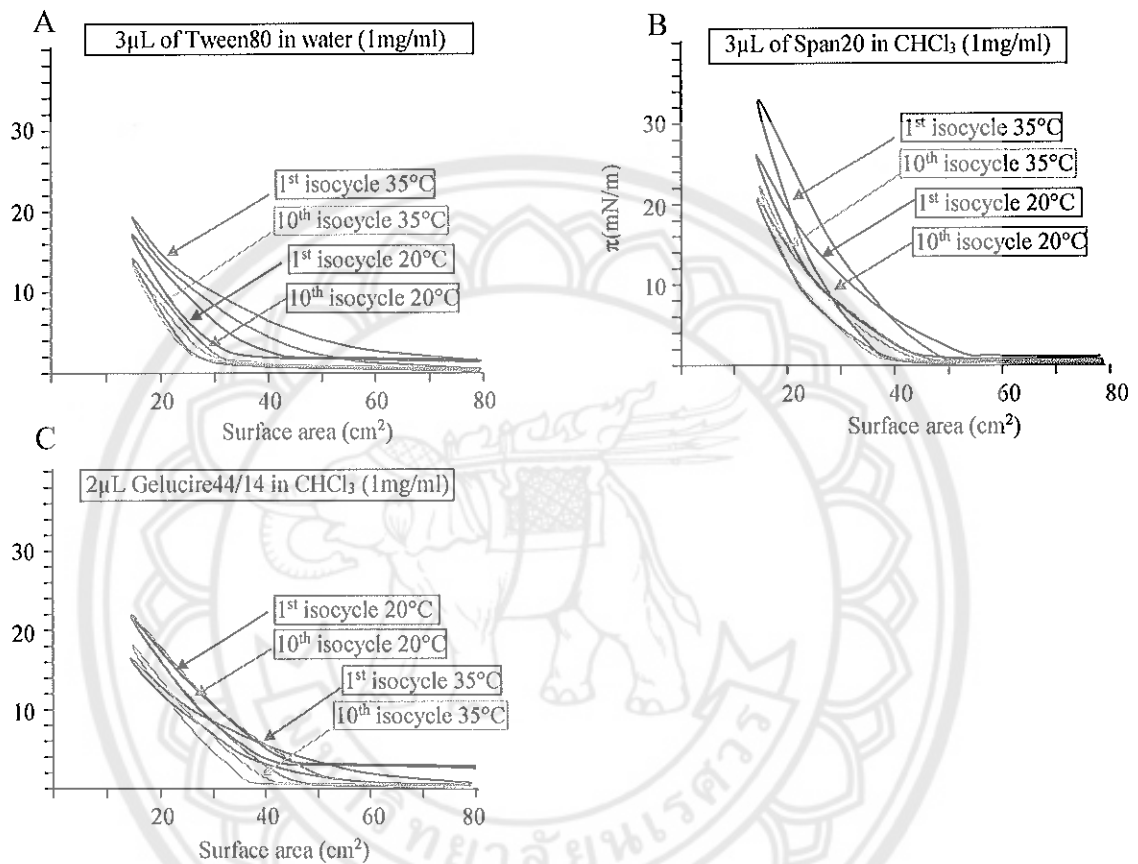
**Appendix C Pressure area curves films of A) Lexol and B) Squalene when spread at  $34 \pm 1$  °C and then decreased to  $20 \pm 1$  °C**



**Appendix D Pressure area curves films of A) Compritol, B) Gelucire 43/01, C) cetyl palmitate, and C) E900 when spread at  $34 \pm 1^\circ\text{C}$  and then decreased to  $20 \pm 1^\circ\text{C}$**



**Appendix E Pressure area curves films of A) Tween 80, B) Span 20, and C) Gelucire 44/14 when spread at  $34 \pm 1^\circ\text{C}$  and then decreased to  $20 \pm 1^\circ\text{C}$**





**REFERENCES**

## REFERENCES

- [1] Cwiklik, L. (2016). Tear film lipid layer: A molecular level view. *Biochimica et Biophysica Acta (BBA) - Biomembranes*, 1858(10), 2421-2430.
- [2] Bron, A.J., & J.M. Tiffany. (2004). The contribution of meibomian disease to dry eye. *Ocul Surf*, 2(2), 149-165.
- [3] Millar, T.J., & B.S. Schuett. (2015). The real reason for having a meibomian lipid layer covering the outer surface of the tear film – A review. *Experimental Eye Research*, 137, 125-138.
- [4] Butovich, I.A., J.C. Wojtowicz, & M. Molai. (2009). Human tear film and meibum. Very long chain wax esters and (O-acyl)-omega-hydroxy fatty acids of meibum. *Journal of Lipid Research*, 50, 2471-2485.
- [5] Lam, S.M., Tong, L., Yong, S.S., Li, B., Chaurasia, S.S., Shui, G., & Wenk, M.R. (2011). Meibum Lipid Composition in Asians with Dry Eye Disease. *PLOS ONE*, 6(10), e24339.
- [6] Stevenson, W., S.K. Chauhan, & R. Dana. (2012). Dry eye disease: an immune-mediated ocular surface disorder. *Arch Ophthalmol*, 130(1), 90-100.
- [7] Barabino, S. (2012). Ocular surface immunity: Homeostatic mechanisms and their disruption in dry eye disease. *Progress in Retinal and Eye Research*, 31(3), 271-285.
- [8] Araújo, J. (2009). Nanomedicines for ocular NSAIDs: safety on drug delivery. *Nanomedicine: Nanotechnology, Biology and Medicine*, 5(4), 394-401.
- [9] Hao, J. (2012). Development and optimization of baicalin-loaded solid lipid nanoparticles prepared by coacervation method using central composite design. *European Journal of Pharmaceutical Sciences*, 47(2), 497-505.
- [10] Tian, B.-C. (2013). Further investigation of nanostructured lipid carriers as an ocular delivery system: In vivo transcorneal mechanism and in vitro release study. *Colloids and Surfaces B: Biointerfaces*, 102, 251-256.
- [11] Schuett, B.S., & T.J. Millar. (2013). An investigation of the likely role of (O-acyl)  $\omega$ -hydroxy fatty acids in meibomian lipid films using (O-oleyl)  $\omega$ -hydroxy palmitic acid as a model. *Experimental Eye Research*, 115, 57-64.

- [12] Georgiev, G.A. (2012). Surface chemistry study of the interactions of pharmaceutical ingredients with human meibum films. *Invest Ophthalmol Vis Sci*, 53(8), 4605-4615.
- [13] Heurtault, B. (2003). Interfacial stability of lipid nanocapsules. *Colloids and Surfaces B: Biointerfaces*, 30(3), 225-235.
- [14] Herok, G.H., P. Mudgil, & T.J. Millar. (2009). The effect of Meibomian lipids and tear proteins on evaporation rate under controlled in vitro conditions. *Curr Eye Res*, 34(7), 589-597.
- [15] Bhamla, M.S. (2016). Instability and Breakup of Model Tear Films. *Invest Ophthalmol Vis Sci*, 57(3), 949-958.
- [16] Mudgil, P., M. Torres, & T.J. Millar. (2006). Adsorption of lysozyme to phospholipid and meibomian lipid monolayer films. *Colloids and Surfaces B: Biointerfaces*, 48(2), 128-137.
- [17] Seyfoddin, A., & R. Al-Kassas. (2013). Development of solid lipid nanoparticles and nanostructured lipid carriers for improving ocular delivery of acyclovir. *Drug Development and Industrial Pharmacy*, 39(4), 508-519.
- [18] Seyfoddin, A., J. Shaw, & R. Al-Kassas. (2010). Solid lipid nanoparticles for ocular drug delivery. *Drug Delivery*, 17(7), 467-489.
- [19] Huang, Z.R. (2008). Development and evaluation of lipid nanoparticles for camptothecin delivery: a comparison of solid lipid nanoparticles, nanostructured lipid carriers, and lipid emulsion. *Acta Pharmacologica Sinica*, 29(9), 1094-1102.
- [20] Schuett, B.S., & T.J. Millar. (2013). An investigation of the likely role of (O-acyl)  $\omega$ -hydroxy fatty acids in meibomian lipid films using (O-oleyl)  $\omega$ -hydroxy palmitic acid as a model. *Experimental Eye Research*, 115(Supplement C), 57-64.



## CHAPTER IV

### NANOSTRUCTURED LIPID CARRIERS AS A BIONIC TEAR FILM IN RABBIT EVAPORATIVE DRY EYE MODEL

This chapter has been submitted to the Cornea and is currently being reviewed. This chapter provide the information about characterizing the developed NLCs eye drop as tear replacement and evaluate the efficacies of NLCs eye drop in order to improve the stability of tear film and decrease the ocular surface epithelial cells damaged from desiccation condition in rabbit evaporative dry eye model.

#### Introduction

The tear film is a liquid layer covering the cornea and acting as a barrier between the eye and environment [1]. The outermost layer of the tear film is coated by lipids which well-known as a tear film lipid layer (TFLL). This TFLL is responsible for reducing the surface tension of the tear film and increasing the tear film stability that related to dry eye disease (DED) [1]. The major component of the TFLL is meibum; a lipid secretion from holocrine glands in the eyelid [2]. It has been hypothesized that abnormal secretion of meibum or changing of the meibum composition can cause tear film instability, a major cause of evaporative dry eye [3, 4]. In general, artificial tear drops are the most widely used to relief dry eye symptomatic [5]. These drops are designed to target the TFLL or to provide a viscous aqueous substitute [6]. However, the efficacy of the drops is transient and the drops need frequent instillation because of they are rapidly clearance by tear and blinking. These limitations put a burden on the patient and diminish patient compliance.

To overcome these problems, nanostructured lipid carriers (NLCs) has been proposed to solve the short residence time of topical eye drop [7]. In particular, the NLCs made from lipid assemblages have been shown to have strong mucoadhesiveness to corneal epithelium [8, 9]. Thus, they have a higher dwell time in the eye and hence could release its lipids through disintegration over a much longer period. This would markedly decrease the frequent application of a NLCs eye drop. In

addition, our previous study suggested that NLCs could provide the means to develop efficient formulations for targeting dry eye conditions related to a non-functional TFLL [10].

According to our previous study, the surface activities of different NLCs formulation and the effect of NLCs on the meibomian lipid film were tested using a Langmuir trough [10]. We found that NLCs possess strongly surface active and interact with meibomian lipid films. They also provide the possibility of designing NLCs to treat deficiencies in the TFLL in evaporative dry eye. The type of interaction can be tailored by altering the solid lipids used in the formulation of the NLCs. Thus, the optimized NLCs formulation prepared with cetyl palmitate as solid lipid was selected in this study. They were autoclavable that suitable for ophthalmic formulation and mixed more evenly with the meibomian lipids when compared to other NLCs formulations.

Although we previously demonstrated the NLCs can be directly improve the lipid tear film structure and provide the possibility of designing NLCs to treat deficiencies in the TFLL in evaporative dry eye. To the best of our knowledge, there is no report about NLCs eye drop behaviour *in vivo* model. Therefore, the aims of this study were to characterize the optimized NLCs eye drop as a tear replacement and evaluate its efficacies in order to improve the stability of tear film and decrease the ocular epithelial cell damaged from desiccation condition in rabbit model.

## **Materials and methods**

### **1. Materials**

Lexol GT865 (medium chain triglyceride), cetyl palmitate and squalene were purchased from Namsiang trading (Bangkok, Thailand). Tween 80 (Polysorbate 80) was acquired from AjexFinechem (Sydney, Australia). Emulmetik 900 was purchased from Lucas Meyer (Ludwigshafen, Germany). Amicon Ultra 10K centrifugal filter was kindly gifted from Merck Millipore (Massachusetts, USA). Normal saline solution (sodium chloride 0.9%) was purchased from General Hospital Products Public (Pathum Thani, Thailand). Fluorescein sodium ophthalmic strips 1.0 mg (Flu-Glo®) was purchased from Akorn (Illinois, USA).

Keratinocyte serum-free medium (K-SFM), bovine pituitary extract, recombinant human epidermal growth factor (EGF), and Gibco antibiotic-antimycotic (100x) were purchased from Invitrogen (California, USA). Hydrocortisone solution, human insulin solution, bovine serum albumin (BSA), bovine collagen type I, and human fibronectin were obtained from Sigma-Aldrich (Steinheim, Germany).

## **2. NLCs eye drop preparation**

The NLCs was prepared by a high pressure homogenization (HPH) technique. Briefly, the lipid phase contained 2% (w/w) squalene, 2% (w/w) phosphatidylcholine, 2% (w/w) Lexol GT865, and 3% (w/w) cetyl palmitate. It was heated to 85°C to melt the lipids. The aqueous phase, consisting of 5% (w/w) Tween 80 dispersed in distilled water was slowly added to the oil phase at the same temperature while gently stirring with a glass rod. This primary emulsion was then stirred at 5000 rpm using a high speed homogenizer (IKA®-T18, Staufen, Germany) for 1 min and then subjected to a high pressure homogenizer (Microfluidics M-110P, Massachusetts, USA) applying 5 cycles at 1500 bar. The resulting hot o/w microemulsion was rapidly cooled to 25°C, re-solidifying the lipid and forming the NLCs. The resulting NLCs were washed twice with 0.9% NaCl solution in purified water (pH 7.4) using an ultrafiltration system (Amicon 8400, Massachusetts, USA) fitted with a molecular weight cut off 100kDa membrane to remove the excess starting components. After preparation process, the NLCs eye drop was placed in a glass vial and sealed with rubber stoppers and aluminum caps. Then, the sample was sterilized by steam sterilization at 121 °C for 15 min at 2 bar.

## **3. Characterization of the NLCs eye drop**

Mean particle size and polydispersity index (PI) of NLCs were determined by dynamic light scattering (DLS) with a ZetaPALS® analyzer (Brookhaven 90Plus, New York, USA). The zeta potential of NLCs was determined by measuring the particle electrophoretic mobility using ZetaPAL® analyzer. Samples were dispersed in DI water at ambient temperature, and 10 measurement cycles were performed. All samples were performed in triplicate.

The pH of the NLCs formulation was determined using a pH meter (SevenEasy S20, Mettler Toledo, Barcelona, Spain) calibrated at pH 4.01, 7.00, and 9.21 with standard solutions (InLab<sup>®</sup> Solution, Mettler Toledo, Greifensee, Switzerland). Measurements were performed in triplicate.

The osmolality was analysed by osmometer (Osmomet 010, Gonotec, Berlin, Germany) after calibration with 300 mOsm NaCl solution. Measurements were performed in triplicate at 35 °C, which corresponding to ocular surface temperature.

The surface tension of NLCs formulation was measured with a tensiometer (K6, Kruss, Hamburg, Germany) by Du nouy ring method in triplicate at 35 °C.

#### **4. Cytotoxicity of NLCs eye drop in primary porcine corneal epithelial (PCE) cells**

Primary porcine corneal epithelial (PCE) cells from primary tissue explant technique were cultured [11, 12]. Briefly, the cornea was excised from the freshly isolated porcine eye, then sterilized with 1% (v/v) povidone-iodine for 5 min and rinsed thrice with PBS containing 1% (v/v) antibiotic-antimycotic. The explant was then placed epithelial side down onto 6-well tissue pre-coated culture plate with coating solution contained BSA, bovine collagen I, and human fibronectin. The explant was further cultured in K-SFM with supplements at 37 °C, in a humidified atmosphere containing 5% CO<sub>2</sub>. The cornea was removed after 5 days, and the outgrowing cells were maintained in culture medium for 2 - 3 weeks.

The cytotoxicity was assessed by the STE test using MTT assay as described by Kojima et al. but with some modifications [13]. The PCE cells were seeded on 96-well plate at  $2 \times 10^4$  cells/well until reaching the semi-confluence (2 - 3 days). Then, the cells were exposed to 200  $\mu$ L of 0.05% (v/v) NLCs and 5% (v/v) NLCs dispersed in PBS for 5 min at room temperature. In addition, PBS and 0.01% (w/v) sodium lauryl sulfate (SLS) were used as vehicle and positive control, respectively. After exposure, the cells were washed with PBS twice, and 200  $\mu$ L of methyl thiazol diphenyl-tetrazolium bromide (MTT) solution (0.5 mg/mL) in culture medium was added. After incubated for 2 h, MTT formazan was extracted with 200  $\mu$ L of a mixture of 0.04 N HCl in absolute isopropanol and DMSO (1:1, v/v) for 30 min. The absorbance was measured at 570 nm with a microplate reader (BioStack Ready, Vermont, USA). The relative cell viability was calculated comparing to the

vehicle, then, category and rank classification was determined as described by Takahashi et al. [14].

### **5. Animals**

Nine-week-old male New Zealand white rabbits, weighing approximately 1.5 - 2.0 kg, were obtained from National Laboratory Animal Center, Mahidol University, Nakorn Pathom Province. All rabbits were housed in separate standard rabbit cage (2 rabbits/cage) under temperature ( $20 \pm 1^\circ\text{C}$ ), relative humidity ( $55 \pm 10\%$ ) and light (12-hour light-dark cycle) conditions at Naresuan University, Center for Animal Research (NUCAR). They were fed the standard diet and RO water ad libitum and were allowed for acclimatization for at least 5 days before use in any experiments. Only healthy rabbits with no corneal infection, infiltration, or leukoma were used. All experiments were approved by the Naresuan University Animal Care and Use Committee (NU-AE580611).

### **6. The retention of NLCs eye drop on corneal surface**

Five male New Zealand white rabbits were used in this study (Appendix A). The retention of NLCs eye drop and the improvement of tear film stability on the corneal surface was examined using a custom-built slit-lamp microscopy (CSLM, Nikon FS-2, Mikon Inc., New York, USA) attached with a Nikon D5300 DSLR for digital photography. Briefly, the rabbits were anesthetized by subcutaneous injection of a mixture of 35 mg/kg ketamine and 5 mg/kg xylazine. Then, they were maintained with isoflurane 2 - 3% in 100% oxygen. The depth of anesthesia was verified by pedal withdrawal reflex or ear pinch response before perform any experimental maneuver. During the anesthesia, the color of the mucous membranes (eye, lip, and tongue) were observed and the respiratory rate, the heart beat and the rectal temperature were monitored using PhysioSuite® system (Kent Scientific Corporation, Connecticut, USA). Following the absence of reflexes, rabbit's eyes were gently held open with tape on the eyelids under temperature of  $20 \pm 1^\circ\text{C}$  and relative humidity of  $55 \pm 10\%$ . A single instillation of 50  $\mu\text{L}$  of NLCs eye drop contained 0.2% (w/v) fluorescein sodium (flu-NLC) was administered topically onto the right eye of each rabbit ( $n = 5$ ). While, the left eyes of a total of five rabbits, were treated with 50  $\mu\text{L}$  of NSS contained 0.2% (w/v) fluorescein sodium (flu-NSS) and used as the control ( $n = 5$ ). The appearance of the tear film on the corneal surface was determined at 1, 5, 10, 15,

30, and 60 min after the instillation of the samples. In addition, the fluorescein intensity (%) on the corneal surface of tear film images was quantified by Image J software.

#### **7. The effect of NLCs eye drop on ocular surface epithelial cells of rabbit after exposure with desiccation conditions**

The effect of NLCs eye drop on evaporative-type dry eye in rabbits was investigated according to the previously described study [15]. A total six rabbits (12 eyes) were used in this study with separated into four groups, including closed eye (3 eyes), opened eye (3 eyes), commercial artificial tears (3 eyes), and NLCs eye drop (3 eyes).

In this study, the rabbits were anesthetized as described above and kept under desiccation conditions at 22 – 25 °C, 45 ± 10 % relative humidity (Appendix B). Immediately, after held the eye open with tape, a single instillation of 50 µL of NLCs eye drop and commercial artificial tears was dropped into the right and left eyes of 3 rabbits ( $n = 3$ ), respectively. Then, the eyes were kept open for 3 h. In addition, another 3 rabbits were used as control groups, the right and left eyes were kept close and open ( $n = 3$ ) for 3 h, respectively.

After 3 h, the corneas were stained with 50 µL of 1% methylene blue (MB) solution, which a vital stain is taken up by dead or damaged cells but not by living cells. The excess MB was rinsed off with NSS and the rabbits were euthanized by an overdose of sodium pentobarbital 100 mg/kg IP. The eyes were enucleated and the corneas were stained with 50 µl of 1% MB solution again, and then rinsed with NSS to remove excess MB. After that, the cornea tissue was isolated and the MB in the isolated cornea tissue was extracted with acetone/sodium sulfate solution for 3 days. Finally, the amount of MB was determined with a spectrophotometer at 660 nm.

The data was represent as the absorbance of MB extracted per mg.protein, which the amount of protein from each tissue was determined by BCA assay.

## Results

### 1. Physicochemical characterizations of the NLCs eye drop

The physicochemical characteristics of NLCs eye drop before and after autoclaving were reported in Table 4.1. After sterilization, the NLCs showed good physical stability without the appearance of oil droplets, phase separation, or particle aggregation. The NLCs eye drop showed a particle size of ~ 35 nm with a narrow size distribution (<0.3) and exhibited a high zeta potential of ~ -30 mV, which would provide a long-term physical stability. In addition, the optimized NLCs achieved values for pH, osmolarity, and surface tension close to the physiological range as presented in Table 4.1. Moreover, no significant difference in all the parameters was observed before and after autoclaving (Table 4.1).

**Table 4.1 Physicochemical properties of the NLCs eye drop before and after autoclaving**

Property	Formulation	
	NLCs	NLCs (after autoclave)
Mean size (nm) ± SD	35 ± 6	37±5
Polydispersity index ± SD	0.27 ± 0.02	0.29 ± 0.03
Zeta potential (mV) ± SD	-29 ± 4	-30 ± 2
pH ± SD	6.98 ± 0.02	6.90 ± 0.01
Osmolarity (mOsm/L) ± SD	281 ± 2	273 ± 1
Surface tension (mN/m) ± SD	38 ± 0	39 ± 1

### 2. Cytotoxicity test of NLCs eye drop

As shown in Table 4.2, exposure of PCE cells to 0.5 and 5% NLCs, showed cell viability of > 70%. Based on Takahashi et al., they could be classified as non-irritants [14]. On the other hand, 0.01% of SLS (positive control) exhibited cell viability (%) of  $46.70 \pm 2.68$ , confirming its irritation potential [14].

**Table 4.2 Summary of short time exposure (STE) tests performed by MTT assay**

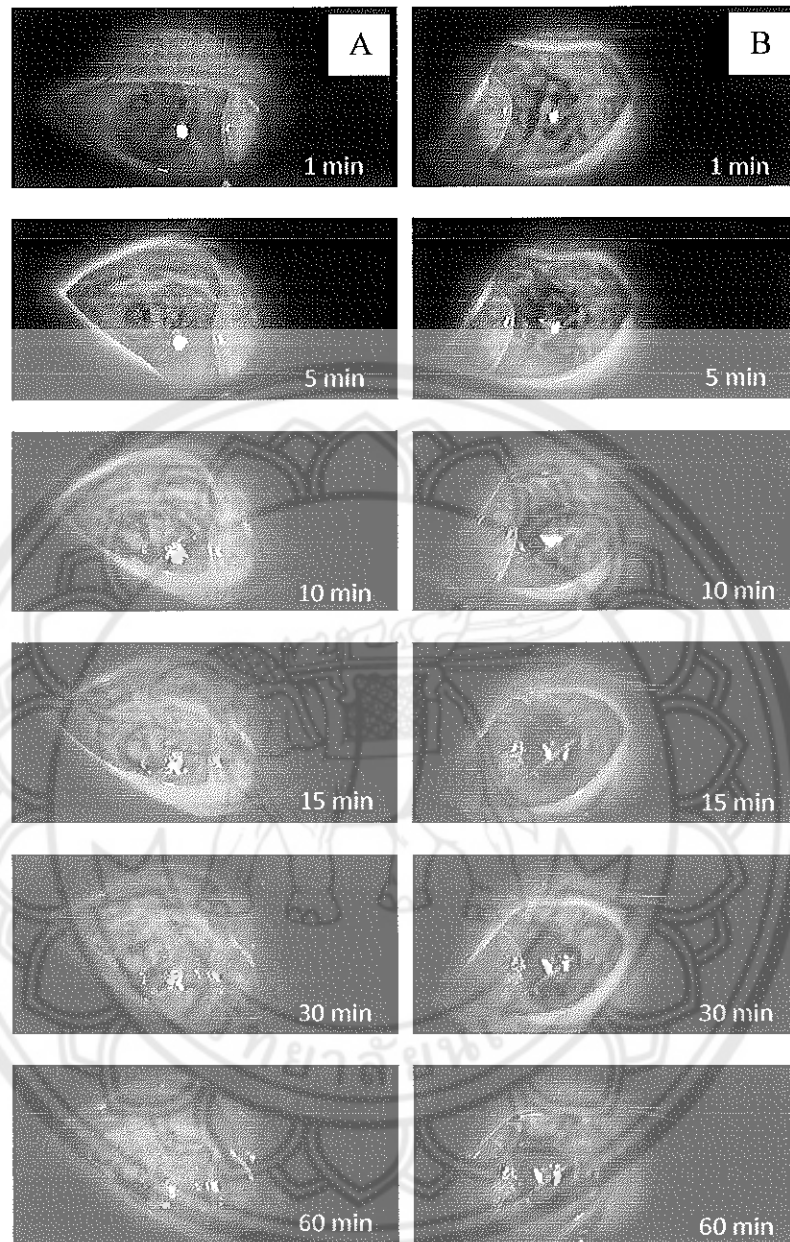
<b>Sample (w/v)</b>	<b>Cell viability (%) (mean <math>\pm</math> SD)</b>	<b>STE classification<sup>a</sup></b>
<b>5 % NLCs</b>	85.75 $\pm$ 7.54	non-irritant
<b>0.05 % NLCs</b>	96.34 $\pm$ 2.84	non-irritant
<b>0.01% SLS</b>	56.70 $\pm$ 2.68	irritant

<sup>a</sup>Eye irritation potential classification STE; Cell viability > 70% is classified as non-irritant [21].

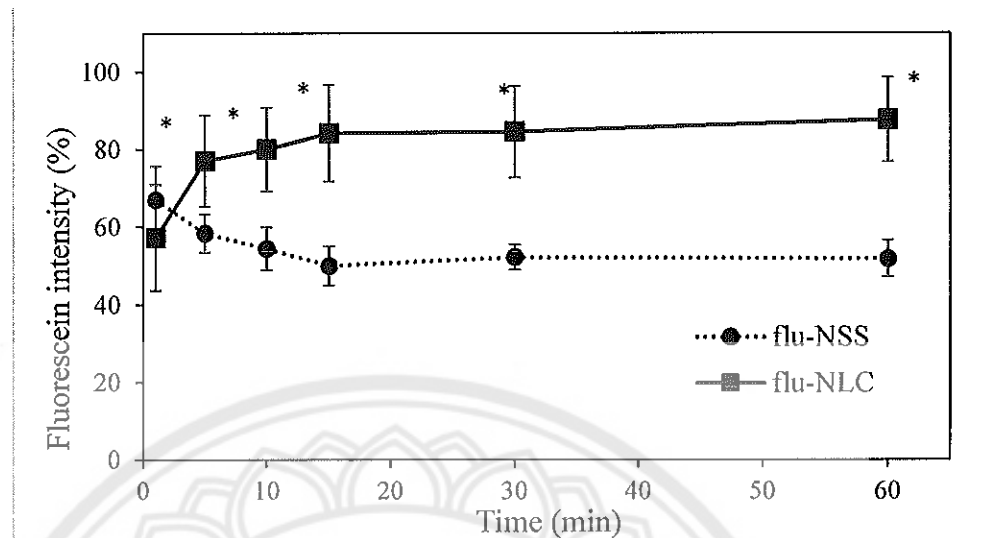
### 3. The retention of NLCs eye drop on corneal surface in rabbit eyes

Figure 4.1 showed fluorescence images of the rabbit precorneal surface at various time points after administration of NLCs eye drop compared with NSS. The NLCs eye drop was mixed with fluorescein sodium (flu-NLC) for tear film visualization. As shown in Fig. 4.1A, flu-NLC formed a stable precorneal film on the rabbit eye and was retained longer up to 60 min after administration, while the flu-NSS formed a weakly short-lived fluorescent film on the corneal surface and mostly disappeared from the eye after 15 min administration. Moreover, the fluorescein intensity (%) of the rabbit precorneal surface was quantified using Image J software and represented in Figure 4.2. After 1 min instillation of flu-NLC, the fluorescein intensity was 57.26  $\pm$  13.66 % and increased to 87.63  $\pm$  10.83 % after 60 min instillation. In contrast, the fluorescein intensity of flu-NSS was decreased from 67.05  $\pm$  8.58 to 51.74  $\pm$  4.76 % after 1 min and 60 min instillation, respectively. This result indicated that flu-NSS could not strongly adhere to the cornea surface and was quickly cleared by nasolacrimal drainage system. As expected, flu-NLC showed strong fluorescein intensity up to the end of experiment suggesting NLCs formulations enhanced the retention on the corneal surface and replenish tear film stability of rabbit eyes. In addition, instillation of flu-NLC did not show to cause local toxicity or irritation to the rabbit eyes.





**Figure 4.1** The fluorescence images of the rabbit preocular surface at 1, 5, 15, 30, and 60 min after administration of A) flu-NLCs and B) flu-NSS obtained with custom-built slit-lamp microscopy attached with a Nikon D5300 DSLR for digital photography (n=5)



**Figure 4.2** The fluorescence intensity (%) of fluorescence images of the rabbit preocular surface after instillation of flu-NLC compared with flu-NSS at various time points analyzed by ImageJ software ( $n = 5$ ; mean  $\pm$  SD). Student *t* test between flu-NLC and flu-NSS: \* =  $p < 0.05$

#### 4. Effect of NLCs eye drop on ocular surface epithelial cells of rabbit after exposure with desiccation conditions

To evaluate the effect of the NLCs eye drop on corneal epithelium cells after exposure with desiccation conditions, the rabbit evaporative-type dry eye model was used. The absorbance of MB extracted per mg.protein from the cornea of closed eye (negative control) and opened eye (positive control) showed statistically significant difference ( $P = 0.023$ ),  $0.04 \pm 0.01$  and  $0.08 \pm 0.02$ , respectively (Figure 4.3). This result indicated that the opened eye illustrated significant epithelial cell damage compared to the closed eye. Interestingly, the MB absorbance per mg.protein of cornea exposed to the NLCs eye drop ( $0.04 \pm 0.01$ ) was similar those of closed eye, and lower than the cornea exposed to the commercial artificial tears ( $0.07 \pm 0.02$ ), indicating that the NLCs eye drop had a higher ability to protect the ocular surface contact with desiccation conditions than commercial artificial tears.

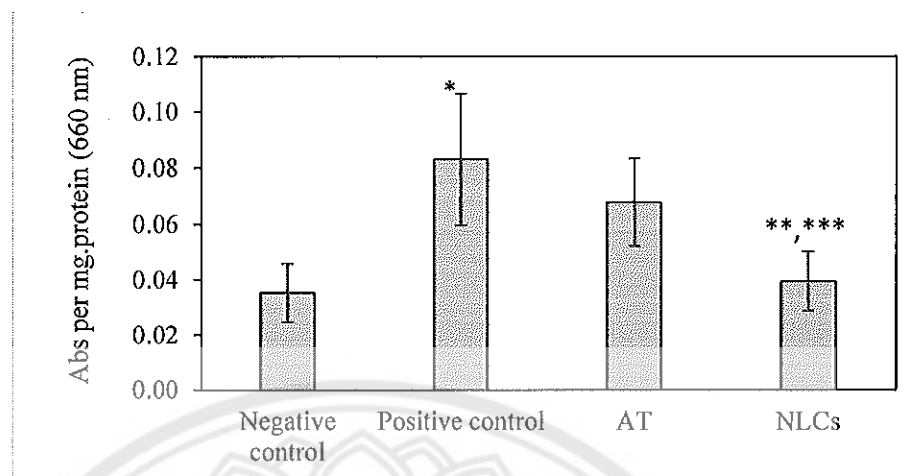


**Figure 4.3** The absorbance of MB per mg.protein of rabbit cornea tissue in different conditions; closed eye (negative control), open eye (positive control), treated with commercial artificial tear (AT), and treated with a NLCs eye drop (NLCs) (n = 3; mean  $\pm$  SD). Statistically significant differences were determined by one-way ANOVA, Turkey multiple comparison test; \* =  $p < 0.05$  compared with negative control; \*\* =  $p < 0.05$  compared with positive control; \*\*\* =  $p < 0.1$  compared with commercial artificial tears

## Discussion

Evaporative dry eye is the most common form of dry eye disease (DED), which usually associated with alterations and instability of the tear film. Therefore, the tear film stability enhancement is a fundamental in DED treatment. In general, artificial tear eye drop has long been used as a first line for DED treatment. Unfortunately, its major advantages are transient effects and frequent application requirement. According to the extremely complex in composition of natural tears, the tear replacements have been recently developed to more closely mimic the combination of aqueous and lipid layers of tear film. As suggested by several studies, the lipid-based eye drops are composed of natural components of the tear film and have surface-active properties. Thus, many researchers have focused on lipid-based nanocarriers, such as emulsions, cationic emulsions, and liposomes [16]. Among the lipid-based nanocarriers, NLCs possess a unique characteristic that is useful for the

treatment of DED. NLCs have been developed to combine the advantages of other colloidal carriers but without their disadvantages [17]. Particularly, NLCs can be prepared using physiological lipid similar to emulsions and liposomes, but NLCs shows better physical stability than those.

The optimized NLCs prepared with cetyl palmitate as solid lipid was used in this study due to it can be mixed more evenly with the meibomian lipids when compared to other NLCs formulations. In addition, NLCs composed of phosphatidylcholine and squalene owing to they usually detected in human meibum, which could mimic closely to the natural tear [18]. Also, Tween 80 used as surfactant could help stabilized the TFL at the tear interface [18]. As consider to the component of the developed NLCs eye drop, this could had a potential to resemble natural tear and replenish the tear film [5].

To formulate a suitable NLCs eye drop for ophthalmic applications, the important physicochemical properties such as particle size, zeta potential, sterility, pH, osmolarity, and surface tension should be considered [19, 20]. The developed NLCs showed the mean size of  $39 \pm 5$  nm which is considered optimum for ocular application because it is unlikely to cause mechanical abrasions and blurred vision after topical administration [21]. In addition, this NLCs is possible to sterile by autoclaving method which is the strongest advantage of NLCs for the ophthalmic formulation [22]. The NLCs eye drop showed a pH of  $\sim 7$  which is in a good agreement with the pH range of normal tears (7.0 - 7.4) and most of commercial products (5 - 7) [23]. If the pH value gets outside the range of 4 - 8 which is tolerated by eye, the patient may feel discomfort, irritation, and increase the tearing. It has been known that the osmolarity of tears is a highly relevant challenge to the normal cell function in human corneal epithelial cells. Generally, the tear osmolarity is higher in a patient with dry eye (311 - 360 mOsm/L) compared to that of non-dry eye [24]. Therefore, the ophthalmic product with osmolarity closes to the normal tears (270 - 310 mOsm/L) would be suggested. In addition, the surface tension of NLCs eye drop was  $39 \pm 1$  mN/m, which similar to the physiological range of normal tears (40 - 46 mN/m) [25] suggesting a good spreading of NLCs over the ocular surface [1]. Furthermore, the surface tension of dry eye tears was  $49.6 \pm 2.2$  mN/m, therefore, we hypothesized that the lower surface tension of NLCs eye drop could balance the dry

eye tears to within the normal tears range. Additionally, NLCs eye drop showed no evidence of aggregation over 6 months at ambient temperature (data not shown). While others lipid-based nanocarrier such as liposome has a poor stability in aqueous media. As reported by Vicario-de-la-Torre et al., the liposome size remained stable for 2 months when stored at 4°C [5]. From these studies, we hypothesized that the NLCs eye drop provided an appropriate physicochemical properties for dry eye management.

One of the critical factors should be taken into consideration for ophthalmic formulation is toxicity. For many years, the method of choice to determine eye irritation potential is the Draize rabbit eye test. However, ethical considerations and the limited value of animal models including lack of reproducibility and overestimation of human response led to the development of alternative *in vitro* tests [23]. Short time exposure (STE) *in vitro* test is recommended for assessing eye irritation potential. The STE method is straightforward and known to provide rapid results with the excellent predictive ability [26]. As expected, NLCs eye drop showed much less toxicity by a PCE cells compared to 0.1% SLS (positive control). These can be explained by its composition, physiological lipids and non-ionic surfactant (Tween 80), were reported as non-irritation to the rabbit eye [20, 27]. In accordance with the *in vivo* experiment, no adverse effects were observed in the rabbit eyes after instillation of NLCs eye drop.

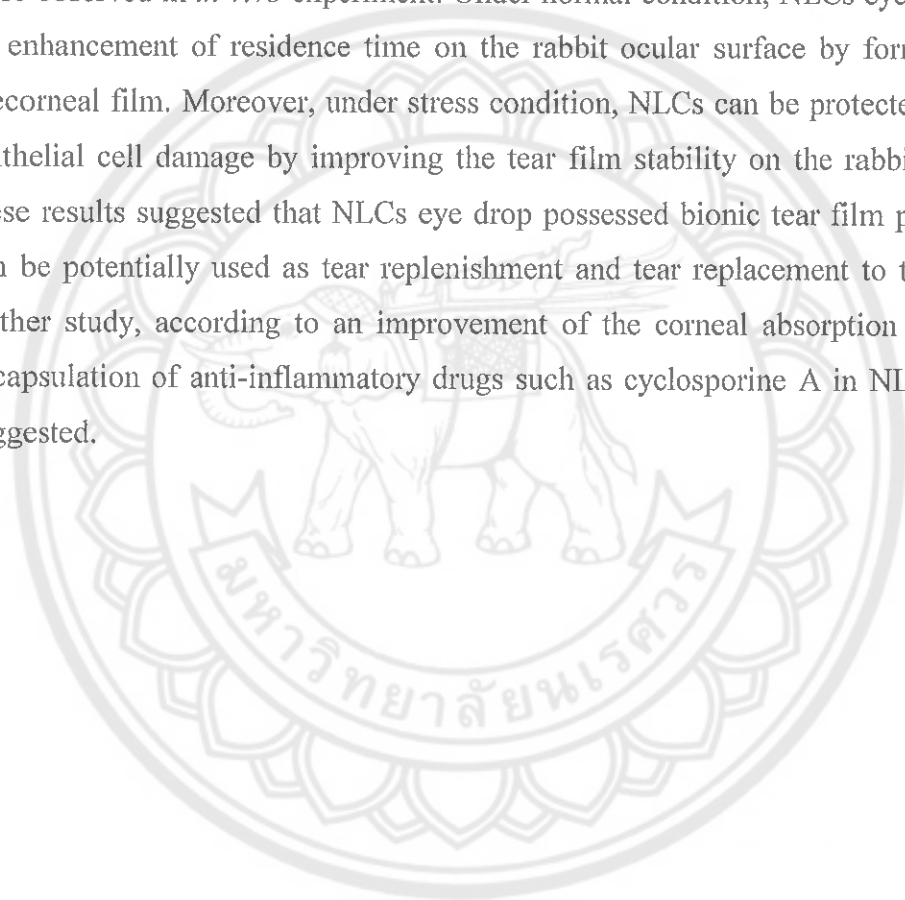
The ability of developed NLCs eye drop to act as a bionic tear film has been further investigated in rabbit eye under normal and stress condition. Under normal condition, NLCs eye drop showed significantly longer retained on the rabbit ocular surface by forming a stable precorneal film compared with NSS as the control. This finding is in agreement with Jinyu Li et al., reporting that the fluorescent-loaded NLCs was longer retained on the rabbit cornea compared with an aqueous fluorescent solution [28]. The stable precorneal film of NLCs is possibly due to their mucoadhesive property and strong intrinsic surface activity [29, 30] (unpublished data). In general, the tear film is composed of three layers: the outermost tear film lipid layer (TFL), the middle aqueous layer, and the innermost mucous layer. We hypothesized that the factors that enable the tear film to spread properly over the ocular surface are increasing adhesion tension of the mucous layer and decreasing the surface tension of the tear film [30]. After NLCs eye drop was instilled into the eye,

the NLCs could possibly distribute into the 3 layers of tear film (Appendix C). Firstly, NLCs with small particle size of ~40 nm would facilitate NLCs retained in the mucin layer covering the corneal epithelium [17, 31]. Secondly, at the air-lipid interface, the TFLL is primarily composed of lipid. Thus, the surface-active properties of NLCs and its lipid nature could favour NLCs to integrate with the TFLL. In accordance with our previous study showing that NLCs can be integrated with the human meibomian lipid films. However, owing to its highly surface activity, NLCs would then gradually penetrate from aqueous layer to the TFLL in a time-dependent manner, as evidence from an increase in the fluorescence signal on the rabbit eye after 5 min of instillation. Thus, our finding indicating that NLCs could directly improve the stability of tear film on ocular surface.

Then, we further examined NLCs protective effect under stress condition using the desiccating stress animal model. It is considered popular means to induce the dry eye and suggested suitable for evaluating the efficacy of artificial tears [15, 18, 32]. In general, this condition was induced by environment stresses including low temperature (22 – 25 °C) and low relative humidity (45 ± 10 %) [15]. During the desiccation conditions, the prevention from blinking of rabbit eyes leads to the rabbit corneal epithelial cells damaged and induction of dry spots within 1 – 3 h [32]. Hence, these apoptosis of corneal epithelial cells could be determined by staining with methylene blue (MB). As expected, NLCs could protect the corneal epithelial cell damage from desiccation as evident from inhibiting the MB staining similar to control group (closed eye). Moreover, NLCs showed higher ability to protect the corneal surface from desiccation than those of commercial artificial tear (polymer based formulation). This phenomenon suggested that NLCs could protect the ocular surface from environmental stress by improving the tear film stability as discussed before. In dry eye person, the tear film appears instability within ~10 seconds or less than that, while the tear film provide longer stable in healthy eye (more than ~15 second) [18]. Instability of the tear film can caused excessive water evaporation from aqueous layer and insufficient tear production that leads to symptoms of discomfort and ocular damage [33]. Therefore, an improving the stability of tear film by NLCs could be helpful to retard water evaporation, enhance the spreading of tear film, and resemble tear film institute that could be benefit as a tear replacement in DED.

### Conclusion

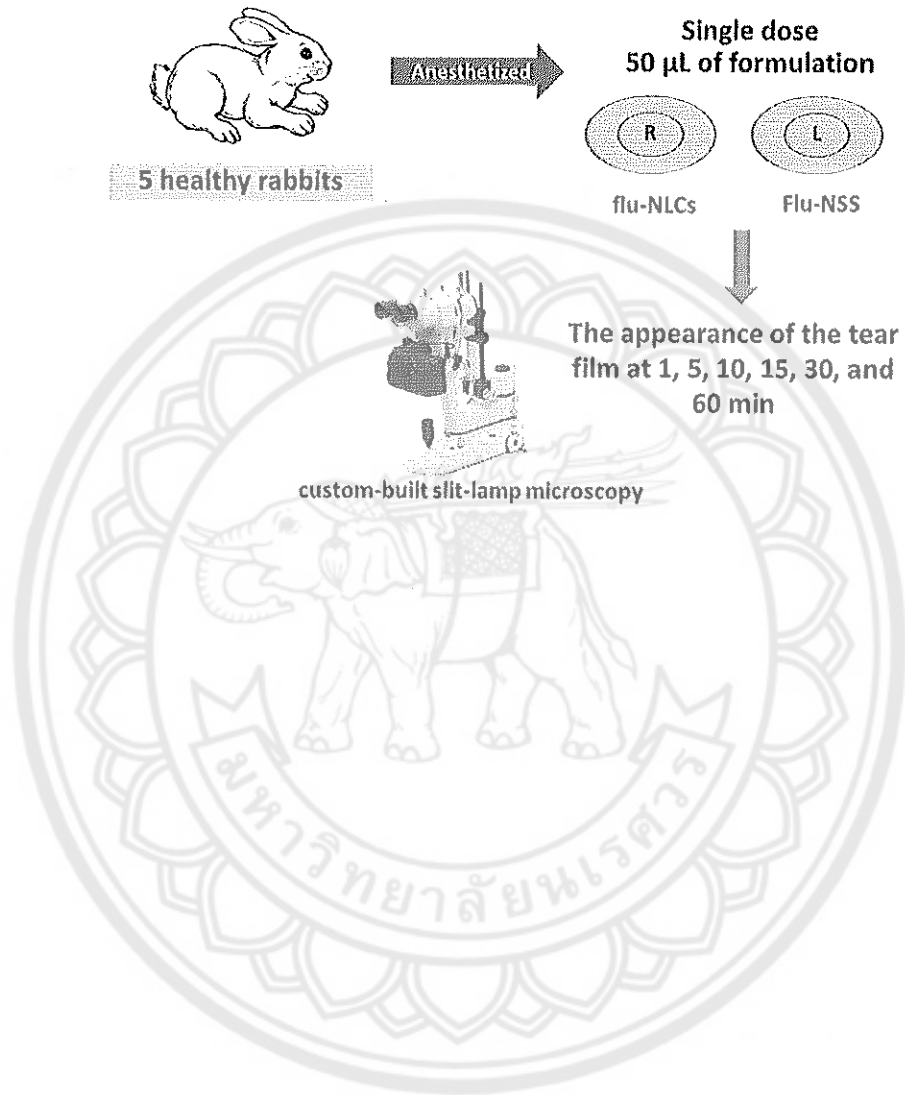
In this study, the NLCs eye drop was successfully developed for the dry eye management. As evidenced of the particle size, zeta potential, sterility, pH, osmolarity, stability, and surface tension of NLCs eye drop, it can be assumed that the developed NLCs should be suitable for topical ophthalmic formulations. In addition, the developed NLCs eye drop showed non-irritation to PCE cells and no adverse effects were observed in *in vivo* experiment. Under normal condition, NLCs eye drop showed an enhancement of residence time on the rabbit ocular surface by forming a stable precorneal film. Moreover, under stress condition, NLCs can be protected the corneal epithelial cell damage by improving the tear film stability on the rabbit eyes. Thus, these results suggested that NLCs eye drop possessed bionic tear film properties and can be potentially used as tear replenishment and tear replacement to treat DED. In further study, according to an improvement of the corneal absorption of NLCs, an encapsulation of anti-inflammatory drugs such as cyclosporine A in NLCs would be suggested.



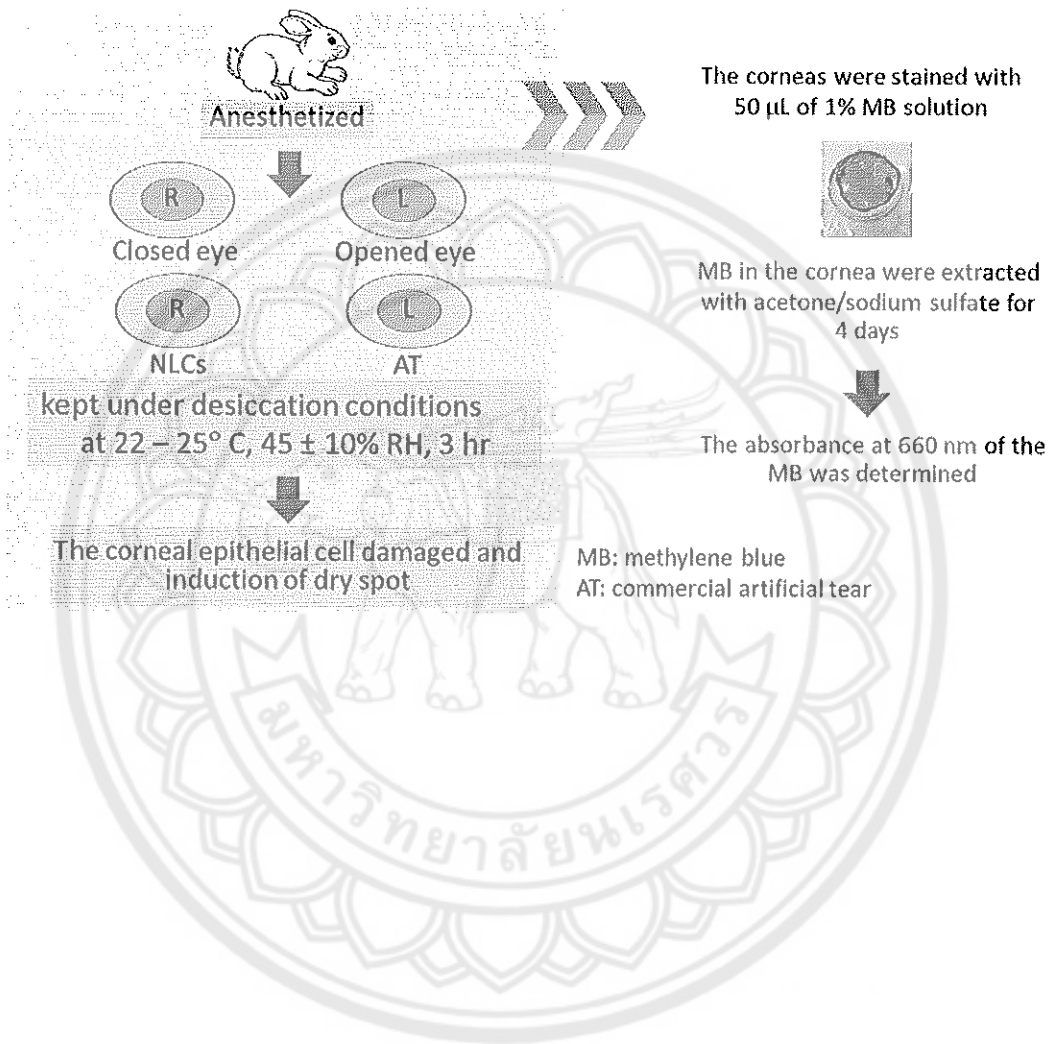




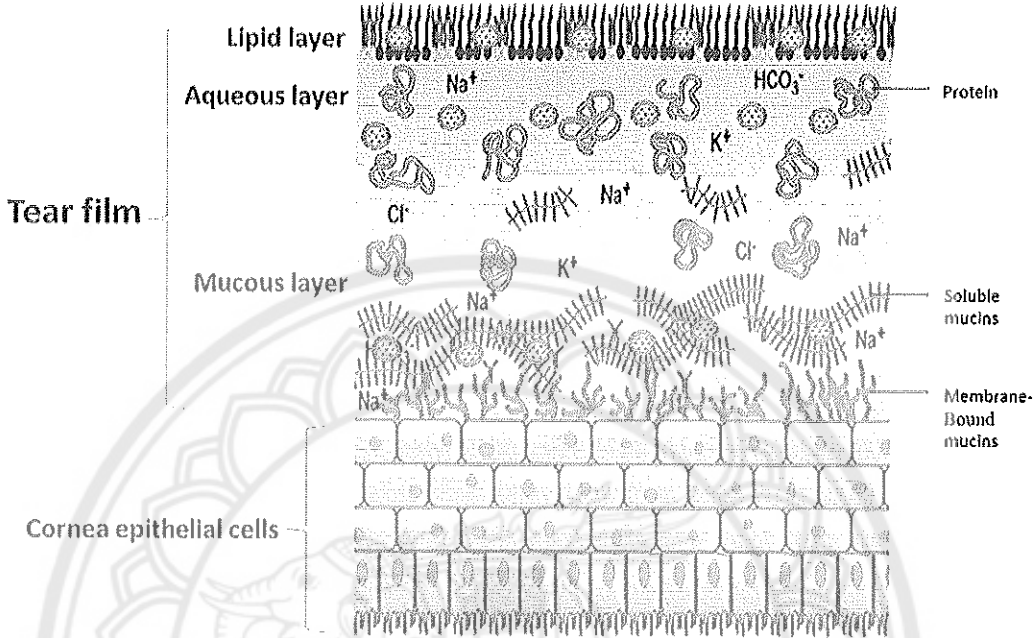
**Appendix A Schematic diagram of the experimental of the retention of NLCs eye drop on the rabbit's corneal surface**



**Appendix B Schematic diagram of the experimental of the effect of NLCs eye drop on ocular surface epithelial cells of rabbit after exposure with desiccation conditions**



Appendix C The mechanisms of NLCs after instilled on the ocular surface





**REFERENCES**

## REFERENCES

- [1] Cwiklik, L. (2016). Tear film lipid layer: A molecular level view. *Biochimica et Biophysica Acta (BBA) - Biomembranes*, 1858(10), 2421-2430.
- [2] Bron, A.J., & J.M. Tiffany. (2004). The contribution of meibomian disease to dry eye. *Ocul Surf*, 2(2), 149-65.
- [3] Stevenson, W., S.K. Chauhan, & R. Dana. (2012). Dry eye disease: An immune-mediated ocular surface disorder. *Arch Ophthalmol*, 130(1), 90-100.
- [4] Barabino, S. (2012). Ocular surface immunity: Homeostatic mechanisms and their disruption in dry eye disease. *Progress in Retinal and Eye Research*, 31(3), 271-285.
- [5] Vicario-de-la-Torre, M. (2018). Novel Nano-Liposome Formulation for Dry Eyes with Components Similar to the Preocular Tear Film. *Polymers*, 10(4), 425.
- [6] Essa, L., D. Laughton, & J.S. Wolffsohn. (2018). Can the optimum artificial tear treatment for dry eye disease be predicted from presenting signs and symptoms?. *Contact Lens and Anterior Eye*, 41(1), 60-68.
- [7] Araújo, J. (2009). Nanomedicines for ocular NSAIDs: Safety on drug delivery. *Nanomedicine: Nanotechnology, Biology and Medicine*, 5(4), 394-401.
- [8] Hao, J. (2012). Development and optimization of baicalin-loaded solid lipid nanoparticles prepared by coacervation method using central composite design. *European Journal of Pharmaceutical Sciences*, 47(2), 497-505.
- [9] Tian, B.-C. (2013). Further investigation of nanostructured lipid carriers as an ocular delivery system: In vivo transcorneal mechanism and in vitro release study. *Colloids and Surfaces B: Biointerfaces*, 102, 251-256.
- [10] Niamprem, P. (n.d.). *Interaction of nanostructured lipid carriers with human meibum*. N.P.: Submitted to Molecular vision.
- [11] Takahashi, H. (2015). Novel primary epithelial cell toxicity assay using porcine corneal explants. *Cornea*, 34(5), 567-575.
- [12] Chaiyasan, W. (2017). Penetration of mucoadhesive chitosan-dextran sulfate nanoparticles into the porcine cornea. *Colloids and Surfaces B: Biointerfaces*, 149, 288-296.

- [13] Kojima, H. (2013). Second-phase validation study of short time exposure test for assessment of eye irritation potency of chemicals. *Toxicology in Vitro*, 27(6), 1855-1869.
- [14] Takahashi, Y. (2009). Inter-laboratory study of short time exposure (STE) test for predicting eye irritation potential of chemicals and correspondence to globally harmonized system (GHS) classification. *J Toxicol Sci*, 34(6), 611-626.
- [15] Zheng, X., T. Goto, & Y. Ohashi. (2014). Comparison of in vivo efficacy of different ocular lubricants in dry eye animal models. *Invest Ophthalmol Vis Sci*, 55(1552-5783), 3454-3460.
- [16] Garrigue, J.-S. (2017). Relevance of Lipid-Based Products in the Management of Dry Eye Disease. *Journal of Ocular Pharmacology and Therapeutics*, 33(9), 647-661.
- [17] Li, H. (2016). Size-exclusive effect of nanostructured lipid carriers on oral drug delivery. *International Journal of Pharmaceutics*, 511(1), 524-537.
- [18] Willcox, M.D.P. (2017). TFOS DEWS II Tear Film Report. *The Ocular Surface*, 15(3), 366-403.
- [19] Han, K., O.E. Woghiren, & R. Priefer. (2016). Surface tension examination of various liquid oral, nasal, and ophthalmic dosage forms. *Chem Cent J*, 10, 31.
- [20] Acar, D. (2018). Novel liposome-based and in situ gelling artificial tear formulation for dry eye disease treatment. *Contact Lens and Anterior Eye*, 41(1), 93-96.
- [21] Zimmer, A., & J. Kreuter. (1995). Microspheres and nanoparticles used in ocular delivery systems. *Advanced Drug Delivery Reviews*, 16(1), 61-73.
- [22] Baudouin, C. (2010). Preservatives in eyedrops: The good, the bad and the ugly. *Progress in Retinal and Eye Research*, 29(4), 312-334.
- [23] Wroblewska, K. (2015). Characterization of new eye drops with choline salicylate and assessment of their irritancy by in vitro short time exposure tests. *Saudi Pharmaceutical Journal*, 23(4), 407-412.
- [24] Utine, C.A. (2011). Tear osmolarity measurements in dry eye related to primary Sjogren's syndrome. *Curr Eye Res*, 36(8), 683-690.

- [25] Tiffany, J.M., N. Winter, & G. Bliss. (1989). Tear film stability and tear surface tension. *Curr Eye Res*, 8(5), 507-515.
- [26] Sakaguchi, H. (2011). Validation study of the Short Time Exposure (STE) test to assess the eye irritation potential of chemicals. *Toxicology in Vitro*, 25(4), 796-809.
- [27] Jiao, J. (2008). Polyoxyethylated nonionic surfactants and their applications in topical ocular drug delivery. *Advanced Drug Delivery Reviews*, 60(15), 1663-1673.
- [28] Li, J. (2017). Transport mechanism of chitosan-N-acetylcysteine, chitosan oligosaccharides or carboxymethyl chitosan decorated coumarin-6 loaded nanostructured lipid carriers across the rabbit ocular. *Eur J Pharm Biopharm*, 120, 89-97.
- [29] Sánchez-López, E. (2017). Lipid nanoparticles (SLN, NLC): Overcoming the anatomical and physiological barriers of the eye – Part II - Ocular drug-loaded lipid nanoparticles. *European Journal of Pharmaceutics and Biopharmaceutics*, 110(Supplement C), 58-69.
- [30] Millar, T.J., & B.S. Schuett. (2015). The real reason for having a meibomian lipid layer covering the outer surface of the tear film – A review. *Experimental Eye Research*, 137, 125-138.
- [31] Niamprem, P.S., S.P., & Tiyaboonchai, Waree. (2018). Development and characterization of indomethacin-loaded mucoadhesive nanostructured lipid carriers for topical ocular delivery. *International Journal of Applied Pharmaceutics*, 10(2), 91-96.
- [32] Schrader, S., A. Mircheff, & G. Geerling. (2008). Animal models of dry eye. *Dev Ophthalmol*, 41, 298 - 312.
- [33] Foulks, G.N. (2007). The Correlation Between the Tear Film Lipid Layer and Dry Eye Disease. *Survey of Ophthalmology*, 52(4), 369-374.

## CHAPTER V

### PENETRATION OF NILE RED-LOADED NANOSTRUCTURED LIPID CARRIERS ACROSS THE PORCINE CORNEA

This chapter has been submitted to the journal of Saudi Pharmaceutical Journal and is currently being reviewed. This chapter provide the information about the effects of particle size and surface modification of nile red-loaded nanostructured lipid carriers (NR-NLCs) on their transcorneal penetration and mucoadhesion.

#### Introduction

The The administration of eye drops on the ocular surface is the most common approach for the treatment of eye diseases. Unfortunately, the poor drug bioavailability on the ocular surface or in the anterior chamber is usually the main limitation of eye drops [1]. This could be attributed to poor corneal epithelial permeability and rapid clearance of the drug by the continuous nasolacrimal drainage [2]. In addition, conventional formulations such as gels and ointments often produce sticky sensation, blurred vision, ocular and surface discomfort [3, 4, 5, 6, 7]. Thus, currently, nano-carrier systems have been explored to enhance the topical ocular bioavailability of drugs by prolonging their precorneal residence time and facilitating their permeability across the corneal epithelium [8, 9, 10].

Among the nano-carrier systems, nanostructured lipid carriers (NLCs) have been focused on ocular drug delivery [4, 11, 12]. NLCs possess the advantages including sustained release, high drug loading capacity, non-toxicity, non-irritation, and high stability *in vivo* as they remain as a solid at body temperature [12, 13, 14, 15]. In general, NLCs are composed of a solid lipid, liquid lipid, and surfactant. These compositions play a vital role in defining their physicochemical characteristics. Interestingly, it has been reported that the physical characteristics of NLCs could be manipulated to improve drug bioavailability. Li et al. noted that NLCs of 100 nm increased the oral absorption and bioavailability of drugs compared to NLC 200 and 300 nm, indicating that the size of NLCs plays a key role in adhesion to the biological



cells [16]. In addition, altering the particle surface either by coating with a mucoadhesive polymer or modified to be positively charge could further enhance mucoadhesion to the ocular surface [2, 15, 17].

Although previous studies have suggested that size, surface hydrophobicity, and surface charge of NLCs influence the ocular bioavailability [2, 18, 19], the relative impact of the different properties of NLCs on mucoadhesion and transcorneal penetration have not been examined simultaneously. In this study, we have first investigated the effects of altered particle size, surface hydrophobicity and surface charge of NLCs on the corneal mucoadhesion and penetration. In order to make a sensitive transcorneal penetration assay, Nile Red (NR) was used as a model lipophilic drug. The different formulations of NR loaded NLCs were prepared by high-pressure homogenization technique. Their physicochemical properties have been characterized including the mucoadhesiveness, transcorneal penetration, and cellular uptake abilities.

## **Materials and Methods**

### **1. Materials**

Lexol GT865 (Caprylic/Capric Triglyceride), cetyl palmitate, and squalene were purchased from Namsiang trading (Bangkok, Thailand). Gelucire 44/14 (lauryl macrogol-32 glyceride) and Compritol 888 ATO (glyceryl behenate) were gifted by Gattefossé (Cedex, France). Tween 80 was purchased from AjexFinechem (Sydney, Australia). Emulmetik 900 (lecithin) was purchased from Lucas Meyer (Ludwigshafen, Germany). Nile red (NR) was purchased from Sigma-Aldrich (Steinheim, Germany). Amicon Ultra 10K centrifugal filter was gifted by Merck Millipore (Massachusetts, USA).

Keratinocyte serum-free medium (K-SFM), bovine pituitary extract, recombinant human epidermal growth factor (EGF), and Gibco antibiotic-antimycotic (100X) were purchased from Invitrogen (California, USA). Hydrocortisone, human insulin, bovine serum albumin (BSA), bovine collagen type I, and human fibronectin were obtained from Sigma-Aldrich (Steinheim, Germany).

## **2. Preparation of Nile red-loaded NLCs (NR-NLCs) and surface modified NR-NLCs**

NR-NLCs of different particle sizes (NR-NLC-40 and NR-NLC-150) were prepared by a hot, high-pressure homogenization technique as described by Keck et al., but with a few modifications [20]. Briefly, 5 mg of NR was dissolved in an oil phase containing squalene (2%; w/w), lecithin (2%; w/w), Caprylic/Capric Triglyceride (2%; w/w), and solid lipid (cetyl palmitate or glyceryl behenate (3%; w/w)) at 85 °C. The oil phase was then mixed with a water phase consisting of Gelucire 44/14 (5%; w/w) dispersed in distilled water at 85 °C before subjected to a high-pressure homogenizer (Microfluidics M-110P, Massachusetts, USA) at 1500 bar for 5 cycles. The resulting hot O/W nanoemulsion was cooled to 25 °C and the obtained NR-NLCs were washed twice with normal saline solution (NSS, 0.9% NaCl in DI water) using an ultrafiltration system (Amicon 8400, Massachusetts, USA) fitted with a MW cut off 100 kDa membrane to remove the free NR.

Then, two types of surface modifications of NR-NLCs were prepared. Firstly, PEG-coated NLCs (NR-NLC-PEG) was obtained by incubating NR-NLC-40 with 0.1% (w/v) PEG 400 at a 1:1 ratio followed by stirring at 500 rpm for 30 min. Secondly, cationic surface charge NR-NLCs (NR-NLC-SA) were prepared with stearyl amine (0.3%, w/w) as cationic solid lipid and cetyl palmitate (2.7%, w/w) instead of cetyl palmitate (3%, w/w). All samples were prepared in triplicate.

## **3. Physico-chemical characterization of NR-NLCs and surface modified NR-NLCs**

The particle size and polydispersity index (PI) were determined by dynamic light scattering (DLS) using ZetaPALS<sup>®</sup> analyzer (Brookhaven 90Plus, New York, USA). They were obtained in the auto-measurement mode at a fixed angle of 90°. The zeta potential was determined by measuring the particle electrophoretic mobility using the ZetaPAL<sup>®</sup> analyzer. Samples were dispersed in DI water, and 10 measurement cycles were performed. All samples were performed in triplicate.

The transmission electron microscope (TEM, Tecnai 12, Philips, USA) was used to examine the morphology of NR-NLCs. Twenty µL of the sample was deposited on a carbon-coated 300 mesh copper grid and negative staining was performed using 10 µL of 0.5% (w/v) uranyl acetate in 20% ethanol in PBS. The

excessive solvent was removed by Whatman no.1 filter paper, allowed to air-dry at room temperature, and kept in a desiccator for further observation by TEM.

#### **4. Penetration NR-NLCs across the porcine cornea**

The penetration of different NR-NLCs formulations across the freshly isolated porcine cornea was investigated by a custom-built confocal scanning microfluorometer (CSMF) [8, 21, 22]. CSMF is a custom-built confocal microscope capable of depth-resolved trans-corneal fluorescence measurements. It has a depth resolution of 7  $\mu\text{m}$ . It has been our instrument of choice for transcorneal penetration of fluorescent nanoparticles and fluorescent dyes since the instrument is inexpensive when compared to a conventional confocal microscope. Moreover, it does not cause photobleaching and hence is highly suitable for repeated depth scanning over a prolonged period [8, 21, 22].

Briefly, the freshly isolated porcine eyes were obtained from the local slaughterhouse. The eyes were held in ice-cold phosphate-buffered saline with a 1% (v/v) antibiotic solution until use (< 3 h after death). The corneas were exposed to samples at different times (4, 6, and 8 h) in a dark, moist chamber at room temperature. The different NR-NLCs formulations; NR-NLC-40, NR-NLC-150, NR-NLC-PEG, and NR-NLC-SA, were tested. NR dissolved in NSS containing 0.5% DMSO and NR dissolved in castor oil were also investigated. After incubation, the corneas were washed 3 times with Phosphate buffer saline (PBS). Then transcorneal fluorescence measurements were performed with the cornea held underneath the objective lens (Zeiss 40x; 0.75 NA; water immersion and wd = 1.2 mm) on a motorized XYZ linear translation stage (Appendix A). The output of a white LED, which was modulated at 10 kHz as a sine wave, was filtered through an interference filter ( $540 \pm 20$  nm) and led to the excitation port of the CSMF. The NR fluorescence (> 590 nm) and scattered light passing through a confocal exit slit positioned in the eyepiece were detected by two photomultiplier tubes (R928HA, Hamamatsu Inc.) coupled to two lock-in amplifiers. The scatter and fluorescence signals were recorded on a computer.

#### **5. Mucoadhesion Assay**

The retention of NR-NLCs on the freshly isolated porcine corneal tissue was determined using an experimental protocol and set up described previously by

Chaiyasan et al. [5]. The corneal button (6 mm) was cut out with a trephine and held on a glass slide. Ten  $\mu\text{L}$  of the formulation were instilled on the corneal surface. Next, to mimic shear stress mimicking caused by blink action, the tissue was exposed to a continuous stream of NSS (pH 5.5), 34 °C, at a rate of 0.3 mL/min for 60 min (Appendix B). Then, cryostat sections of the corneal tissue were prepared by embedding the cornea in optimum cutting temperature compound (OCT, Tissue-Tek; CellPath, Powys, UK) and frozen at -20 °C for at least 24 h. The OCT-embedded cornea was sectioned at 5  $\mu\text{m}$  using a cryostat (Leica Microsystem, Wetzlar, Germany) and mounted on a glass slide before imaging by fluorescence microscopy (AxioImager Z1; Zeiss, Oberkochen, Germany).

#### **6. Cellular uptake by flow cytometry**

To quantitatively evaluate the internalization of NR-NLCs in porcine corneal epithelium (PCE) cells, flow cytometric analysis was conducted. PCE cells were isolated using cellular outgrowth from primary tissue explant technique. The corneal tissues were excised from the fresh porcine eye and plated epithelial side down onto 6-well plate. The explant was further cultured in Keratinocyte serum-free medium (K-SFM) with supplements (Invitrogen, California, USA) at 37 °C in a humidified atmosphere containing 5 %  $\text{CO}_2$  and removed 5 days later. The outgrowing cells were maintained in culture medium for 10-14 days, with the medium changed every 2 days. After the cells reached 80 % confluence, the culture medium was abandoned, and the cells were treated with serum-free K-SFM medium containing NR-NLCs, equivalent to 10  $\mu\text{g}/\text{mL}$  of NR, for 2 h. After the incubation period, the cells were washed 3 times with ice-cold PBS to remove the un-internalized NR-NLCs. Then, the cells were harvested by trypsinization and resuspended in PBS. The internalized NR-NLCs were determined using a Flow cytometer (Guava easyCyte<sup>TM</sup>5, Merck Millipore, Massachusetts, USA), on an average of 5000 cells from each sample. Experiments were carried out in triplicate and results were analyzed using In-cytes software (Guava soft 3.2, Merck Millipore, Massachusetts, USA).

#### **7. Statistic analysis**

The statistical significance of the differences between nanoparticles and controls to each time point was tested using a one-way analysis of variance (ANOVA)

SPSS software (17.0 version, SPSS Inc., Illinois, USA). The statistical significance was set at  $p < 0.05$ .

## Results and discussion

### 1. Characterization of NR-NLCs

The developed NLCs were prepared by a high-pressure homogenization technique due to its advantages including reliability, ease of scale-up, and cost-effectiveness [23]. Depending on the production process and especially different lipid blended, the different type of NLCs are obtained [23]. Due to the ratio of solid lipid/oil, 5/4, used in developed NR-NLCs formulations, we assumed that the multiple type of NR-NLCs would be achieved (Figure 5.1) [24]. The particle size, PI values, and zeta potential of various NR-NLCs formulations are presented in Table 5.1. The different size of NLCs was successfully developed using different types of solid lipids. In general, the longer fatty acid side chain formed a larger particle size comparing to the shorter fatty acid side chain [13, 25]. As expected, NR-NLC-150 prepared with Compritol 888 ATO (fatty acid side chains, C<sub>22</sub>) showed larger particle size, ~150 nm, than NR-NLC-40 prepared with cetyl palmitate (fatty acid side chains, C<sub>16</sub>), ~40 nm. Both formulations exhibited a negatively charged of ~ -30 mV that could be attributed to the medium chain triglyceride carboxylic group on the particle surface [26].

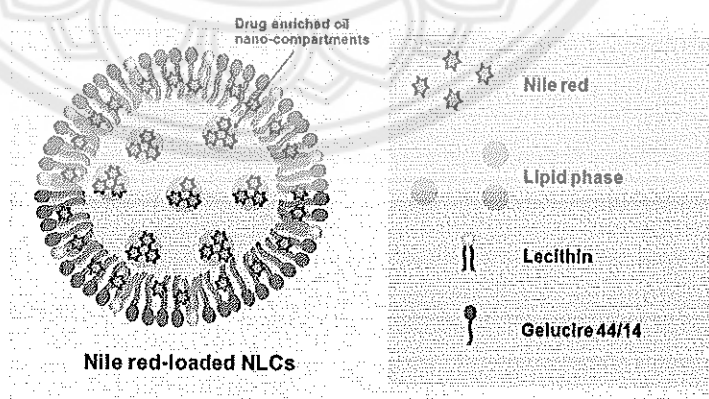


**Figure 5.1 Schematic illustration of multiple type nile red-loaded nanostructured lipid carriers (NR-NLCs)**

**Table 5.1** The effects of solid lipid type and concentration on the particle size, polydispersity index, and zeta potential of NR-NLCs

Formulation	Solid-lipid type and concentration (w/w)	Particle size (nm) ± SD	PI ± SD	Zeta potential (mV) ± SD
NR-NLC-150	Compritol 888 ATO, 3%	154 ± 5	0.27 ± 0.01	-31 ± 4
NR-NLC-40	cetyl palmitate, 3%	39 ± 1	0.17 ± 0.03	-28 ± 2
NR-NLC-PEG	cetyl palmitate, 3%	38 ± 3	0.19 ± 0.04	-28 ± 1
NR-NLC-SA	cetyl palmitate, 2.7%: Stearylamine, 0.3%	38 ± 2	0.14 ± 0.05	20 ± 1

**Note:** SD = standard deviation for n=3, PI = polydispersity index

The surface modification of NR-NLCs was achieved by either coating NR-NLC-40 with PEG 400 (NR-NLC-PEG) or using cationic lipids in the formulation (NR-NLC-SA). The obtained NR-NLC-PEG showed particle size of ~38 nm with a surface charge of ~ -28 mV. In agreement with previous studies [27], possibly due to its short chain, PEG has neither affected the particle size nor the surface charge of NR-NLCs. In contrast, NR-NLC-SA produced a positively charged particle as a result of localization of SA amine group, a cationic lipid, on the particle surface. Based on preliminary study, the particle size and surface charge tended to increase as the amount of SA increased (data not showed). Therefore, the optimized formulation containing SA 0.3% (w/w) was chosen in this study to obtain NR-NLC-SA with a particle size of ~40 nm and a positive charged of ~20 mV. In addition, the PI value of all formulations was less than 0.3 indicating a narrow size distribution.

All prepared NLCs showed a particle size of less than 200 nm which is considered optimum for ocular application because it is unlikely to cause mechanical abrasions after topical administration. Zimmer et al. have suggested a limit of 10 µm above which abrasive injury is induced [28]. Moreover, the obtained particles size of less than 200 nm could enhance mucoadhesion and endocytosis [16].

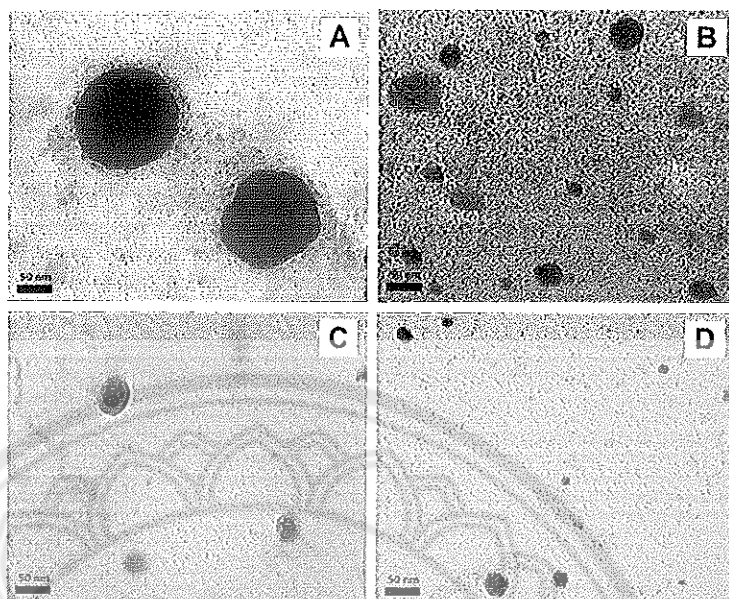


**Figure 5.2** TEM micrographs of (A) NR-NLC-150, (B) NR-NLC-40, (C) NR-NLC-PEG, and (D) NR-NLC-SA

TEM micrographs of NR-NLCs were shown in Figure 5.2. All NR-NLCs formulations were a spherical shape in nanosize range, which was in agreement with DLS determination. As shown in Figure 5.2C, the TEM micrographs of NR-NLC-PEG revealed the light grey border at the periphery, which attributed to the presence of PEG coating around the particle surface.

## 2. Penetration of NR-NLCs across the porcine cornea

The cornea is oil:water:oil matrix corresponding to epithelium, stroma, and endothelium, respectively. Each layer forms a barrier to transcorneal drug penetration, depending on the size of the solute and its lipophilicity. In this context, a lipophilic dye NR can be expected to partition into the epithelium and endothelium readily but not into the stroma. In our preparation of NR-NLCs, NR encapsulation was 100% as confirmed by polarized light microscopy (Appendix C).

The penetration of NR-NLCs across the cornea was investigated using the CSMF. The instrument, in particular, was designed to monitor transcorneal penetration of fluorescence dyes employed as drug analogs. Our previous studies have examined the penetration of rhodamine B, fluorescein, and FITC in mice, bovine, porcine, rabbit, and human corneas [8, 22]. The transcorneal fluorescence and scatter scans obtained

simultaneously during a depth scan were shown in Figure 5.3A. The thick dashed curve referred to light scatter *vs.* depth while the continuous thin line represented fluorescence *vs.* depth. The scatter scan was used to delineate the boundaries of different layers of the cornea [8]. As shown in Figure 5.3A, the peak in the scatter intensity at the beginning of the scan is from the epithelium, followed by the scatter from the stroma (up to the depth of 800  $\mu\text{m}$ ). A minor peak usually observed at the end of the scan is from the endothelium. Unfortunately, the last minor peak of the endothelium was not observed in our study because the scan depth was limited to 800  $\mu\text{m}$  since the working distance of the objective lens was 1.2 mm. However, there was no effect on our results because the deepest penetration was distributed from epithelium to stroma.

### 2.1 Effect of formulations and incubation time

The transcorneal fluorescence and scatter scans after topical NR-CO, NR-NSS, and NR-NLC-40 at different incubation times were shown in Figure 5.3, 5.4, and 5.5, respectively. The results showed that the NR fluorescence intensity increased in a time-dependent manner in all formulations. As expected, NR can be dissolved in castor oil due to its lipophilicity. Therefore, topical NR-CO revealed only an NR intensity peak corresponding to the epithelium but no detectable NR in the stroma up to 8 h. This was attributed to the NR not partitioning into the stroma owing to its high lipophilicity. Interestingly, topical NR-NSS showed increased NR intensity corresponding to the epithelial and stromal layers. This is possibly due to the presence of DMSO, a penetration enhancer, which could disrupt the structure of the corneal epithelium, leading to NR-NSS penetration into the stroma [29]. Similar to NR-NSS, the NR intensity peak of topical NR-NLC-40 significantly increased in the epithelium and anterior stroma compared to NR-CO. This could be explained by the high surface area of the NR-NLC-40 (the nano-size particles), leading to an increase in mucoadhesive property, which can further enhance the penetration of NLCs [30].



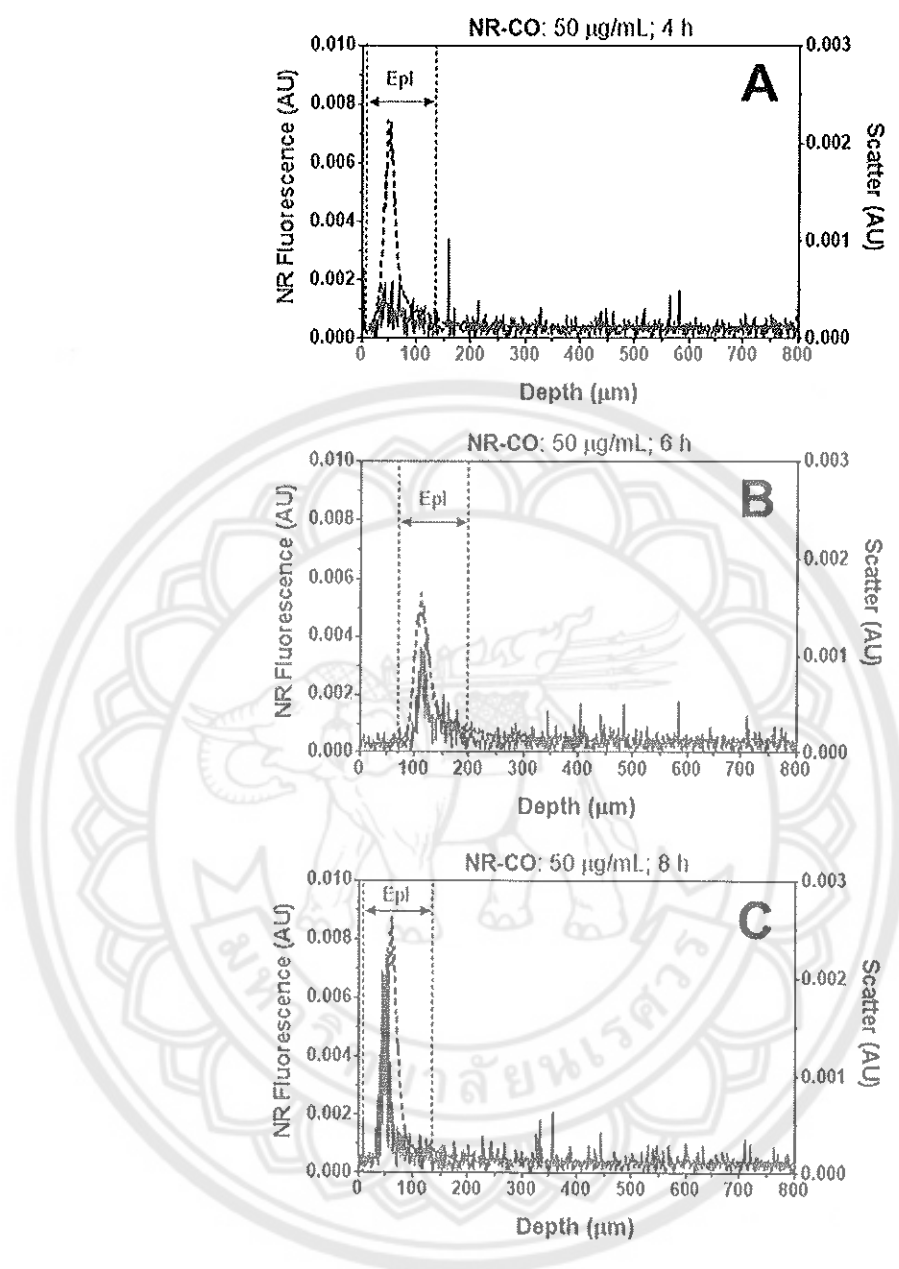


**Figure 5.3** The transcorneal fluorescence (red line) and scatter (blue line) scans obtained after topical NR-CO at (A) 4 h, (B) 6 h, and (C) 8 h. Data shown are typical results after 3 independent trials

Although, the penetration mechanisms for NLCs into the anterior segment of the eye are unclear; the commonly accepted three mechanisms could be explained. Firstly, NR, a lipophilic dye, can diffuse from NR-NLCs into the epithelial membrane. This particle-to-membrane diffusion can subsequently facilitate the penetration of NR

across the entire thickness of epithelium along the connected lipid membranes. Secondly, it has been reported that the presence of Gelucire 44/14 as a surfactant on the NLCs surface can act as a drug penetration enhancer. Similarly, Li Xiang et al. reported that NLCs prepared with Gelucire 44/14 produce higher Ibuprofen permeation across the rabbit cornea than do the NLCs without Gelucire 44/14 [18]. Finally, the NR-NLCs were internalized by the epithelial cells via endocytosis [30]. Regarding the penetration into the stroma, the NLCs could be distributed from the basal epithelium to the stroma by exocytosis [30]. Alternatively, the dye is slowly released into the stroma from the epithelium. However, this latter step is unlikely to occur because the stroma is hydrophilic whereas the NR is lipophilic [2].

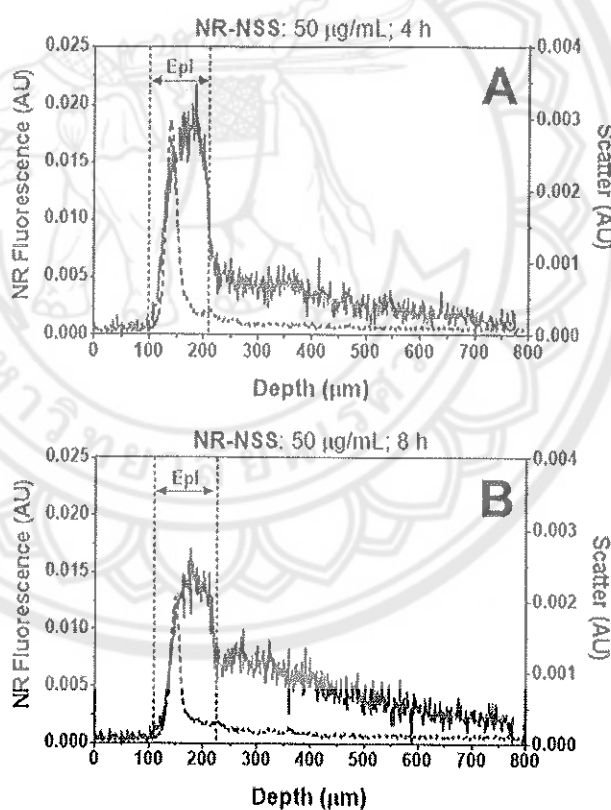


**Figure 5.4** The transcorneal fluorescence (red line) and scatter (blue line) scans obtained after topical NR-NSS at (A) 4 h and (B) 8 h. Data shown are typical results after 3 independent trials

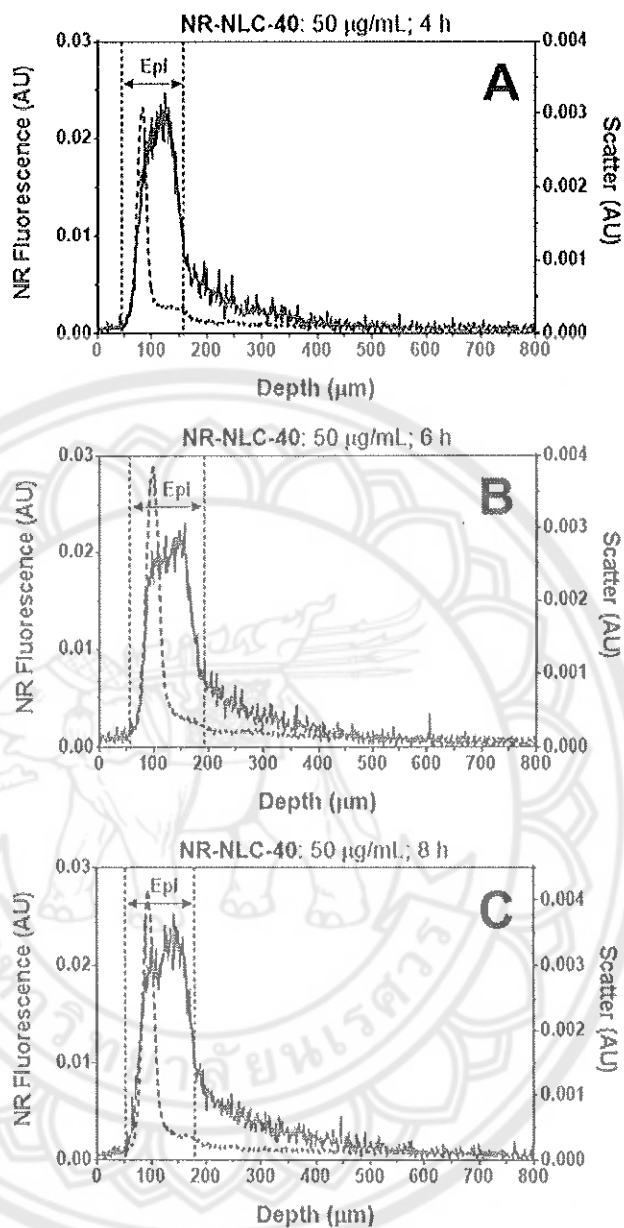


**Figure 5.5** The transcorneal fluorescence (red line) and scatter (blue line) scans obtained after topical NR-NLC-40 at (A) 4 h, (B) 6 h, and (C) 8 h. Data shown are typical results after 3 independent trials

## 2.2 Effect of particle size

It has been reported that the particle size is a key factor that impacts the efficiency of drug delivery systems [31]. To assess the effect of particle size, the transcorneal NR fluorescence after 4 h of exposure to NR-NLC-40 and NR-NLC-150

was investigated. The NR intensity was illustrated corresponding to the epithelium and stroma in both formulations (Figure 5.6A and 5.6B). As expected, NR-NLC-40 showed higher NR intensity in both epithelial and stromal layers compared to that of NR-NLC-150. This attributed to the smaller particles size exhibited higher uptake and penetration across the epithelium in comparison to those of larger particles. Moreover, Oh N et al., suggested that the exocytosis rate of 15 nm was faster than that of 30 nm nanoparticles, indicating the smaller nanoparticles are more favorable for exocytosis to stroma layer [30]. This finding is in agreement with Li Huipeng et al. [16] and Pelin Aksungur et al. [31]. They found that the particle size is considered an important parameter governing cellular uptake.

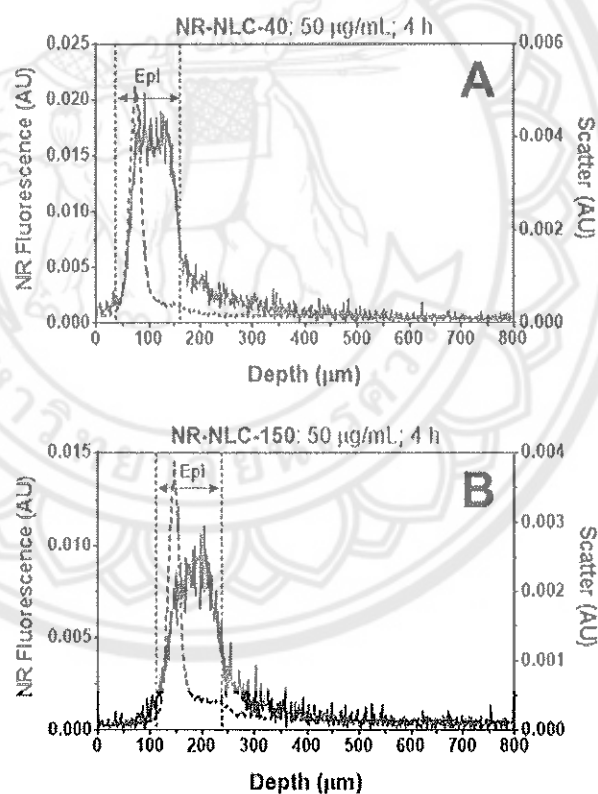


**Figure 5.6** The transcorneal fluorescence (red line) and scatter (blue line) scans obtained after topical (A) NR-NLC-40 and (B) NR-NLC-150 at 4 h. Data shown are the typical result after 3 independent trials.

### 2.3 Effect of surface modification

NR-NLC-40, NR-NLC-PEG, and NR-NLC-SA were prepared with a similar particle size of ~40 nm, but different surface properties of negatively surface charge, a hydrophilic surface, and cationic surface charge, respectively. The NR-NLC-PEG and NR-NLC-SA showed relatively higher NR penetration into the epithelium but lower penetration into the stroma compared to the NR-NLC-40 (Figure 5.7). This could be attributed by the fact that both NR-NLCs modifications facilitated strong mucoadhesion with the mucus. In the case of NR-NLC-PEG, PEG-coated on the NLCs surface could bind with the mucin at the mucus layer, enhancing the mucoadhesive on the cornea surface [32, 33]. Similarly, the positive charged NR-NLC-SA can interact electrostatically with the anionic groups of mucins glycosylated regions, resulting in an increase in the retention time on the cornea [18]. Therefore, both NR-NLCs modifications are more favorably retained in the mucus layer and, thus, slowly penetrate to the epithelium and the stroma, respectively [14]. As a consequent, the NR intensity in the stroma was increased after exposure up to 8 h, indicating that the penetration of both NR-NLCs modifications increased in a time-dependent manner (data not shown).

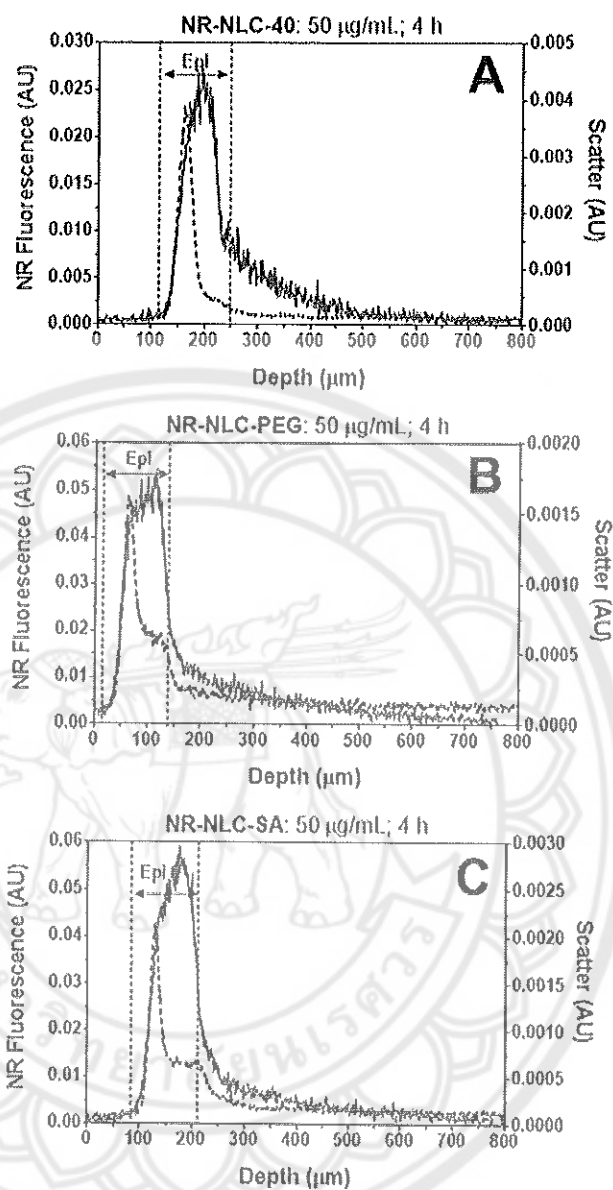


**Figure 5.7** The transcorneal fluorescence (red line) and scatter (blue line) scans obtained after topical (A) NR-NLC-40, (B) NR-NLC-PEG, and (C) NR-NLC-SA at 4 h. Data shown are the typical result after 3 independent trials

### 3. Mucoadhesion

In general, the retention of topical ophthalmic drugs is limited by tear flow secretion and drainage induced by blink action. Therefore, an enhanced mucoadhesive formulation could be considered to improve the corneal penetration of drugs. In this

study, the developed NR-NLCs were put on the porcine button and subjected to a continuous stream of NSS in order to determine their mucoadhesive properties. The NR fluorescence images of the vertical sections of the porcine cornea after instillation with NR-NLCs and NR-NSS at different time points are depicted in Figure 5.8. Also, the NR fluorescence intensity (%) in the epithelium and stroma layers was quantified using Image J software and represented in Figure 5.9. To confirmed that NR signal is only from NR-NLCs, porcine cornea and blank NLCs, without NR, were examined and showed no fluorescence response (data not shown). After the instillation of NR-NSS, the NR fluorescence intensity both in the epithelium and stroma showed rapidly decreased with time. After 5 min instillation, the NR intensity in epithelium and stroma was  $43.44 \pm 9.60$  % and  $1.41 \pm 0.44$  %, respectively, and decreased to  $10.83 \pm 0.90$  % and  $0.35 \pm 0.13$  %, respectively, after 360 min instillation (Figure 5.9). The decrease in NR fluorescence intensity with time indicated that NR-NSS could not adhere to the cornea surface and was quickly washed off by liquid flow. Interestingly, all NR-NLCs formulations illustrated stronger NR fluorescence intensity than did NR-NSS, suggesting higher NR distribution. In addition, their NR fluorescence intensity tended to increase with time. These could imply that NR-NLCs possessed mucoadhesive properties, and thus, could highly remain on the corneal tissue for a longer time. Consequently, prolonged residence time of NR-NLCs could increase NR penetration into cornea tissue [34, 35]. This finding is similar to Cavalli et al., reporting that the fluorescent-loaded SLN (particle size <100 nm) was retained on the rabbit cornea surface for a longer time when comparing with an aqueous fluorescent solution [36].

Concerning the effect of NR-NLCs modification, the fluorescence images of NR-NLC-PEG and NR-NLC-SA were compared with NR-NLC-40, Figure 5.8. At 5 min instillation (Figure 5.9), NR-NLC-40 showed higher NR intensity than NR-NLC-PEG and NR-NLC-SA in both the epithelial and stroma layers. However, after 360 min, the NR intensity in the epithelial layer of NR-NLC-40 was decreased from ~80 % to ~67 %, while both NLCs modifications showed relatively increased from ~51-56 % up to ~70-80 %. The phenomena could be explained by the stronger mucoadhesion property of both NLCs modification compared to unmodified NLCs. After instillation, NLCs modifications showed strong adhesion to the porcine cornea

surface due to their interaction with the mucin leading to prolonged pre-corneal residence time. These results are well correlated with the CSMF experiment (section 3.2.3) and in agreement with previous studies, which conclude that NLCs with PEG-coating or cationic surface charge resulted to an enhancement of mucoadhesion on ocular surface [18, 27].

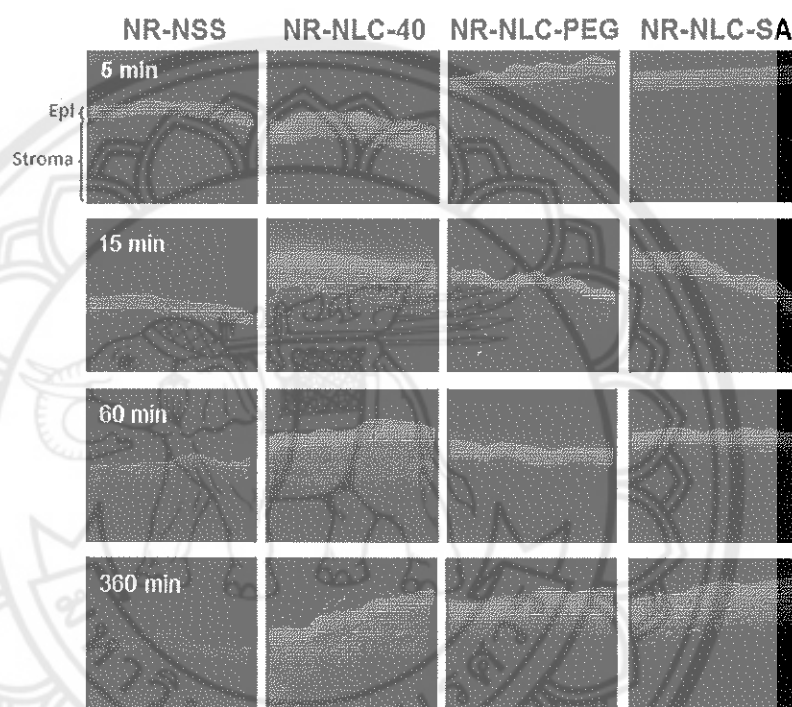


**Figure 5.8** Fluorescence images of vertical slices of the cornea surface after instillation of different NR-NLCs compared with NR-NSS at 5, 15, 60, and 360 min (n=3). Magnification  $\times 20$



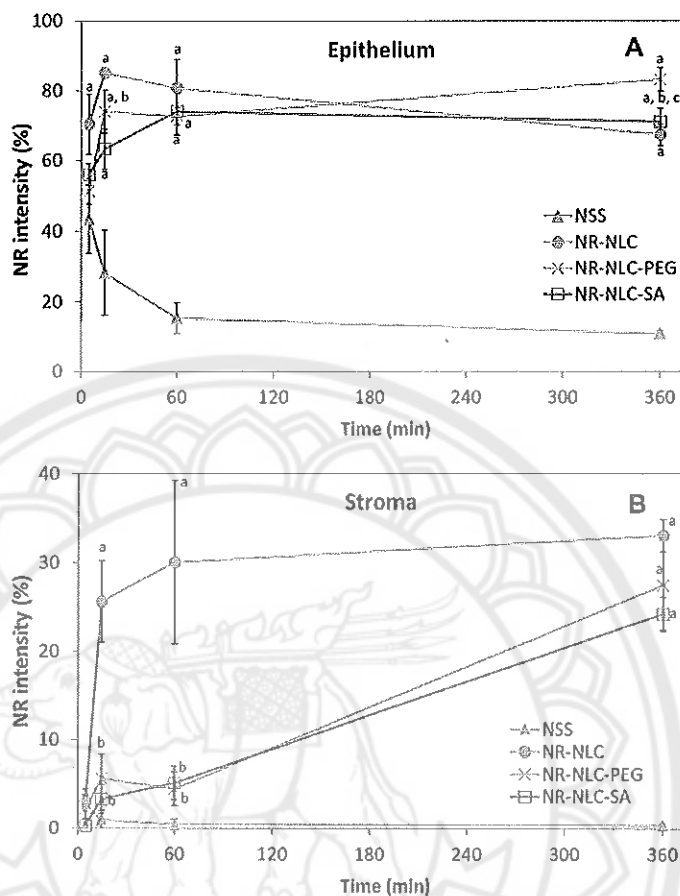


**Figure 5.9** The fluorescence intensity (%) of fluorescence images of the cornea tissue after instillation of different NR-NLCs compared with NR-NSS at 5, 15, 60, and 360 min analyzed by ImageJ software. Statistically significant differences were determined by one-way ANOVA, Turkey multiple comparison test; <sup>a</sup>  $p < 0.05$  compared with NR-NSS; <sup>b</sup>  $p < 0.05$  compared with NR-NLC-40; <sup>c</sup>  $p < 0.05$  compared with NR-NLC-PEG. Error bars indicate SD for  $n=3$

#### 4. Cellular uptake by flow cytometric analysis

The nano-sized particles are commonly known to be taken up by the cell via endocytosis. Thus, to confirm the PCE cell uptake ability of NR-NLCs, the flow cytometric experiment was conducted. The uptake ability was expressed by the fluorescence-positive PCE cells (%). As expected, the PCE cells treated with NR-NLCs illustrated a higher percentage of fluorescence-positive cells compared to

untreated control group, Figure 5.10. When comparing among NR-NLCs formulations after 2 h incubation, NR-NLC-40 possessed the highest cell uptake, with the fluorescence-positive cells (%) of  $54.77 \pm 3.97$ , followed by NR-NLC-PEG,  $46.74 \pm 2.33$ , and NR-NLC-SA,  $9.92 \pm 3.69$ , respectively. NR-NLC-PEG provided lower detectable fluorescence cell than that of NR-NLC-40 could be a result of its mucoadhesive properties. Generally, mucin expression in cell culturing could be observed leading to possible NR-NLC-PEG entrapment in the mucin [37]. Furthermore, the lowest level of NR-NLC-SA internalization into PCE cells could be attributed to its positively charged property resulting in mucoadhesion and also toxicity. Its mucoadhesion retarded the cell uptake via ionic interaction with mucin, while its positive charge may reduce the PCE cell viability as supported by a flow cytometric analysis. The PCE cells treated with NR-NLC-SA revealed a decrease in the cell size (Forward Scatter, FSC) coupled with the increase in cell granularity (Side Scatter, SSC), a typical pattern for apoptosis as previously reported (Appendix D) [38]. These observations indicated that the present results correlated well with CSMF experiment and fluorescence microscopy.

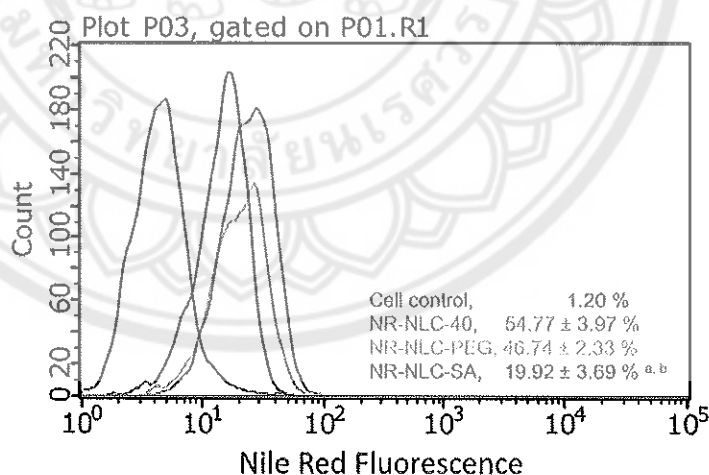


**Figure 5.10** Cell uptake of NR-NLC-40, NR-NLC-PEG, and NR-NLC-SA in PCE cells analyzed by flow cytometry. Histogram for different samples corresponds to the mean NR fluorescence intensity (%). Statistically significant differences were determined by one-way ANOVA, Turkey multiple comparison test; <sup>a</sup>  $p < 0.05$  compared with NR-NLC-40; <sup>b</sup>  $p < 0.05$  compared with NR-NLC-PEG

## Conclusion

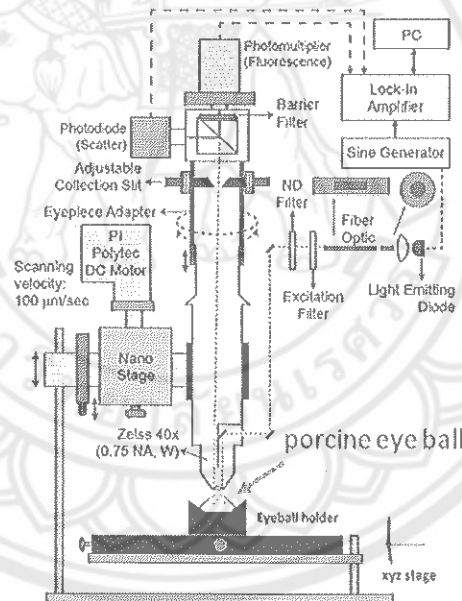
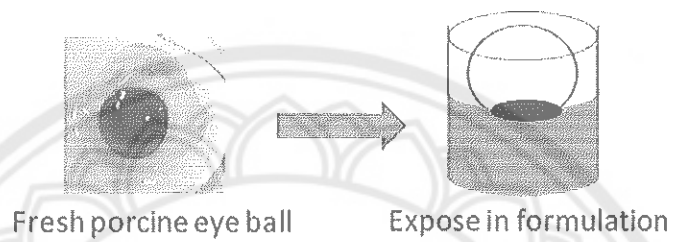
In this study, the different size and surface modifications of NLCs containing lipophilic model drug were successfully prepared to improve the transcorneal penetration and mucoadhesion of topical ophthalmic formulations. Surface modifications of NR-NLCs by PEG-coating or cationic lipid altered the hydrophilic surface or cationic surface charge, respectively, which the modifications did not affect the particle size. We have demonstrated that incubation time, particle size, and surface modification affect the penetration of the ocular surface. Smaller NR-NLCs (~40 nm) showed greater penetration across the epithelium compared with the larger particles (~150 nm). Both NR-NLCs modifications showed an enhancement of the mucoadhesive property on the corneal surface more than unmodified NR-NLCs and hence lead to slowly penetrate to the epithelium and the stroma. However, the unmodified NR-NLCs revealed significantly higher internalization uptake compared to the NR-NLCs modifications in PCE cells. Thus, these results suggest that NLCs can be helpful for lipophilic drug delivery to the anterior segment of the eye, while the modified-NLCs could be potentially used to treat ocular surface disorders.



**APPENDIX**

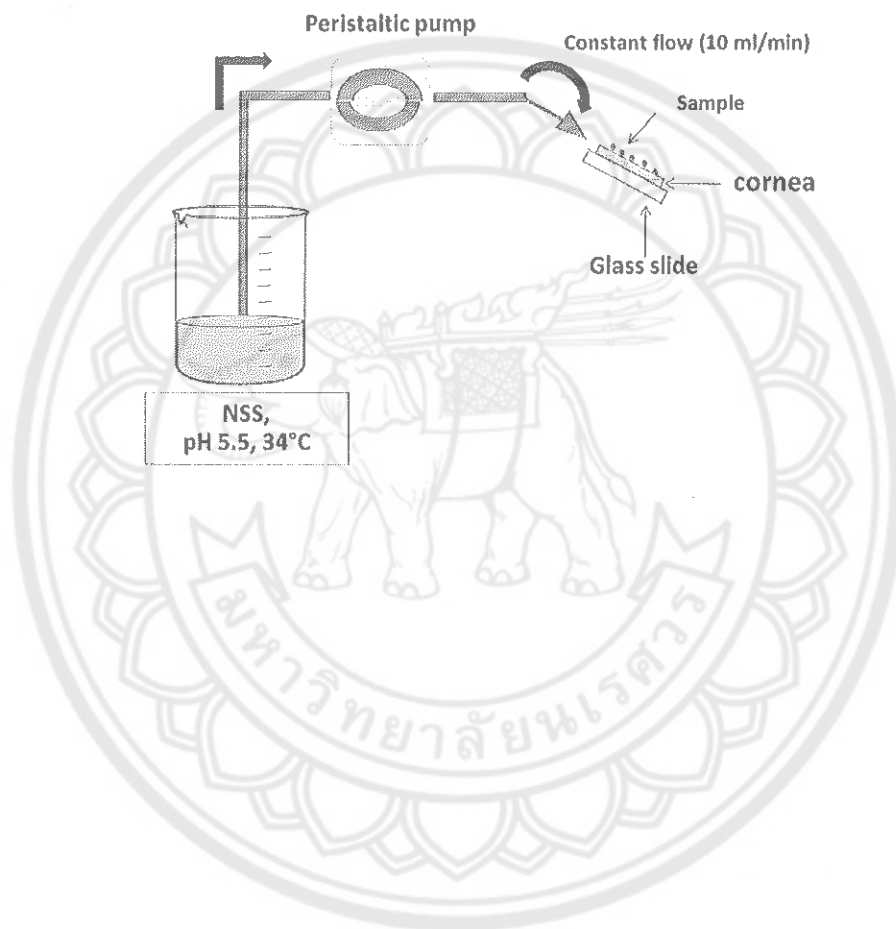
มหาวิทยาลัยราชภัฏสุรินทร์

**Appendix A Schematic diagram of the experimental of the penetration of different NR-NLCs formulations across the freshly isolated porcine cornea. The corneas were exposed to samples at different times and the transcorneal fluorescence measurements were performed with the cornea held underneath the objective lens of CSMF**

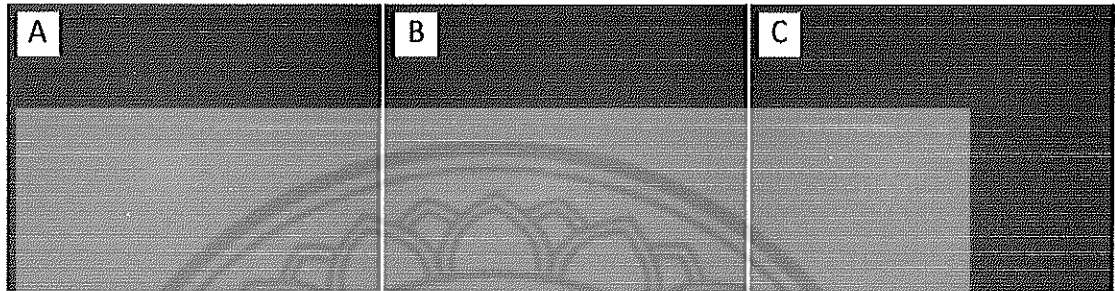


**Confocal Scanning Micro Fluorometer (CSMF)**

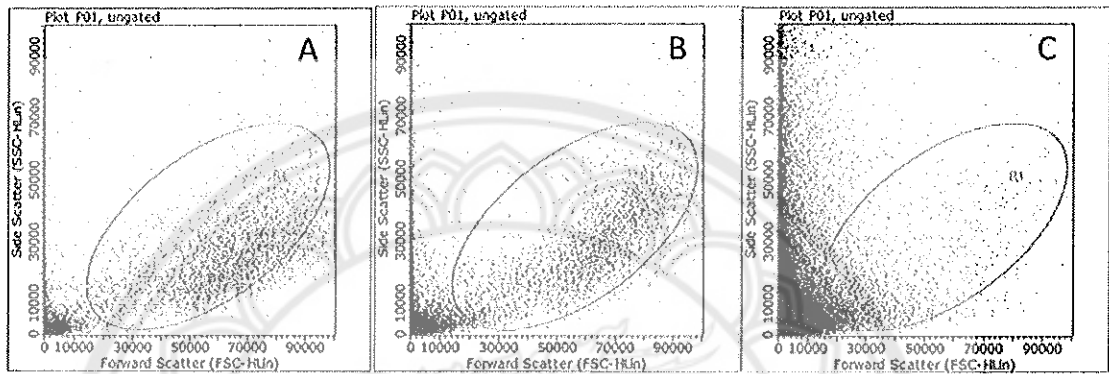
**Appendix B Schematic diagram of the apparatus for *ex vivo* mucoadhesion test. The retention of NR-NLCs on the freshly isolated porcine corneal tissue was determined using an experimental protocol and set up described previously by Chaiyasan et al. [5]. The corneal button (6 mm) was cut out with a trephine and held on a glass slide**



**Appendix C Images obtained by Polarized light microscopy of NR-NLCs prepared with different concentrations (% w/w) of Tween 80: (A) 3 %, (B) 5 %, and (C) 7%, at 100X magnification.**



**Appendix D** Flow cytometry of light scatter of PCE cells treated with (A) NR-NLC-40, (B) NR-NLC-PEG, and (C) NR-NLC-SA for 2 h. Each dot on the plot represents an individual cell that passed through the laser. The gating on scatter plot is shown in red line (R1)







**REFERENCES**

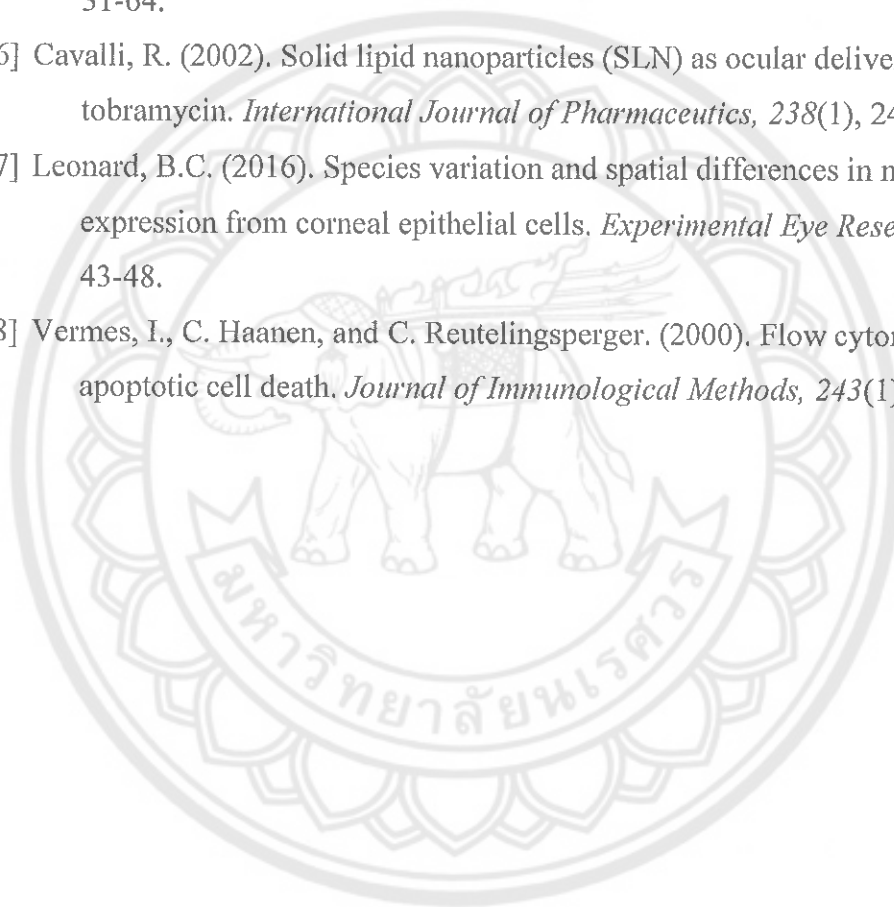
## REFERENCES

- [1] Sanchez-Lopez, E. (2017). Lipid nanoparticles (SLN, NLC): Overcoming the anatomical and physiological barriers of the eye - Part I - Barriers and determining factors in ocular delivery. *European Journal of Pharmaceutics and Biopharmaceutics*, 110, 70-75.
- [2] Alvarez-Trabado, J., Y. Diebold, & A. Sanchez. (2017). Designing lipid nanoparticles for topical ocular drug delivery. *International Journal of Pharmaceutics*, 532(1), 204-217.
- [3] Yao, W.J. (2010). Effect of poly(amidoamine) dendrimers on corneal penetration of puerarin. *Biol Pharm Bull*, 33(8), 1371-1377.
- [4] Balguri, S.P., G.R. Adelli, & S. Majumdar. (2016). Topical ophthalmic lipid nanoparticle formulations (SLN, NLC) of indomethacin for delivery to the posterior segment ocular tissues. *European Journal of Pharmaceutics and Biopharmaceutics*, 109, 224-235.
- [5] Chaiyasan, W., S.P. Srinivas, & W. Tiyaboonchai. (2013). Mucoadhesive chitosan-dextran sulfate nanoparticles for sustained drug delivery to the ocular surface. *Journal of Ocular Pharmacology and Therapeutics*, 29(2), 200-207.
- [6] Li, N. (2009). Liposome coated with low molecular weight chitosan and its potential use in ocular drug delivery. *International Journal of Pharmaceutics*, 379(1), 131-138.
- [7] Onoue, S. (2014). Self-micellizing solid dispersion of cyclosporine A with improved dissolution and oral bioavailability. *European Journal of Pharmaceutical Sciences*, 62, 16-22.
- [8] Chaiyasan, W. (2017). Penetration of mucoadhesive chitosan-dextran sulfate nanoparticles into the porcine cornea. *Colloids and Surfaces B: Biointerfaces*, 149, 288-296.
- [9] Diebold, Y. (2007). Ocular drug delivery by liposome-chitosan nanoparticle complexes (LCS-NP). *Biomaterials*, 28(8), 1553-1564.
- [10] Gupta, H. (2010). Sparfloxacin-loaded PLGA nanoparticles for sustained ocular drug delivery. *Nanomedicine: Nanotechnology, Biology and Medicine*, 6(2), 324-333.

- [11] Balguri, S.P. (2017). Ocular disposition of ciprofloxacin from topical, PEGylated nanostructured lipid carriers: Effect of molecular weight and density of poly (ethylene) glycol. *International Journal of Pharmaceutics*, 529(1), 32-43.
- [12] Sánchez-López, E. (2017). Lipid nanoparticles (SLN, NLC): Overcoming the anatomical and physiological barriers of the eye – Part II - Ocular drug-loaded lipid nanoparticles. *European Journal of Pharmaceutics and Biopharmaceutics*, 110(Supplement C), 58-69.
- [13] Seyfoddin, A., J. Shaw, & R. Al-Kassas. (2010). Solid lipid nanoparticles for ocular drug delivery. *Drug Delivery*, 17(7), 467-489.
- [14] Beloqui, A. (2016). Nanostructured lipid carriers: Promising drug delivery systems for future clinics. *Nanomedicine: Nanotechnology, Biology and Medicine*, 12(1), 143-161.
- [15] Battaglia, L. (2016). Application of lipid nanoparticles to ocular drug delivery. *Expert Opinion on Drug Delivery*, 13(12), 1743-1757.
- [16] Li, H. (2016). Size-exclusive effect of nanostructured lipid carriers on oral drug delivery. *International Journal of Pharmaceutics*, 511(1), 524-537.
- [17] Mansfield, E.D.H. (2016). Side chain variations radically alter the diffusion of poly(2-alkyl-2-oxazoline) functionalised nanoparticles through a mucosal barrier. *Biomaterials Science*, 4(9), 1318-1327.
- [18] Li, X. (2008). A controlled-release ocular delivery system for ibuprofen based on nanostructured lipid carriers. *International Journal of Pharmaceutics*, 363(1-2), 177-182.
- [19] Azhar Shekoufeh Bahari, L., & H. Hamishehkar. (2016). The Impact of Variables on Particle Size of Solid Lipid Nanoparticles and Nanostructured Lipid Carriers; A Comparative Literature Review. *Advanced Pharmaceutical Bulletin*, 6(2), 143-151.
- [20] Keck, C.M. (2014). Oil-enriched, ultra-small nanostructured lipid carriers (usNLC): A novel delivery system based on flip-flop structure. *International Journal of Pharmaceutics*, 477(1), 227-235.
- [21] Gupta, C. (2010). Measurement and modeling of diffusion kinetics of a lipophilic molecule across rabbit cornea. *Pharmaceutical Research*, 27(4), 699-711.

- [22] Gupta, C., A. Chauhan, & S.P. Srinivas. (2012). Penetration of Fluorescein Across the Rabbit Cornea from the Endothelial Surface. *Pharmaceutical Research*, 29(12), 3325-3334.
- [23] Müller, R.H., M. Radtke, & S.A. Wissing. (2002). Solid lipid nanoparticles (SLN) and nanostructured lipid carriers (NLC) in cosmetic and dermatological preparations. *Advanced Drug Delivery Reviews*, 54(Supplement), S131-S155.
- [24] Jennings, V., A.F. Thünnemann, & S.H. Gohla. (2000). Characterisation of a novel solid lipid nanoparticle carrier system based on binary mixtures of liquid and solid lipids. *International Journal of Pharmaceutics*, 199(2), 167-177.
- [25] Seyfoddin, A., & R. Al-Kassas. (2013). Development of solid lipid nanoparticles and nanostructured lipid carriers for improving ocular delivery of acyclovir. *Drug Development and Industrial Pharmacy*, 39(4), 508-519.
- [26] Huang, Z.R. (2008). Development and evaluation of lipid nanoparticles for camptothecin delivery: a comparison of solid lipid nanoparticles, nanostructured lipid carriers, and lipid emulsion. *Acta Pharmacologica Sinica*, 29(9), 1094-1102.
- [27] Shen, J. (2009). Mucoadhesive effect of thiolated PEG stearate and its modified NLC for ocular drug delivery. *Journal of Controlled Release*, 137(3), 217-223.
- [28] Zimmer, A., & J. Kreuter. (1995). Microspheres and nanoparticles used in ocular delivery systems. *Advanced Drug Delivery Reviews*, 16(1), 61-73.
- [29] Marren, K. (2011). Dimethyl sulfoxide: an effective penetration enhancer for topical administration of NSAIDs. *Phys Sportsmed*, 39(3), 75-82.
- [30] Oh, N. and J.H. Park. (2014). Endocytosis and exocytosis of nanoparticles in mammalian cells. *International Journal of Nanomedicine*, 9(Suppl 1), 51-63.
- [31] Aksungur, P. (2011). Development and characterization of Cyclosporine A loaded nanoparticles for ocular drug delivery: Cellular toxicity, uptake, and kinetic studies. *Journal of Controlled Release*, 151(3), 286-294.
- [32] Ludwig, A. (2005). The use of mucoadhesive polymers in ocular drug delivery. *Advanced Drug Delivery Reviews*, 57(11), 1595-1639.

- [33] Huckaby, J.T., & S.K. Lai. (2018). PEGylation for enhancing nanoparticle diffusion in mucus. *Advanced Drug Delivery Reviews*, 124, 125-139.
- [34] Souza, J.G. (2014). Topical delivery of ocular therapeutics: carrier systems and physical methods. *J Pharm Pharmacol*, 66(4), 507-530.
- [35] Janagam, D.R., L. Wu, & T.L. Lowe. (2017). Nanoparticles for drug delivery to the anterior segment of the eye. *Advanced Drug Delivery Reviews*, 122, 31-64.
- [36] Cavalli, R. (2002). Solid lipid nanoparticles (SLN) as ocular delivery system for tobramycin. *International Journal of Pharmaceutics*, 238(1), 241-245.
- [37] Leonard, B.C. (2016). Species variation and spatial differences in mucin expression from corneal epithelial cells. *Experimental Eye Research*, 152, 43-48.
- [38] Vermes, I., C. Haanen, and C. Reutelingsperger. (2000). Flow cytometry of apoptotic cell death. *Journal of Immunological Methods*, 243(1), 167-190.



## CHAPTER VI

### DEVELOPMENT AND CHARACTERIZATION OF INDOMETHACIN-LOADED MUCOADHESIVE NANOSTRUCTURED LIPID CARRIERS FOR TOPICAL OCULAR DELIVERY

This chapter has been published in the International Journal of Applied Pharmaceutics, volume 10, Issue 2, page 91 – 96, published 7 March 2018. This chapter has been developed and characterized the indomethacin loaded-nanostructured lipid carriers (IND-NLCs) for topical ophthalmic delivery with different particle sizes and polymer coating to improve the mucoadhesive property on the ocular surface.

#### Introduction

Indomethacin (IND), a common non-steroidal anti-inflammatory drug (NSAID) in ocular therapeutics, is administered topically on the ocular surface for clinical management of conjunctivitis, anterior uveitis, and post-operative inflammation following cataract surgery [1]. Although it is stable at lower pH, IND possesses a low solubility of 3 - 5 mg/100 ml at pH 5.6 [2]. IND can be rendered soluble in aqueous buffers at pH 7.5 - 8.0 but with a risk of its hydrolysis into 5-methoxy-2-methylindolyl-3-acetic acid and 4-chlorobenzene acid [3]. Therefore, IND is formulated in the form of gels and suspensions to improve the solubility and stability [2, 3]. A polyethylene glycol (PEG)- based formulation of 0.1% indomethacin solution (Indocollyre®) is commercially available but it is known to exhibit poor bioavailability and cause irritation, superficial punctuate keratitis, and local pain [4]. Accordingly, nano-carriers drug delivery systems have been proposed as potential alternatives [5, 6, 7, 8].

Nano-carrier systems, in general, are able to encapsulate drug and thereby protect them against degradation. Also, nanoparticles can be mucoadhesive, and accordingly show increased their retention time on the ocular surface. These characteristics are suitable for enhanced stability and topical bioavailability of IND

[9]. Among the nano-carrier systems, nanostructured lipid carriers (NLCs) possess unique characteristics that are promising for ophthalmic drug delivery. They have been developed to combine the advantages of other colloidal carriers but without their disadvantages [10]. For example, NLCs can be prepared using physiological lipids similar to nanoemulsions and liposomes, thus, providing less significant toxicity and acidic related inflammation problems compared to polymeric nanoparticles such as PLGA nanoparticles [11, 12]. Moreover, NLCs show better physical stability than nanoemulsions and liposomes by remaining in a solid state at room and body temperature. NLCs are composed of the imperfect crystalline structure of lipid matrix which formed by a mixture of solid and liquid lipid and stabilized by surfactants. Therefore, the drug payload is increased, and expulsion of the drug during storage is avoided as compared to solid lipid nanoparticles (SLNs) [13].

A major challenge of topical ocular drug delivery is the poor bioavailability of the drug at the ocular surface and the anterior chamber [12]. Employing nano-carrier systems, the topical bioavailability can be improved by enhancing their residence time and corneal epithelial uptake [12]. Both parameters are strongly affected by the particle size and surface modification [11]. Although, Balguri et al. have recently reported increased bioavailability of IND to ocular tissues with IND-loaded NLCs [7], the effect of particle size and surface modifications have not been delineated.

Therefore, the aim of this study was to develop IND-loaded NLCs (IND-NLCs) with different types of solid lipids and surfactants which improve the mucoadhesive property on the corneal surface. Surface-modification of IND-NLCs with polyethylene glycol 400 (PEG) was also undertaken. Physicochemical properties of the developed IND-NLCs were evaluated in terms of particle size, zeta potential, drug entrapment efficacy, and *in vitro* release study. The effect of the autoclaving method on the physicochemical stability of IND-NLCs was investigated. The retention of IND-NLCs on porcine cornea mucosa was determined using *ex vivo* mucoadhesive studies. In addition, *in vitro* cytotoxicity of the optimized IND-NLCs was investigated by the short time exposure test (STE) in primary porcine corneal epithelial (PCE) cells.

## **Materials and methods**

### **1. Materials**

Gelucire 44/14 (G44/14, lauryl macrogol-32 glyceride) and Compritol 888 ATO (CATO, Compritol, glyceryl behenate) were kindly gifted by Gattefossé (Cedex, France). Lexol GT865 (medium chain triglyceride), cetyl palmitate (CP) and squalene were purchased from Namsiang trading (Bangkok, Thailand). Tween 80 (T80, Polysorbate 80) was acquired from AjexFinechem (Sydney, Australia). Emulmetik 900 was purchased from Lucas Meyer (Ludwigshafen, Germany). Indomethacin (Lot BCBK0293) was acquired from Sigma-Aldrich (China). Amicon Ultra 10K centrifugal filter was kindly gifted from Merck Millipore (Massachusetts, USA). Methanol and Acetonitrile used as HPLC solvent were purchased in HPLC grade quality from Lab Scan.

Keratinocyte serum-free medium (K-SFM), bovine pituitary extract, recombinant human epidermal growth factor (EGF), and Gibco antibiotic-antimycotic (100x) were purchased from Invitrogen (California, USA). Hydrocortisone solution, human insulin solution, bovine serum albumin (BSA), bovine collagen type I, and human fibronectin were obtained from Sigma-Aldrich (Steinheim, Germany).

### **2. Preparation of blank-NLCs and IND-NLCs**

IND-NLCs were prepared by a high-pressure homogenization technique. Briefly, the lipid phase contained 50 mg of IND, 2% (w/w) of squalene, 2% (w/w) of Emulmetik 900, 2% (w/w) of Lexol GT865, and 3% (w/w) of solid lipid was heated at 80 °C. Meanwhile, the aqueous phase consisting of 7% (w/w) of surfactant dissolved in distilled water was heated at 80 °C and slowly added to the oil phase. The obtained a primary emulsion was subjected to a high-speed homogenizer at 5000 rpm (T18, IKA, Staufen, Germany) for 1 min before subjected to a high-pressure homogenizer (M-110P, Microfluidics, Massachusetts, USA) applying 5 cycles at 1500 bar. The resulting hot o/w microemulsion was cooled at 25 °C, re-solidification the lipid and forming the NLCs. Finally, the obtained NLCs was washed twice with normal saline solution (NSS) using an ultrafiltration system (Amicon 8400, Massachusetts, USA) fitted with a molecular weight cut off 100 kDa membrane to remove the excess components and unencapsulated IND. Blank-NLCs were prepared with the same method as described above without adding IND. NLCs were prepared by varying the



type of solid lipid and surfactant namely; NLC1 (Compritol 888 ATO and Tween 80 ); NLC2 (cetyl palmitate and Tween 80 ); NLC3 (Compritol 888 ATO and Gelucire 44/4 ); and NLC4 (cetyl palmitate and Gelucire 44/4 ). The selection of these variables was based on preliminary experiments.

To prepare the mucoadhesive NLCs, NLC2 and IND-NLC2 were incubated with 0.1% (w/v) PEG 400 at a ratio of 1:1 and stirred at 500 rpm for 30 min (C-MAG HS7, Guangzhou, China). The obtained polymer coated NLC2 (NLC2-PEG) and polymer coated IND-NLC2 (IND-NLC2-PEG) were washed as described above. All samples were prepared in triplicate.

### **3. Sterilization by autoclaving**

Blank-NLCs and IND-NLCs were placed in a glass vial and sealed with rubber stoppers and aluminum caps. Then, the samples were sterilized by steam sterilization at 121 °C for 15 min at 2 bar. After the autoclaving process, the sterilized formulations were characterized the particle size, zeta potential, and drug remaining (%).

### **4. Drug incorporation efficiency**

The content of IND incorporated into NLCs was determined by extraction method. Briefly, 100  $\mu$ L of IND-NLCs was mixed with 900  $\mu$ L of a mixture of 1 M HCl and methanol (1:90, v/v) and sonicated at 40% amplitude for 30 seconds by the ultrasonic probe (VCX130, Connecticut, USA). The sample was then centrifuged at  $31,514 \times g$  for 10 min; then the supernatant was collected to determine the amount of IND using a modified high performance liquid chromatography (HPLC) assay of Nováková L et al. [14]. The HPLC system (LC10AT, Shimadzu, Kyoto Japan) composed of an autosampler model SIL-10ADVP, a pump system model LC20-AT, and a UV/VIS detector model SPD-20A. Twenty  $\mu$ L of the sample was injected onto a Gemini 5u C18 110A (5  $\mu$ m, 150 x 4.6 mm) which was kept at 25 °C. The mobile phase consisted of acetonitrile and 0.2% (v/v) orthophosphoric acid at the volume ratio of 65:35 (v/v) was delivered at a flow rate of 1.2 mL/min. The UV detection was set at 270 nm. IND was quantified from its peak area using calibration curve of IND established from the range of 1 to 50  $\mu$ g/mL. The percentage of drug incorporation efficiency was calculated as  $[(\text{Amount of extracted IND}) \times 100] / (\text{Initial amount of IND})$ .

### 5. Physico-chemical characterization of blank-NLCs and IND-NLCs

The mean particle size and polydispersity index (PI) were determined by dynamic light scattering (DLS) with a ZetaPALS® analyzer (Brookhaven 90Plus, New York, USA). This instrument was equipped with a 35 mW HeNe laser diode operating at 632.8 nm and a BI-200SM Goniometer connected to a BI-9010AT digital correlator. Samples were dispersed in DI water and run for 10 measurement cycles. The mean particle size and PI values were obtained by the auto measuring mode at a fixed angle of 90°. All samples were performed in triplicate.

The zeta potential determined by measuring the particle electrophoretic mobility using the ZetaPAL® analyzer. The measurement was then carried out at 25 °C and angle of 14.8° to the incident light. The zeta potential was calculated based on the Smoluchowski equation. The measurement was performed for 5 cycles.

The transmission electron microscope (TEM, Tecnai 12, Philips, USA) was used to examine the morphology of NLCs and IND-NLCs by negative staining method. Twenty µL of sample was deposited on a carbon-coated 300 mesh copper grid. Then, 10 µL of 0.5% (w/v) uranyl acetate in ethanol was dropped onto the grid. The excessive solvent was removed by Whatman no.1 filter paper and allowed to air-dry at room temperature. The dried sample was kept in a desiccator for further observation by TEM.

### 6. *In vitro* release study

The shake-flask method was employed to evaluate the dissolution profile of IND-NLCs formulations [15]. IND is a poorly water-soluble drug. Therefore, NSS (pH 5.5) contained 0.6% (v/v) Tween 80 was used as a dissolution medium to provide sink condition [16]. One ml of IND-NLCs (containing IND 0.4 mg) was mixed into 10 mL of dissolution medium and stirred at 200 rpm at  $34 \pm 0.5$  °C. An aliquot (500 µL) of the sample was taken at pre-determined time intervals of 5, 30, 60, 120, 180, 240, and 360 min. The fresh medium was replaced immediately after sampling to maintain a constant volume. Samples were then centrifuged using 10K Amicon centrifugal filter at  $17,508 \times g$  for 10 min. The filtrate was collected and mixed with mobile phase before performed on HPLC system as described above.

### 7. *Ex vivo* mucoadhesive study

The retention of IND-NLCs on the corneal surface was determined using an experimental setup previously described by Chaiyasan et al. [17]. Porcine eyes were obtained from the local slaughterhouse. The eyes were kept on the ice and kept moist with 1% (v/v) antibiotic solution until use (<8 h after death). The corneal tissue was cut out with a trephine (6 mm diameter) and mounted on a glass slide. IND-NLCs (10  $\mu$ L) was instilled on the cornea surface. Then, the tissue was exposed to a continuous stream of pH 5.5 NSS, 34 °C, at a flow rate of 0.3 mL/min for 5, 15, 30, and 60 min to induce shear stress mimicking blink action. Finally, the cornea tissue was collected and extracted to determine the IND-NLCs adhered to the tissue using HPLC method. The percentage of IND retained on the ocular surface calculated as  $[(\text{Amount of extracted IND from cornea tissue}) \times 100] / (\text{Initial amount of IND-NLCs})$ .

### 8. Cytotoxicity of IND-NLC in primary porcine corneal epithelial (PCE) cells

Primary porcine corneal epithelial (PCE) cells from primary tissue explant technique were cultured as before [18, 19]. Briefly, the cornea was excised from the freshly isolated porcine eye, then sterilized with 1% (v/v) povidone-iodine for 5 min and rinsed thrice with PBS containing 1% (v/v) antibiotic-antimycotic. The explant was then placed epithelial side down onto 6-well tissue pre-coated culture plate with coating solution contained BSA, bovine collagen I, and human fibronectin. The explant was further cultured in K-SFM with supplements at 37 °C, in a humidified atmosphere containing 5% CO<sub>2</sub>. The cornea was removed after 5 days, and the outgrowing cells were maintained in culture medium for 2 - 3 weeks.

For several years, the method of choice to determine eye irritation potential was the Draize rabbit eye test. However, ethical considerations and the limited value of animal models including lack of reproducibility and overestimation of human response led to the development of alternative *in vitro* tests [20]. The short time exposure (STE) *in vitro* test is recommended for assessing eye irritation potential. The STE method is straightforward to use and known to provide rapid results with the excellent predictive ability [21].

The cytotoxicity was assessed by the STE test using MTT assay as described by Kojima et al. but with some modifications [20]. The PCE cells were seeded on 96-well plate at  $2 \times 10^4$  cells/well until reaching the semi-confluence (2 - 3 days). Then, the cells were exposed to 200  $\mu$ L of IND-NLCs dispersed in PBS containing 5 and 0.05% (w/v) indomethacin for 5 min at room temperature. In addition, 5 and 0.05% (w/v) IND solution, PBS, and 0.01% (w/v) sodium lauryl sulfate (SLS) were used as sample test, vehicle, and positive control, respectively. After exposure, the cells were washed with PBS twice, and 200  $\mu$ L of methyl thiazol diphenyl-tetrazolium bromide (MTT) solution (0.5 mg/mL) in culture medium was added. After incubated for 2 h, MTT formazan was extracted with 200  $\mu$ l of a mixture of 0.04 N HCl in absolute isopropanol and DMSO (1:1, v/v) for 30 min. The absorbance was measured at 570 nm with a microplate reader (BioStack Ready, Vermont, USA). The relative cell viability was calculated comparing to the vehicle, then, category and rank classification was determined as described by Takahashi et al. [22].

## Results

### 1. Physicochemical characteristics of blank-NLCs

Table 6.1 shows the effect of different solid lipids, surfactants, and PEG coating on the physical characteristics of NLCs. NLC1 and NLC3, prepared with Compritol 888 ATO as solid lipid, showed a larger particle size of  $307 \pm 29$  and  $144 \pm 8$  nm, respectively. While preparing with cetyl palmitate, NLC2 and NLC4, reduced the particle size to  $39 \pm 4$  and  $34 \pm 1$  nm, respectively. Moreover, NLC1 and NLC2, prepared with Tween 80 as a surfactant, demonstrated a larger particle size compared to those with Gelucire 44/14, NLC3 and NLC4. The PI value of all formulations was less than 0.3 indicating a narrow size distribution. The hydrophilic coating with PEG, NLC2-PEG, did not affect neither the particle size nor zeta potential ( $p > 0.05$ ).

The effects of sterilization by autoclaving on the physical characteristics of the blank-NLCs formulations were presented in Table 6.1. The surfactant used in the formulations showed a critical effect on physical stability. NLC3 and NLC4, prepared by Gelucire 44/14 could not autoclave as evidenced by the appearance of oil droplets, phase separation, and particle aggregation. However, NLC1, NLC2, and NLC2-PEG,

prepared with Tween 80, provided stable NLCs. No significant difference in all the parameters was observed before and after autoclaving ( $p > 0.05$ ).

**Table 6.1 The components and physicochemical properties of NLCs**

Formula	Type of Solid lipid : Surfactant	Mean size	Polydispersity	Zeta potential
		(nm) $\pm$ SD before autoclave (after autoclave)	index $\pm$ SD before autoclave (after autoclave)	(mV) $\pm$ SD before autoclave (after autoclave)
NLC1	CATO : T80	307 $\pm$ 29 (261 $\pm$ 10)	0.24 $\pm$ 0.02 (0.31 $\pm$ 0.03)	-27 $\pm$ 1 (-26 $\pm$ 2)
NLC2	CP : T 80	39 $\pm$ 4 (40 $\pm$ 3)	0.34 $\pm$ 0.02 (0.21 $\pm$ 0.08)	-30 $\pm$ 3 (-24 $\pm$ 3)
NLC2- PEG	CP : T 80	42 $\pm$ 2 (37 $\pm$ 3)	0.16 $\pm$ 0.05 (0.19 $\pm$ 0.03)	-28 $\pm$ 1 (-31 $\pm$ 2)
NLC3	CATO : G 44/14	144 $\pm$ 8(PS)	0.32 $\pm$ 0.02 (PS)	-30 $\pm$ 6 (PS)
NLC4	CP : G44/14	34 $\pm$ 1(PS)	0.33 $\pm$ 0.00 (PS)	-28 $\pm$ 5 (PS)

**Note:** SD: standard deviation for n=3; PS: phase separation

## 2. Physicochemical characterization of IND-NLCs

Table 6.2 showed the effect of different solid lipids, surfactants, and PEG coating on the physical characteristics of IND-NLCs. Compared to blank NLCs, IND-NLCs were slightly larger ( $p < 0.05$ ). However, IND loading showed no significant influence on the zeta potential and PI ( $p > 0.05$ ). The entrapment efficiency (EE) of IND-NLC1, IND-NLC2, and IND-NLC2-PEG was  $74.11 \pm 2.81$ ,  $65.09 \pm 3.16$ , and  $62.75 \pm 4.10$ , respectively. Table 6.2 also showed lack of any significant effect of sterilization on the physicochemical characteristics of all IND-NLCs formulations.

The morphology examined by TEM was shown in Figure 6.1, both uncoated IND-NLC2, and PEG-coated IND-NLC2 exhibited spherical shape. The light grey border at the periphery (Figure 6.1B) was attributed to the presence of PEG coating around the particle surface.

**Table 6.2 Physicochemical characterizations of the optimized IND-NLCs**

Formula	Mean size	Polydispersi	Zeta potential	Entrapment
	(nm) $\pm$ SD	ty index $\pm$ SD	(mV) $\pm$ SD	efficacy (%) $\pm$
	before	before	before	SD before
	autoclave	autoclave	before autoclave	autoclave
	(after	(after	(after autoclave)	(after
	autoclave)	autoclave)		autoclave)
IND-NLC1	333 $\pm$ 19 (261 $\pm$ 10)	0.27 $\pm$ 0.05 (0.31 $\pm$ 0.03)	-25 $\pm$ 5 (-26 $\pm$ 2)	74.11 $\pm$ 2.81 (73.91 $\pm$ 0.37)
IND-NLC2	46 $\pm$ 5 (40 $\pm$ 3)	0.34 $\pm$ 0.06 (0.21 $\pm$ 0.08)	-26 $\pm$ 4 (-24 $\pm$ 3)	65.09 $\pm$ 3.16 (61.10 $\pm$ 2.84)
IND-NLC2-PEG	43 $\pm$ 2 (40 $\pm$ 3)	0.12 $\pm$ 0.02 (0.21 $\pm$ 0.08)	-28 $\pm$ 1 (-24 $\pm$ 3)	62.75 $\pm$ 4.10 (60.35 $\pm$ 1.49)

**Note:** SD: standard deviation for n=3

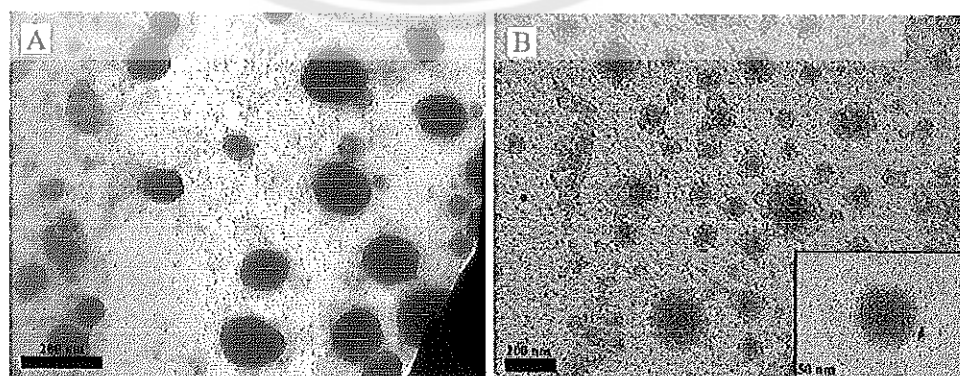


**Figure 6.1 TEM micrographs of (A) IND-NLC2 and (B) IND-NLC2-PEG**

### 3. *In vitro* release study

IND has a poor solubility of  $0.83 \pm 0.04 \mu\text{g/mL}$  in NSS at ambient temperature. Therefore, 0.6% (w/v) Tween 80 was added to the NSS to provide a sink condition by increasing the solubility of IND to  $206.67 \pm 7.08 \mu\text{g/mL}$ . As shown in Figure 6.2, all formulations showed a biphasic release profile with a burst release during 5 min followed by a prolonged release up to 6 h following Higuchi's model (Appendix A). At the first 5 min, the cumulative release of IND from the IND-NLC1 and IND-NLC2 was  $48.24 \pm 3.15$  and  $56.14 \pm 9.86\%$ , respectively. Then, they increased to  $93.89 \pm 4.76$  and  $98.25 \pm 4.20\%$ , respectively, after 6 h. Moreover, in the case of IND-NLC2-PEG, the cumulative released of IND at 5 and 360 min was  $47.64 \pm 0.92$  and  $80.04 \pm 4.72\%$ , respectively. The results showed that the smaller particle size showed faster drug release rate than larger ones. Moreover, IND-NLC2-PEG showed slower drug release rate than uncoated ones (IND-NLC2).

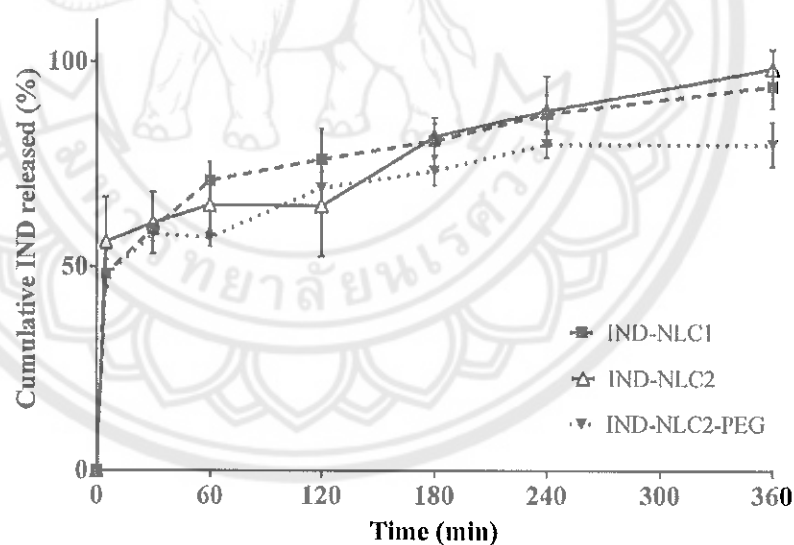


**Figure 6.2** *In vitro* release profiles of IND from IND-NLC1, IND-NLC2, and IND-NLC2-PEG in NSS with 0.6% (w/v) Tween 80 at 34°C. Error bars represent standard deviation for n=3

#### 4. *Ex vivo* mucoadhesion test

The percentage of IND remaining on the porcine cornea tissue after instillation was depicted in Figure 6.3. After 5 min of fluid flow, cornea tissue instilled with IND solutions showed ~28% remaining while those instilled with IND-NLC1, IND-NLC2, and IND-NLC2-PEG showed ~59%, ~70%, and ~73% remaining, respectively. Moreover, nearly 100% loss occurred after 60 min of fluid flow when instilled with IND solutions, IND-NLC1, and IND-NLC2. On the other hand, IND-NLC-PEG showed ~8% remaining after 60 min of continuous fluid flow. These results indicated that small NLCs (IND-NLC2) showed higher mucoadhesive property than larger NLCs (IND-NLC1), especially, NLCs coating with PEG provided the highest mucoadhesiveness on ocular surface.

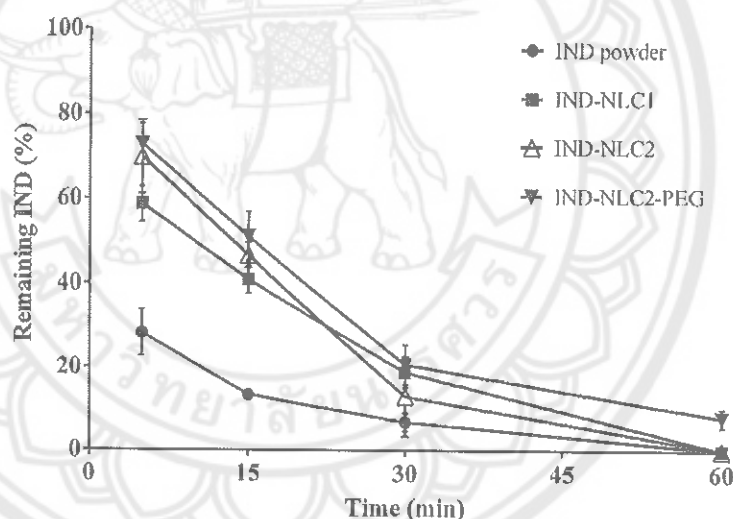


**Figure 6.3** The percentage of IND remaining on porcine cornea tissue after a steady flow of NSS for 60 min. Error bars represent standard deviation for n=3

#### 5. Cytotoxicity of IND-NLC

As shown in Table 6.3, exposure of PCE cells to IND-NLC2 and IND-NLC2-PEG, contained 0.5 and 5% IND, showed cell viability of > 70%. Based on Takahashi et al., they could be classified as non-irritants [22]. On the other hand, 5% of IND-solutions and SLS (positive control) exhibited cell viability (%) of  $56.16 \pm 4.23$  and  $59.69 \pm 3.96$ , respectively, confirming their irritation potential [22].



**Table 6.3 Summary of short time exposure (STE) tests performed by MTT assay**

Sample	IND (% w/v)	Cell viability (%) (mean $\pm$ SD)	STE classification <sup>a</sup>
IND-NLC2	5	72.47 $\pm$ 1.51	non-irritant
	0.05	92.76 $\pm$ 2.54	non-irritant
IND-NLC2-PEG	5	73.63 $\pm$ 1.05	non-irritant
	0.05	91.24 $\pm$ 4.81	non-irritant
IND-solution	5	56.16 $\pm$ 4.23	irritant
	0.05	72.56 $\pm$ 2.47	non-irritant
SLS	0.01	59.69 $\pm$ 3.96	irritant

<sup>a</sup>Eye irritation potential classification STE; Cell viability > 70% is classified as non-irritant [21]

### Discussion

Topical NSAIDs frequently produce side effects and adverse reactions ranging from burning sensation, stinging, and to minor signs of ocular irritation [23]. Stroobant et al., reported several formulations of topical NSAIDs eye drops to impact the rabbit corneal epithelial adversely [24]. Hence, safe and effective formulations of topical NSAIDs remain an unmet need in ophthalmic therapeutics [25]. In this study, NLC was employed as a drug carrier with the goal not only to overcome the adverse effects of topical NSAIDs but also to provide enhanced bioavailability, which could be improved by enhanced residence time on the cornea surface.

IND-NLCs were successfully prepared by a high-pressure homogenization technique. This technique has been used extensively because of its advantages including reliability, ease of scale up, and cost-effectiveness [26]. The particles produced were found to be suitable for ophthalmic applications with size ranging ~40 - 300 nm. In addition, all IND-NLCs formulations exhibited a high zeta potential of -30 mV, which would provide a long-term physical stability. The negative charge could

be attributed to the presence of medium chain triglyceride carboxylic group on the particle surface [27].

In agreement with previous reports, the number of fatty acid side chain on solid lipid and surfactant had a significant effect on the particle size of NLCs [28, 29]. In case of solid lipid type, NLC prepared with Compritol 888 ATO (fatty acid side chains, C<sub>22</sub>) resulted in larger particle size than NLC prepared with cetyl palmitate (fatty acid side chains, C<sub>16</sub>). Similarly, NLC stabilized with Tween 80 (fatty acid side chains, C<sub>18</sub>), showed larger size than NLC stabilized with Gelucire 44/14 (fatty acid side chains, C<sub>12</sub>). These could be attributed to the solid lipid and surfactant with long fatty acid side chain commonly forms larger particle size.

The type of liquid lipid, solid lipid, and surfactant all play an important role in incorporating a drug into NLCs [30]. In general, the incorporation of a liquid lipid consisting of a medium chain triglyceride along with a solid lipid consisting of a long chain triglyceride is known to increase the loading capacity and also enable controlled release [31]. Therefore, Lexol GT865 (medium chain triglyceride, C<sub>8</sub> and C<sub>10</sub>) was chosen as a liquid lipid in all formulations [32]. As expected, IND-NLC1 prepared with Compritol 888 ATO (fatty acid side chains, C<sub>22</sub>) showed higher EE compared to IND-NLC2 prepared with cetyl palmitate (fatty acid side chains, C<sub>16</sub>). This could be explained by increasing the space created between the solid fatty acid chain and the medium chain triglyceride, allowing more drug to be accommodated [33, 34]. In addition, the complete IND incorporation was confirmed by polarized light microscopy (data not shown).

Sterilization of ophthalmic formulation is critical for topical application as microbial contamination should be prevented [35, 36]. One of the strongest advantages of these NLCs is possible to sterile by an autoclaving method which is a commonly used and reliable technique. Taken together, the components for the preparation of NLCs must withstand the conditions of sterilization. As shown in Table 6.1, the physicochemical properties of NLCs were not affected by the type of solid/liquid lipids and polymer after autoclaving. However, the type of surfactant appears to have a profound influence. We found that NLCs prepared with Tween 80 withstood the sterilization by autoclaving in agreement with previous reports [37, 36]. The phenomena could be explained by the difference in the fatty acid side chain of the

surfactants. During autoclaving, the lipid matrix melts and then recrystallizes again during cooling at room temperature. As Tween 80 has a side chain of 18 carbon atoms, its long chain could have more chance to penetrate to the solid lipid phase, consequently lead to more compact and stronger particles. Gelucire 44/14, on the other hand, is composed of 12-carbon short side chain and hence it would be harder to stabilize the particles leading to phase separation.

Depending on the production process and especially different lipid blended, the different type of NLCs are obtained [26]. Due to the ratio of solid lipid/oil, 5/4, used in developed NLCs formulations, we assumed that the multiple type of NLCs would be achieved [31]. According to Müller et al., high levels of the oil can exceed their solubility in the solid lipid leading to precipitation as tiny oil nano compartments within the lipid matrix during the cooling process [26]. These oil nano compartments can contain higher amount of IND. However, the release of the drug would still be controlled by the surrounding solid lipid barrier. These observations help explain *in vitro* release data as discussed below.

As shown in Figure 6.2, we found biphasic IND release, with the burst phase contributing up to 50%. This burst release arguably would be beneficial since therapeutic drug levels can be reached after the administration [39]. The burst release of IND could be attributed to the re-distribution of IND during preparation process [26]. During hot homogenization, heating leads to an increased IND solubility in the water phase, thus, some drug partition from the melt lipid droplet to the water phase. However, during cooling, the solubility of the drug in water phase decreases leading to a re-partitioning of the drugs into the lipid phase. At the same time, the lipid phase starts to solidify and thus, the drugs are not accessible for the re-partitioning. Therefore, some of IND are accumulated at the matrix surface leading to the burst release characteristics.

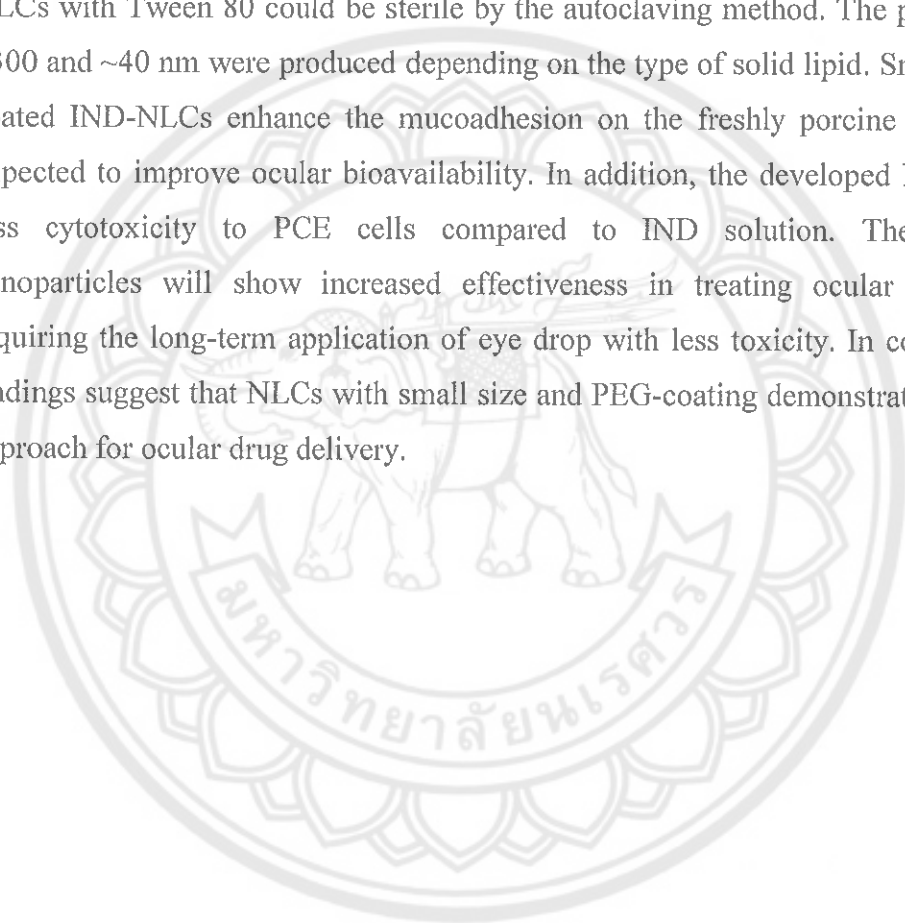
However, after the burst release, the release profile could be the best fit to the Higuchi square root model. This indicates that IND released from the NLCs in the second phase occurs by a diffusion-controlled mechanism from oil nano-compartment to the matrix for subsequent release to the medium. Also, the release of IND-NLC2 coated with PEG, an uncharged hydrophilic polymer, is slightly reduced possibly due to the presence of the polymer in the outer regions of the particles.

IND-NLCs showed greater adhesion on the porcine cornea tissue compared to IND solutions. It was found that the small IND-NLC2 (~40 nm) showed higher retention than large IND-NLC1 (~300 nm). Li et al., had suggested that NLCs with a particle size of 100 nm could be easily inserted into the branching sugar chains of mucin and thereby led to a stronger mucoadhesive property, compared to NLCs with a particle size of 200 and 300 nm [11]. This could be attributed to the small particle size exhibits more surface area to adhere on the corneal surface, surface modification of NLCs by coating with PEG could further improve ocular mucoadhesion. As Kashanian et al., noted that NLCs coating with PEG lead to an increment of nanoparticles penetration through mucus layer of the ocular surface possibly via PEG interpenetrating the mucus network aided by hydrogen bonding [40-42].

As a first step, we assessed the *in vitro* cytotoxicity of IND-NLCs in PCE cells following STE test protocol recommended as a potential alternative method for the assessment of ocular irritation in place of animal testing [20]. We have found the two candidates NLC formulations (IND-NLC2 and IND-NLC2-PEG) caused much less toxicity compared to IND in solutions. Interestingly, IND nanoparticles eye drops (containing 0.5% indomethacin) prepared using zirconia beads and Bead Smash 12, the particle size of  $76 \pm 59$  nm, are much tolerated better by a human cornea epithelial cell line (HCE-T) and rat corneal epithelial cells than commercial IND eye drops [5]. This could be explained by its sustained release, which lowers the risk of locally high concentrations, decreasing the direct cells stimulation leads to minimize local irritation. Therefore, the releasing of IND from IND-NLCs to the cells provided a less toxicity compared to direct cells stimulation form IND-solutions. Moreover, the nanoparticle formulations may decrease in the drug dose via an increase in bioavailability, thus resulting in a reduction in drug toxicity. Furthermore, IND-NLCs can be easily developed avoiding the use of organic solvents, and the selection of Tween 80 as a surfactant was reported to be non-irritating to the rabbit eye up to a concentration of 10% and has been used in a number of marketed ophthalmic solution eye drop [43].

## Conclusion

IND-NLCs were successfully prepared by a high-pressure homogenization technique to overcome the problems of IND on the topical ophthalmic formulations. Additionally, NLCs are solid at room and body temperature which can be formulated as nano-dispersions in liquid dosage forms. Therefore, they can be administered as an eye drop to avoid blurred vision and comfortable due to the nano size. The developed NLCs with Tween 80 could be sterile by the autoclaving method. The particle size of ~300 and ~40 nm were produced depending on the type of solid lipid. Small and PEG-coated IND-NLCs enhance the mucoadhesion on the freshly porcine cornea which expected to improve ocular bioavailability. In addition, the developed NLCs showed less cytotoxicity to PCE cells compared to IND solution. Therefore, these nanoparticles will show increased effectiveness in treating ocular inflammation requiring the long-term application of eye drop with less toxicity. In conclusion, our findings suggest that NLCs with small size and PEG-coating demonstrate a promising approach for ocular drug delivery.





**APPENDIX**

มหาวิทยาลัยสุรินทร์

**Appendix A Regression linear equation and correlation coefficient ( $R^2$ ) of three different drug release models**

Formulations	Regression linear equation ( $R^2$ )		
	Zero order	First order	Higuchi
IND-NLC1	$y = 0.1162x + 57.4300$ (0.8622)	$y = 0.0007x + 1.7591$ (0.7904)	$y = 2.6725x + 45.5755$ (0.9705)
IND-NLC2	$y = 0.1215x + 56.3597$ (0.9587)	$y = 0.0007x + 1.7598$ (0.9454)	$y = 2.5803x + 46.2487$ (0.9188)
IND-NLC2-PEG	$y = 0.0905x + 53.7274$ (0.8433)	$y = 0.0006x + 1.7307$ (0.8061)	$y = 2.0771x + 44.5482$ (0.9441)



**REFERENCES**



## REFERENCES

- [1] Weber, M. (2013). Efficacy and safety of indomethacin 0.1% eye drops compared with ketorolac 0.5% eye drops in the management of ocular inflammation after cataract surgery. *Acta Ophthalmologica*, 91(1), e15-e21.
- [2] Vulovic, N. (1989). Some studies into the properties of indomethacin suspensions intended for ophthalmic use. *International Journal of Pharmaceutics*, 55(2), 123-128.
- [3] Ahuja, M. (2008). Topical Ocular Delivery of NSAIDs. *The AAPS Journal*, 10(2), 229-241.
- [4] Hippalgaonkar, K. (2013). Indomethacin-loaded solid lipid nanoparticles for ocular delivery: development, characterization, and in vitro evaluation. *J Ocul Pharmacol Ther*, 29(2), 216-228.
- [5] Nagai, N. (2014). A nanoparticle formulation reduces the corneal toxicity of indomethacin eye drops and enhances its corneal permeability. *Toxicology*, 319, 53-62.
- [6] Ammar, H.O. (2009). Nanoemulsion as a Potential Ophthalmic Delivery System for Dorzolamide Hydrochloride. *AAPS PharmSciTech*, 10(3), 808.
- [7] Balguri, S.P., G.R. Adelli, & S. Majumdar. (2016). Topical ophthalmic lipid nanoparticle formulations (SLN, NLC) of indomethacin for delivery to the posterior segment ocular tissues. *European Journal of Pharmaceutics and Biopharmaceutics*, 109, 224-235.
- [8] Andonova V. (2015). Eye drops with nanoparticles as drug delivery system. *International Journal of Pharmacy and Pharmaceutical Science*, 7, 431-435.
- [9] Battaglia, L. (2016). Application of lipid nanoparticles to ocular drug delivery. *Expert Opinion on Drug Delivery*, 13(12), 1743-1757.
- [10] Sánchez-López, E. (2017). Lipid nanoparticles (SLN, NLC): Overcoming the anatomical and physiological barriers of the eye – Part II - Ocular drug-loaded lipid nanoparticles. *European Journal of Pharmaceutics and Biopharmaceutics*, 110, 58-69.

- [11] Li, H. (2016). Size-exclusive effect of nanostructured lipid carriers on oral drug delivery. *International Journal of Pharmaceutics*, 511(1), 524-537.
- [12] Alvarez-Trabado, J., Y. Diebold, & A. Sanchez. (2017). Designing lipid nanoparticles for topical ocular drug delivery. *International Journal of Pharmaceutics*, 532(1), 204-217.
- [13] Beloqui, A. (2016). Nanostructured lipid carriers: Promising drug delivery systems for future clinics. *Nanomedicine: Nanotechnology, Biology and Medicine*, 12(1), 143-161.
- [14] Nováková, L. (2005). Development and validation of HPLC method for determination of indomethacin and its two degradation products in topical gel. *Journal of Pharmaceutical and Biomedical Analysis*, 37(5), 899-905.
- [15] Niamprem, P., S. Rujivipat, & W. Tiyaboonchai. (2014). Development and characterization of lutein-loaded SNEDDS for enhanced absorption in Caco-2 cells. *Pharmaceutical Development and Technology*, 19(6), 735-742.
- [16] El-Badry, M., G. Fetih, & M. Fathy. (2009). Improvement of solubility and dissolution rate of indomethacin by solid dispersions in Gelucire 50/13 and PEG4000. *Saudi Pharmaceutical Journal*, 17(3), 217-225.
- [17] Chaiyasan, W., S.P. Srinivas, & W. Tiyaboonchai. (2013). Mucoadhesive chitosan-dextran sulfate nanoparticles for sustained drug delivery to the ocular surface. *Journal of Ocular Pharmacology and Therapeutics*, 29(2), 200-207.
- [18] Takahashi, H. (2015). Novel primary epithelial cell toxicity assay using porcine corneal explants. *Cornea*, 34(5), 567-575.
- [19] Chaiyasan, W. (2017). Penetration of mucoadhesive chitosan-dextran sulfate nanoparticles into the porcine cornea. *Colloids and Surfaces B: Biointerfaces*, 149, 288-296.
- [20] Wroblewska, K. (2015). Characterization of new eye drops with choline salicylate and assessment of their irritancy by in vitro short time exposure tests. *Saudi Pharmaceutical Journal*, 23(4), 407-412.
- [21] Sakaguchi, H. (2011). Validation study of the Short Time Exposure (STE) test to assess the eye irritation potential of chemicals. *Toxicology in Vitro*, 25(4), 796-809.

- [22] Takahashi, Y. (2009). Inter-laboratory study of short time exposure (STE) test for predicting eye irritation potential of chemicals and correspondence to globally harmonized system (GHS) classification. *J Toxicol Sci*, 34(6), 611-626.
- [23] Araújo, J. (2009). Nanomedicines for ocular NSAIDs: safety on drug delivery. *Nanomedicine: Nanotechnology, Biology and Medicine*, 5(4), 394-401.
- [24] Stroobants, A., K. Fabre, & P.C. Maudgal. (2000). Effect of non-steroidal anti-inflammatory drugs (NSAID) on the rabbit corneal epithelium studied by scanning electron microscopy. *Bull Soc Belge Ophtalmol*, 276, 73-81.
- [25] Doktorovova, S., E.B. Souto, & A.M. Silva. (2014). Nanotoxicology applied to solid lipid nanoparticles and nanostructured lipid carriers – A systematic review of in vitro data. *European Journal of Pharmaceutics and Biopharmaceutics*, 87(1), 1-18.
- [26] Müller, R.H., M. Radtke, & S.A. Wissing. (2002). Solid lipid nanoparticles (SLN) and nanostructured lipid carriers (NLC) in cosmetic and dermatological preparations. *Advanced Drug Delivery Reviews*, 54(Supplement), S131-S155.
- [27] Huang, Z.R. (2008). Development and evaluation of lipid nanoparticles for camptothecin delivery: a comparison of solid lipid nanoparticles, nanostructured lipid carriers, and lipid emulsion. *Acta Pharmacologica Sinica*, 29(9), 1094-1102.
- [28] Seyfoddin, A., J. Shaw, & R. Al-Kassas. (2010). Solid lipid nanoparticles for ocular drug delivery. *Drug Delivery*, 17(7), 467-489.
- [29] Seyfoddin, A., & R. Al-Kassas. (2013). Development of solid lipid nanoparticles and nanostructured lipid carriers for improving ocular delivery of acyclovir. *Drug Development and Industrial Pharmacy*, 39(4), 508-519.
- [29] Jenning, V., A.F. Thünemann, & S.H. Gohla. (2000). Characterisation of a novel solid lipid nanoparticle carrier system based on binary mixtures of liquid and solid lipids. *International Journal of Pharmaceutics*, 199(2), 167-177.

- [30] Thang LQ. (2017). Study on cause-effect relations and optimization of exemestane-loaded nanostructured lipid carriers. *International Journal of Pharmacy and Pharmaceutical Science*, 9, 68-74.
- [31] Jenning V. (2000). Characterisation of a novel solid lipid nanoparticle carrier system based on binary mixtures of liquid and solid lipids. *International Journal of Pharmaceutics*, 199, 167-177.
- [32] Muchtar, S. (1997). Ex-vivo permeation study of indomethacin from a submicron emulsion through albino rabbit cornea. *Journal of Controlled Release*, 44(1), 55-64.
- [33] Paliwal, R. (2009). Effect of lipid core material on characteristics of solid lipid nanoparticles designed for oral lymphatic delivery. *Nanomedicine: Nanotechnology, Biology and Medicine*, 5(2), 184-191.
- [34] Duarah S. (2016). Nanotechnology-based cosmeceuticals: a review. *International Journal of Applied Pharmaceutics*, 8, 8-12.
- [35] Baudouin, C. (2010). Preservatives in eyedrops: The good, the bad and the ugly. *Progress in Retinal and Eye Research*, 29(4), 312-334.
- [36] M H, Gowda DV. (2016). Nanotechnology for ophthalmic preparations. *International Journal of Current Pharmaceutical Research*, 8, 5-11.
- [37] Pardeike, J. (2012). Formation of a physical stable delivery system by simply autoclaving nanostructured lipid carriers (NLC). *International Journal of Pharmaceutics*, 439(1-2), 22-27.
- [38]. Ibrahim, S.S. (2009). Comparative effects of different cosurfactants on sterile prednisolone acetate ocular submicron emulsions stability and release. *Colloids and Surfaces B: Biointerfaces*, 69(2), 225-231.
- [39] Gupta, H. (2010). Sparfloxacin-loaded PLGA nanoparticles for sustained ocular drug delivery. *Nanomedicine: Nanotechnology, Biology and Medicine*, 6(2), 324-333.
- [40] Kashanian, S., & E. Rostami. (2014). PEG-stearate coated solid lipid nanoparticles as levothyroxine carriers for oral administration. *Journal of Nanoparticle Research*, 16(3), 2293.

- [41] De Campos, A.M. (2003). The effect of a PEG versus a chitosan coating on the interaction of drug colloidal carriers with the ocular mucosa. *European Journal of Pharmaceutical Sciences*, 20(1), 73-81.
- [42] Deore S. (2016). Nanoparticle: as targeted drug delivery system for depression. *International Journal of Current Pharmaceutical Research*, 8, 7-11.
- [43] Jiao, J. (2008). Polyoxyethylated nonionic surfactants and their applications in topical ocular drug delivery. *Advanced Drug Delivery Reviews*, 60(15), 1663-1673.



## CHAPTER VII

### CONCLUSION

NLCs eye drop has been successfully developed as an effective formulation for treating DED related to a non-functional TFLL and also useful as ocular drug delivery to deliver the drug to anterior segment. NLCs are new generation of lipid-based colloidal carriers which composed of mixture of liquid and solid lipid. In addition, they are solid at room and body temperature, which can be formulated as nano-dispersions in liquid dosage forms. Therefore, they can be administered as an eye drop to avoid blurred vision and comfortable due to the nano size. In this study, the particle size of NLCs eye drop in the range of ~300 - 40 nm were produced depending on the type of solid lipid and surfactant. In addition, all NLCs formulations exhibited a high zeta potential of -30 mV, which would provide a long-term physical stability. One of the strongest advantages of these NLCs eye drop is possible to sterile by an autoclaving method which is a commonly used and reliable technique. As we expected, the developed NLCs eye drop with Tween 80 as surfactant can be autoclaved which the microbial contamination can be avoided. The optimized NLCs eye drop achieved values of particle size, zeta potential, sterility, pH, osmolarity, stability, and surface tension close to the physiological range that suitable for tear replacement. In addition, NLCs eye drop showed non-irritation to PCE cells and no adverse effects were observed in *in vivo* experiment.

Generally, the evaporative type of DED is the most common form which caused of high evaporation that resulting from environment stress and unstable of tear film. In order to improve tear film stability, NLCs eye drop designed to more closely mimic the combination of aqueous and tear film lipid layers. Thus, the surface activity and interaction of the developed NLCs eye drop on meibomian lipid were investigated using *in vitro* Langmuir trough model. Our finding suggested that NLCs can interact with meibomian lipid films by both directly and diffusing from the subphase owing to its high surface activity. It can conclude that NLCs eye drop do not disrupt meibomian lipid layer and could improve tear film stability.

To support this conclusion, we further evaluated the appearance of NLCs eye drop in rabbit eye under normal condition. Surprisingly, the fluorescent signal of NLCs eye drop was significantly increased with a time manner. This phenomenon could be explained by its high surface activity and the mechanisms of NLCs eye drop after instilled into the eye. In general, the tear film is composed of three layers: the outermost tear film lipid layer (TFLL), the middle aqueous layer, and the innermost mucous layer. After NLCs eye drop was instilled into the eye, the NLCs eye drop would first attach to the tear film and hence have the opportunity to interact with all of three layers. Firstly, at the air-lipid interface, the TFLL is primarily composed of lipid. Thus, the NLCs eye drop could have interaction with this lipid layer due to a lipid property of the NLCs eye drop. Secondly, the NLCs eye drop also includes surfactant that this surfactant could stabilize the lipid-aqueous mixture as found in natural TFLL. Therefore, some of the NLCs eye drop would bind to the lipid-aqueous interface and play a key role in enhance tear film stability. Lastly, as suggested by previous studies, the NLCs eye drop with particle size of ~40 nm could be easily inserted into the branching sugar chains of mucin. Thereby, the NLCs eye drop would also bind within the mucous layer. Furthermore, due to its highly surface activity of these NLCs eye drop, they would then adsorb and penetrate from aqueous or mucous layer to the TFLL, leading to an increase in the fluorescence signal on the rabbit eye. These could be attributing to the NLCs eye drop improves the stability of TFLL on ocular surface and correlated well with previous *in vitro* Langmuir trough model. We next studied the protecting effect of the NLCs eye drop on corneal epithelium cells in the rabbit model desiccating stress-induced dry eye. Interestingly, we have found that the NLCs eye drop reduced the corneal epithelial cell damage and showed greater corneal epithelium cell protection than positive control (untreated) and commercial artificial tear (polymer based formulation). Therefore, the results confirmed that NLCs eye drop can form a stable bionic tear film and protect the ocular surface from environmental stress. Thus, NLCs can be potentially used as tear replenishment and tear replacement formulation for treating DED.

Apart from the artificial tear, anti-inflammatory agents are widely accepted to suppress the chronic inflammation of DED. However, anti-inflammatory agents are usually used as eye drops which also exhibited poor bioavailability and caused eye irritation. To overcome this problem, the mucoadhesive nanostructured lipid carriers (NLCs) eye drop has been successfully developed by surface modification with polyethylene glycol 400 or stearylamine (the cationic lipid) to obtain hydrophilic polymer coated surface or positively charged surface, respectively. The surface modification did not affect the particle size. We have demonstrated that size of the particle, surface hydrophobicity, and surface charge affects the penetration and mucoadhesion of NLCs. Although, the penetration mechanisms for NLCs into the anterior segment of the eye are unclear; the commonly accepted three mechanisms could be explained. Firstly, drugs can diffuse from NLCs into the epithelial membrane. This particle-to-membrane diffusion can subsequently facilitate the penetration of drug across the entire thickness of epithelium along the connected lipid membranes. Secondly, the presence of surfactant on the NLCs surface can act as a drug penetration enhancer. Finally, the NR-NLCs were internalized by the epithelial cells via endocytosis. It can be suggested that NR-NLC-40 can be useful for lipophilic drug delivery to the anterior segment. Moreover, hydrophilic surface or positive surface charge improved the ocular mucoadhesive property of NR-NLCs and could be potentially used to treat ocular surface disorders.

In addition, Indomethacin (IND), the lipophilic model drug, was successfully entrapped into the NLCs. High entrapment efficiency up to ~70% and biphasic release profile was observed. After the burst release, the release profile could be best fit to the Higuchi square root model indicating that drugs released from the NLCs by a diffusion-controlled mechanism. Depending on the production process and especially different lipid blended, the different type of NLCs is obtained. Due to the ratio of solid lipid/oil, 5/4, used in developed NLCs formulations, we assumed that the multiple types of NLCs would be achieved. Also, the type of liquid lipid, solid lipid, and surfactant all play an important role in incorporating a drug into NLCs. Moreover, we found that the developed NLCs showed less cytotoxicity compared to IND solution suggesting NLCs provide effectiveness in long-term application of eye drop for treating ocular inflammation.



In conclusion, our findings suggest that NLCs eye drop is an effective formulation for treating DED related to a non-functional TFLL and also useful for ocular drug delivery to treat ocular surface disorders.

